Measurement of the Hydrodynamic Radius, R_h

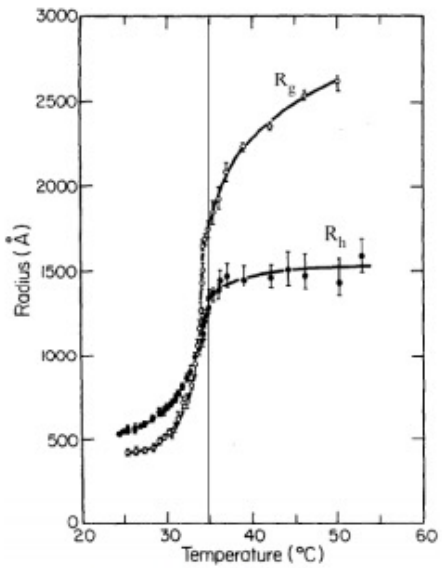

Figure 3. Radius of gyration, R_g, and hydrodyamic radius R_h versus temperature for polystyrene in cyclohexane. Vertical line indicates the phase separation temperature. From Reference [21].

R_g/R_h
1.5 Theta
1.6 Expanded
0.774 Sphere
0.92 Draining Sphere

$$[\eta] = \frac{4/3\pi R_H^3}{N} \qquad R_H = \frac{kT}{6\pi\eta D} \qquad \frac{1}{R_H} = \frac{1}{2N^2}\sum_{i=1}^{N}\sum_{j=1}^{N}\left\langle \frac{1}{|r_i - r_j|} \right\rangle$$

Kirkwood, J. Polym. Sci. **12** 1(1953).

http://theor.jinr.ru/~kuzemsky/kirkbio.html

A Harmonic Mean

(based on an average of transport rates, $D = kT/(6\pi\eta R_h)$)

http://www.eng.uc.edu/~gbeaucag/Classes/Properties/HydrodyamicRadius.pdf

An Arithmetic Mean

$$R_g^2 = \frac{1}{N}\sum_{n=1}^{N}\left\langle\left(R_n - \frac{1}{N}\sum_{m=1}^{N}R_m\right)^2\right\rangle = \frac{1}{N}\sum_{n=1}^{N}\left\langle\frac{1}{2N}\sum_{m=1}^{N}(R_n - R_m)^2\right\rangle = \frac{1}{2N^2}\sum_{n=1}^{N}\sum_{m=1}^{N}\langle(R_n - R_m)^2\rangle$$

Measurement of the Hydrodynamic Radius, R_h

$[\eta] = \frac{4}{}$

R_g/R_H Ratio

Table III
ρ Factor and Molecular Polydispersity P_w/P_n for Some Selected Models[a]

model		ρ	P_w/P_n
linear chains			
monodisperse	1.5	$8/3\pi^{1/2}$	1
polydisperse ($m = 1$)		$3^{1/2}$	2
polydisperse (m coupled chains)		$\frac{(m+2)^{1/2}}{m+1} 2\Sigma\left(1 + \frac{k-1}{m}\right)c(k)$	$1 + (1/m)$
star molecules			
regular stars		$\left(\frac{3f-2}{f\pi}\right)^{1/2} \frac{8}{3} \frac{(2-f) + 2^{1/2}(f-1)}{f}$	1
polydisperse stars		$\left(\frac{6f}{f+1}\right)^{1/2} \frac{f+3}{2(f+1)}$	$1 + (1/f)$
polycondensates			
A_f type	1.73	$3^{1/2}$	$P_w\left(1 - \frac{f}{2(f-1)}\right)$
ABC type		$\left(\frac{3}{4}\frac{1+2B}{1+B}\right)^{1/2}\left(\frac{2+B}{1+B}\right)$	$2(1+B)$
randomly cross-linked chains (polydisperse ($m = 1$) primary chains)		$3^{1/2}$ 1.73	$2(P_w/P_w p)$
monodisperse spheres	0.77	$(3/5)^{1/2}$	1

[a] $\rho = \langle 1/R\rangle_z \langle S^2\rangle_z^{1/2}$; all other notation is as in Tables I and II.

Burchard, Schmidt, Stockmayer, Macro. 13 1265 (1980)
(http://www.eng.uc.edu/~gbeaucag/Classes/Properties/RgbyRhRatioBurchardma60077a045.pdf)

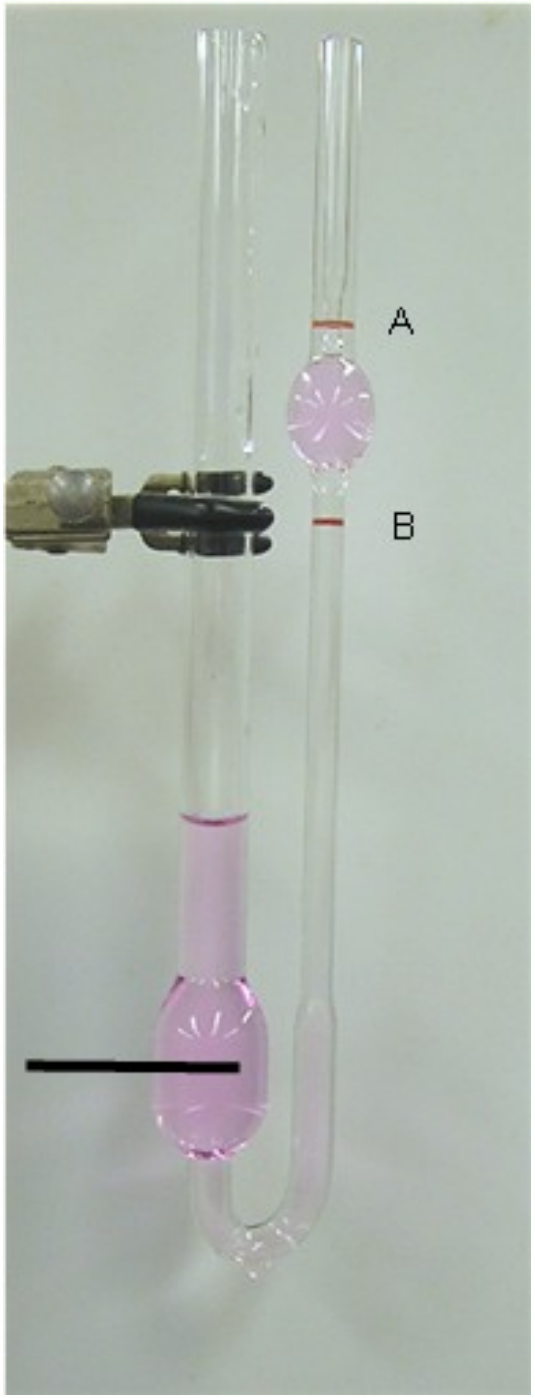

Viscosity

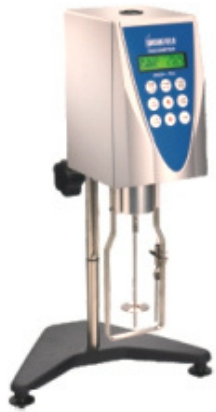

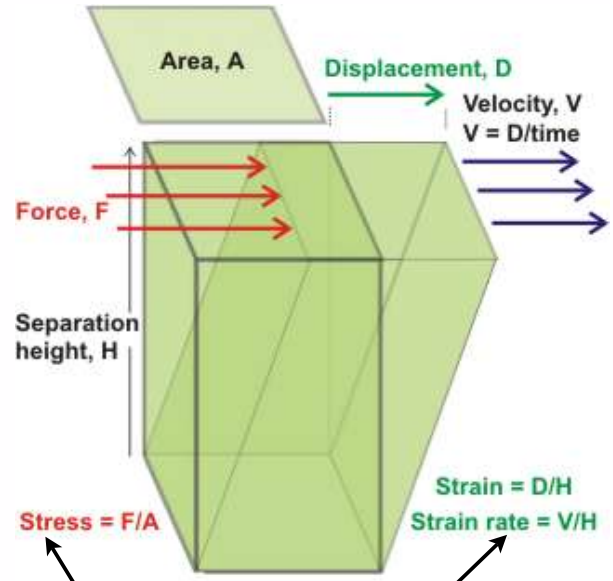

$$\tau = \eta\dot{\gamma}$$

$$\eta_s = \eta_0\left(1+[\eta]\phi\right)$$

$$[\eta] \approx \frac{V_{Molecule}}{M_{Moledule}}$$

Native state has the smallest volume

$$\Delta p = \frac{8\mu LQ}{\pi R^4} = \frac{8\pi\mu LQ}{A^2}$$ Poiseuille's Law ($Q = V/time$)

Intrinsic "viscosity" as a linear displacement law

$$\tau_{xy} = \eta \dot{\gamma}_{xy}$$

$$\tau_{xy} = \frac{dF_x}{dA_y} = \eta \dot{\gamma}_{xy} = \eta \frac{d\left(\frac{\Delta L_x}{L_y}\right)}{dt}$$

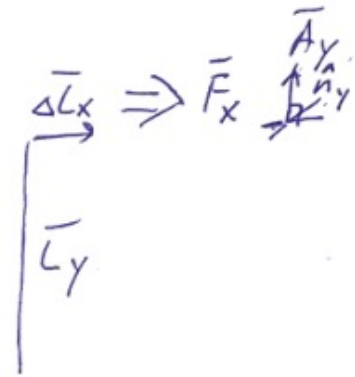

$$\eta = \eta_s(1 + \phi[\eta]) \sim \eta_s \exp(\phi[\eta])$$

At very small ϕ

$$L_y^* = L_y \exp(-\phi[\eta])$$
$$\sim L_y\,(1 - \phi[\eta])$$

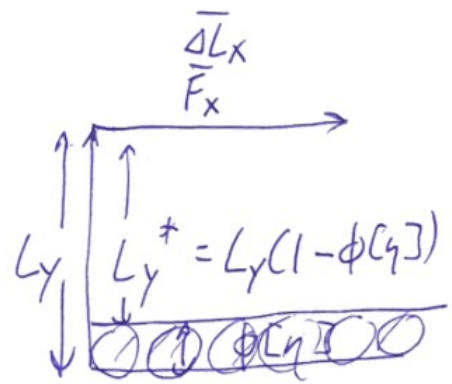

Intrinsic "viscosity" as a linear displacement law

$$L_y^* = L_y \exp(-\phi[\eta])$$
$$\sim L_y\,(1 - \phi[\eta])$$

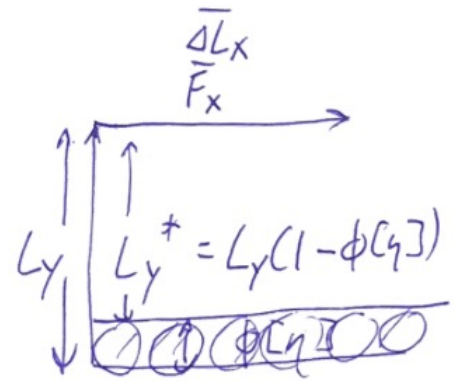

$$\tau_{xy} = \eta_s(1 + \phi[\eta])\,\frac{d\left(\frac{\Delta L_x}{L_y}\right)}{dt}$$
$$= \eta_s\,\frac{d\left(\frac{\Delta L_x}{L_y^*}\right)}{dt}$$

Intrinsic, specific & reduced "viscosity"

$\tau_{xy} = \eta \dot{\gamma}_{xy}$ Shear Flow (may or may not exist in a capillary/Couette geometry)

$$\eta_s = \eta_0 (1+\phi[\eta])$$

$$\eta_{rel} = \eta / \eta_S$$

$$\eta_{sp} = (\eta - \eta_S) / \eta_S = \eta_{rel} - 1$$

$$\eta_{red} = \eta_{sp} / c = (\eta_{rel} - 1) / c$$

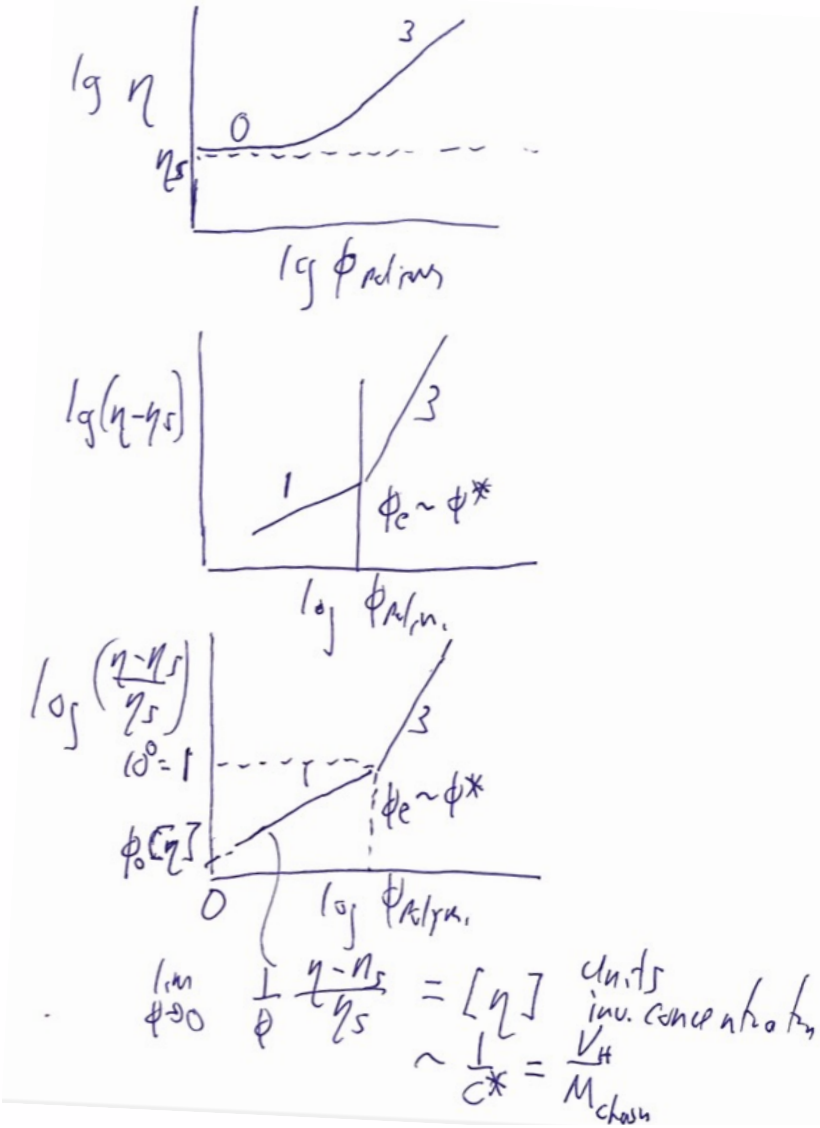

Intrinsic, specific & reduced "viscosity"

$$\tau_{xy} = \eta \dot{\gamma}_{xy}$$ Shear Flow (may or may not exist in a capillary/Couette geometry)

$$\eta = \eta_0 \left(1 + \phi[\eta] + k_1 \phi^2 [\eta]^2 + k_2 \phi^3 [\eta]^3 + \cdots + k_{n-1} \phi^n [\eta]^n\right)$$

Reminiscent of a virial expansion.

n = order of interaction (2 = binary, 3 = ternary etc.)

Reduced Viscosity $$\frac{1}{\phi}\left(\frac{\eta - \eta_0}{\eta_0}\right) = \frac{1}{\phi}(\eta_r - 1) = \frac{\eta_{sp}}{\phi} \xrightarrow{\text{Limit } \phi \Rightarrow 0} [\eta] = \frac{V_H}{M}$$ **Intrinsic Viscosity**

We can approximate (1) as:

Relative Viscosity $$\eta_r = \frac{\eta}{\eta_0} = 1 + \phi[\eta]\exp\left(K_M \phi[\eta]\right)$$ Martin Equation

Utracki and Jamieson "Polymer Physics From Suspensions to Nanocomposites and Beyond" 2010 Chapter 1

Intrinsic, specific & reduced "viscosity"

$$\eta = \eta_0 \left(1 + c[\eta] + k_1 c^2 [\eta]^2 + k_2 c^3 [\eta]^3 + \cdots + k_{n-1} c^n [\eta]^n\right) \qquad (1)$$

n = order of interaction (2 = binary, 3 = ternary etc.)

Reduced Viscosity $\frac{1}{c}\left(\frac{\eta - \eta_0}{\eta_0}\right) = \frac{1}{c}(\eta_r - 1) = \frac{\eta_{sp}}{c} \xrightarrow{\text{Limit } c=>0} [\eta] = \frac{V_H}{M}$

We can approximate (1) as:

Relative Viscosity $\eta_r = \frac{\eta}{\eta_0} = 1 + c[\eta]\exp\left(K_M c[\eta]\right)$ Martin Equation

Reduced Viscosity $\frac{\eta_{sp}}{c} = [\eta] + k_1 [\eta]^2 c$ Huggins Equation

$\frac{\ln(\eta_r)}{c} = [\eta] + k_1' [\eta]^2 c$ Kraemer Equation (exponential expansion)

Utracki and Jamieson "Polymer Physics From Suspensions to Nanocomposites and Beyond" 2010 Chapter 1

Intrinsic, specific & reduced "viscosity"

$$\eta = \eta_0 \left(1 + c[\eta] + k_1 c^2 [\eta]^2 + k_2 c^3 [\eta]^3 + \cdots + k_{n-1} c^n [\eta]^n\right) \qquad (1)$$

n = order of interaction (2 = binary, 3 = ternary etc.)

Reduced Viscosity

$$\frac{1}{c}\left(\frac{\eta - \eta_0}{\eta_0}\right) = \frac{1}{c}(\eta_r - 1) = \frac{\eta_{sp}}{c} \xrightarrow{\text{Limit } c \Rightarrow 0} [\eta] = \frac{V_H}{M}$$

Reduced Viscosity

$$\frac{\eta_{sp}}{\phi}$$

Concentration Effect

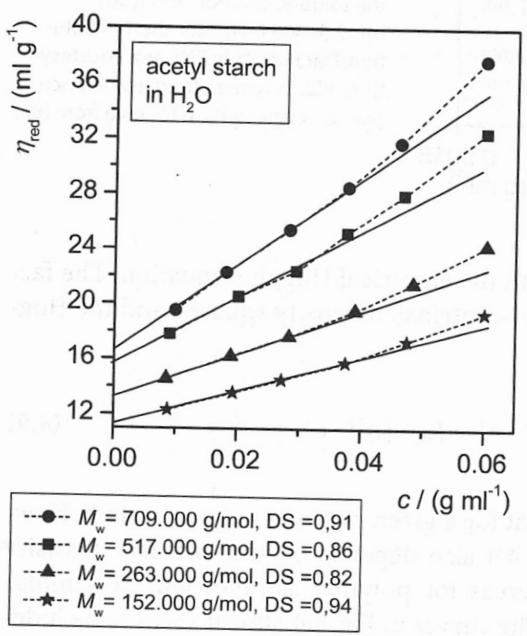

Fig. 4.5. Reduced viscosity η_{red} as a function of the concentration c for acetyl starch of different molar masses in aqueous solution at T=25 °C. The degree of substitution (DS) with acetyl groups is nearly constant at DS≈0.9. Due to the compact structure of the polymer coil the concentrations of the dilution series are relatively high to reach the required relative viscosity range of η_r=1.2–2.5

Kulicke & Clasen "Viscosimetry of Polymers and Polyelectrolytes (2004)

Intrinsic, specific & reduced "viscosity"

$$\eta = \eta_0 \left(1 + c[\eta] + k_1 c^2 [\eta]^2 + k_2 c^3 [\eta]^3 + \cdots + k_{n-1} c^n [\eta]^n\right) \qquad (1)$$

n = order of interaction (2 = binary, 3 = ternary etc.)

$$\frac{1}{c}\left(\frac{\eta - \eta_0}{\eta_0}\right) = \frac{1}{c}(\eta_r - 1) = \frac{\eta_{sp}}{c} \xrightarrow{\text{Limit } c \Rightarrow 0} [\eta] = \frac{V_H}{M}$$

Concentration Effect, c*

Reduced Viscosity

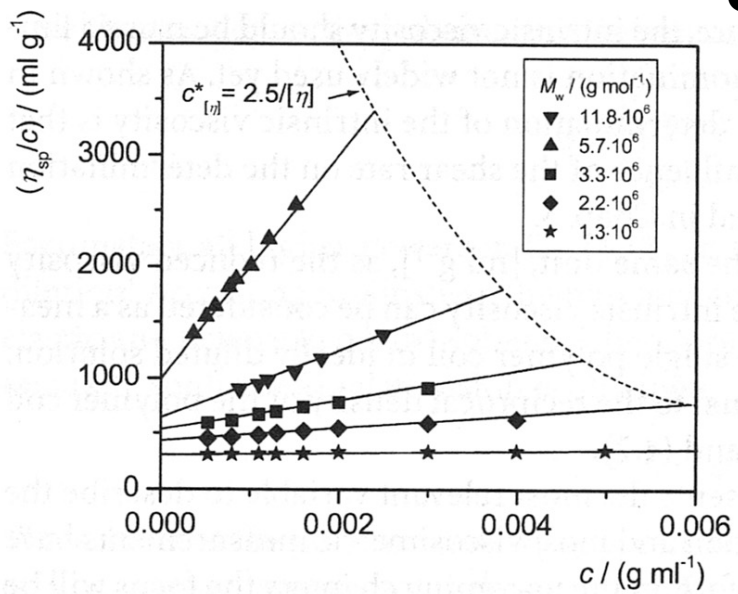

Fig. 4.2. Reduced viscosity η_{red} as a function of the concentration c for different molar masses of the polycation poly(acrylamide-*co*-(*N,N,N*-trimethyl-*N*-[2-methacryloethyl]-ammoniumchloride) (PTMAC) in 0.1 mol/l $NaNO_3$ solution. Data from [87]. All data points are measured at concentrations below the critical concentration $c^*_{[\eta]}$. The copolymer consists of 8 mol% TMAC and 92 mol% AAm

Kulicke & Clasen "Viscosimetry of Polymers and Polyelectrolytes (2004)

Intrinsic, specific & reduced "viscosity"

$$\eta = \eta_0 \left(1 + c[\eta] + k_1 c^2 [\eta]^2 + k_2 c^3 [\eta]^3 + \cdots + k_{n-1} c^n [\eta]^n\right) \qquad (1)$$

n = order of interaction (2 = binary, 3 = ternary etc.)

$$\frac{1}{c}\left(\frac{\eta - \eta_0}{\eta_0}\right) = \frac{1}{c}(\eta_r - 1) = \frac{\eta_{sp}}{c} \xrightarrow{\text{Limit } c \Rightarrow 0} [\eta] = \frac{V_H}{M}$$

Reduced Viscosity $\dfrac{\eta_{sp}}{\phi}$

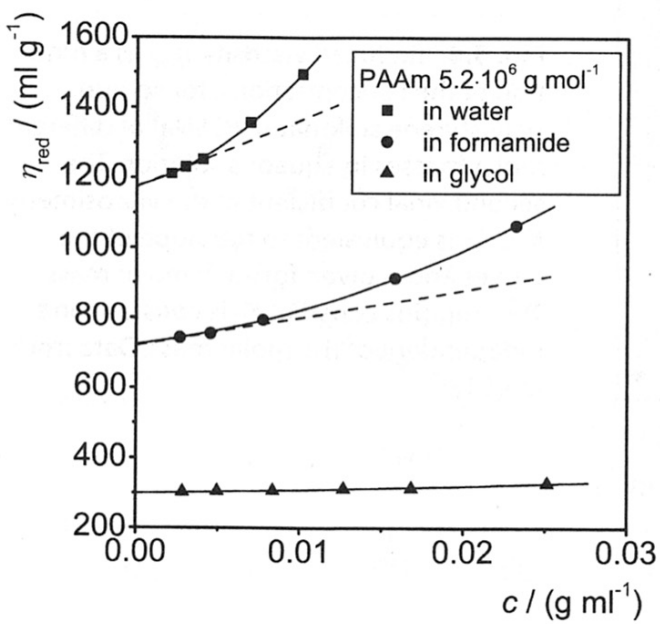

Solvent Quality

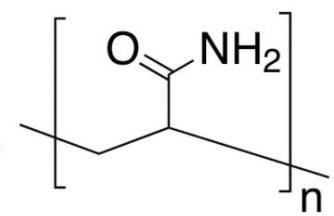

Fig. 5.3. Reduced viscosity η_{red} as a function of the concentration c for a poly(acrylamide) (PAAm) in the solvents H_2O, formamide and ethylene glycol at T=25 °C. Data from [89, 90]. The intrinsic viscosity (intersection with the Y-axis) rises with the solvent quality

Kulicke & Clasen "Viscosimetry of Polymers and Polyelectrolytes (2004)

Intrinsic, specific & reduced "viscosity"

$$\eta = \eta_0 \left(1 + c[\eta] + k_1 c^2 [\eta]^2 + k_2 c^3 [\eta]^3 + \cdots + k_{n-1} c^n [\eta]^n\right) \qquad (1)$$

n = order of interaction (2 = binary, 3 = ternary etc.)

Reduced Viscosity

$$\frac{1}{c}\left(\frac{\eta - \eta_0}{\eta_0}\right) = \frac{1}{c}(\eta_r - 1) = \frac{\eta_{sp}}{c} \xrightarrow{\text{Limit } c \Rightarrow 0} [\eta] = \frac{V_H}{M}$$

Molecular Weight Effect

$$\frac{\eta_{sp}}{\phi}$$

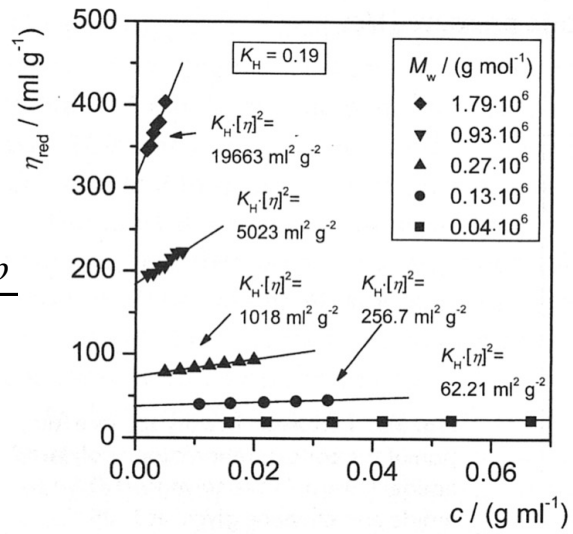

Fig. 5.4. Reduced viscosity η_{red} as a function of the concentration c for sodium poly(styrene sulfonate) (PSSNa) of different molar masses in aqueous solution. The second virial coefficient of the viscosimetry, $K_H \cdot [\eta]^2$, is equivalent to the slope of the curves and is given for each molar mass. The Huggins constant K_H is constant and independent of the molar mass. Data from [35, 91]

$$\eta_{red} = \frac{\eta_{sp}}{c} = [\eta] + k_H [\eta]^2 c$$

Huggins Equation

Kulicke & Clasen "Viscosimetry of Polymers and Polyelectrolytes (2004)

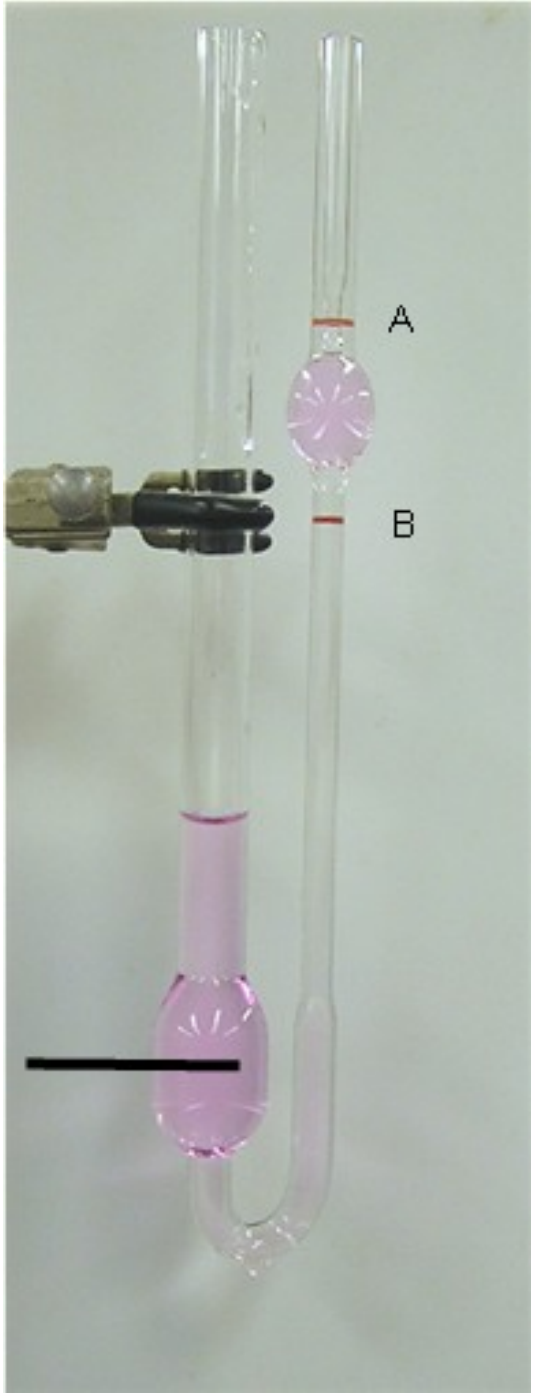

Viscosity

$$\eta_s = \eta_0 \left(1 + [\eta]\phi\right)$$

$$[\eta] \approx \frac{V_{Molecule}}{M_{Moledule}}$$

For the Native State Mass ~ $\rho V_{Molecule}$

Einstein Equation (for Suspension of 3d Objects)

$$\eta_s = \eta_0 \left(1 + 2.5\phi_v\right)$$

$$[\eta] = \frac{2.5}{\rho} \; ml/g$$

For "Gaussian" Chain Mass ~ Size^2 ~ $V^{2/3}$

V ~ Mass$^{3/2}$

For "Expanded Coil" Mass ~ Size$^{5/3}$ ~ $V^{5/9}$

V ~ Mass$^{9/5}$

For "Fractal" Mass ~ Size^{df} ~ $V^{df/3}$

V ~ Mass$^{3/df}$

$$[\eta] \sim M_{Molecule}^{\frac{3}{d_f}-1}$$

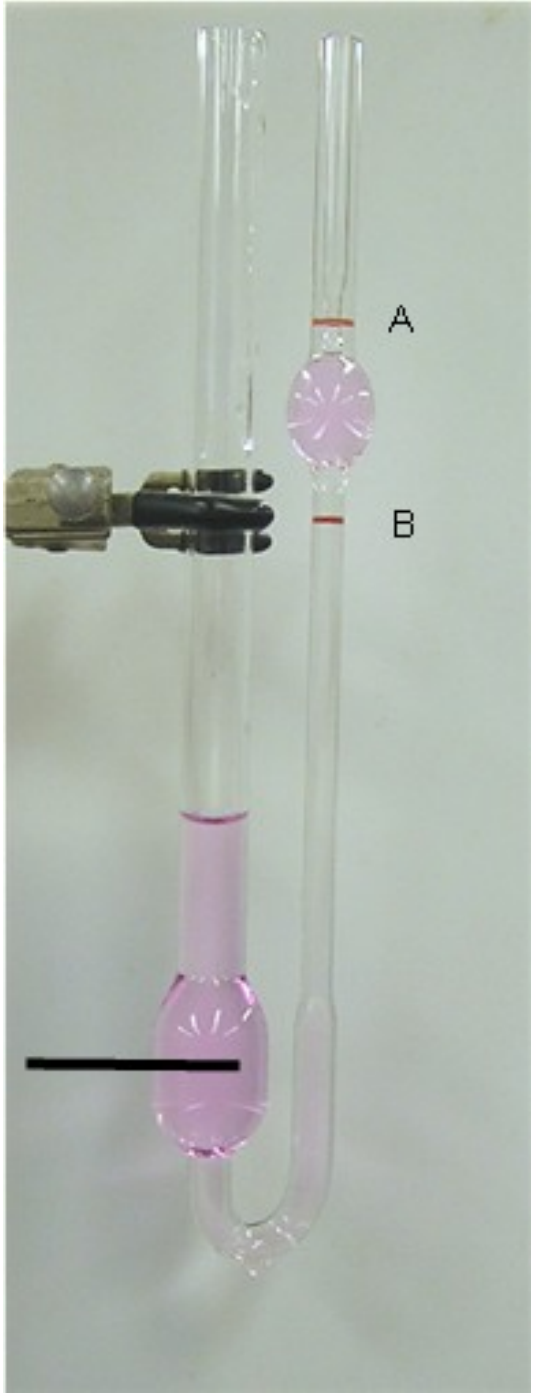

Viscosity

$$\eta_s = \eta_0 \left(1 + [\eta]\phi\right)$$

$$[\eta] \approx \frac{V_{Molecule}}{M_{Moledule}}$$

For the Native State Mass ~ $\rho V_{Molecule}$

Einstein Equation (for Suspension of 3d Objects)

$$\eta_s = \eta_0 \left(1 + 2.5\phi\right)$$

"Size" is the "Hydrodynamic Size"

For "Gaussian" Chain Mass ~ Size^2 ~ $V^{2/3}$

V ~ Mass$^{3/2}$

For "Expanded Coil" Mass ~ Size$^{5/3}$ ~ $V^{5/9}$

V ~ Mass$^{9/5}$

This is the "Zimm Model"
Or
Non-draining model

For "Fractal" Mass ~ Size^{df} ~ $V^{df/3}$

V ~ Mass$^{3/df}$

$$[\eta] \sim M_{Molecule}^{\frac{3}{d_f}-1}$$

Intrinsic, specific & reduced "viscosity"

$$\eta = \eta_0 \left(1 + c[\eta] + k_1 c^2 [\eta]^2 + k_2 c^3 [\eta]^3 + \cdots + k_{n-1} c^n [\eta]^n\right) \qquad (1)$$

n = order of interaction (2 = binary, 3 = ternary etc.)

$$\frac{1}{c}\left(\frac{\eta - \eta_0}{\eta_0}\right) = \frac{1}{c}(\eta_r - 1) = \frac{\eta_{sp}}{c} \xrightarrow{\text{Limit } c=>0} [\eta] = \frac{V_H}{M}$$

Viscosity itself has a strong temperature dependence. But intrinsic viscosity depends on temperature as far as coil expansion changes with temperature (R_H^3).

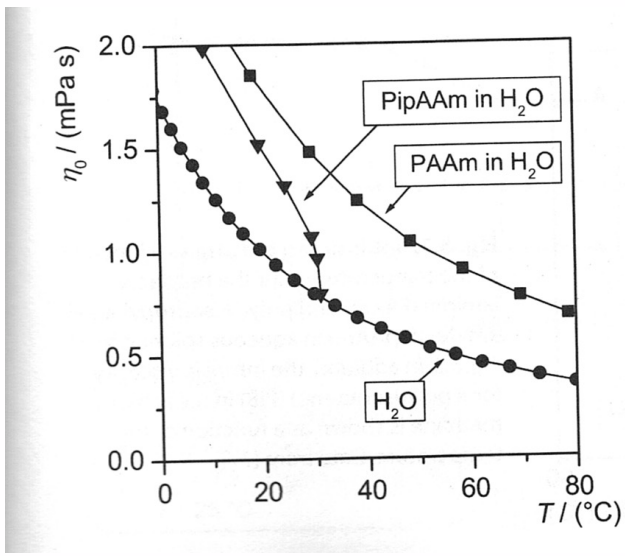

Temperature Effect

Fig. 5.5. Zero-shear viscosity η_0 as a function of the temperature T for poly (acrylamide) (PAAm) and poly(*N*-iso-propyl-acrylamide) (PipAAm) in aqueous solution (c=0.1 wt%). The viscosity for the solvent water as a function of the temperature is plotted as well. Data from [77]

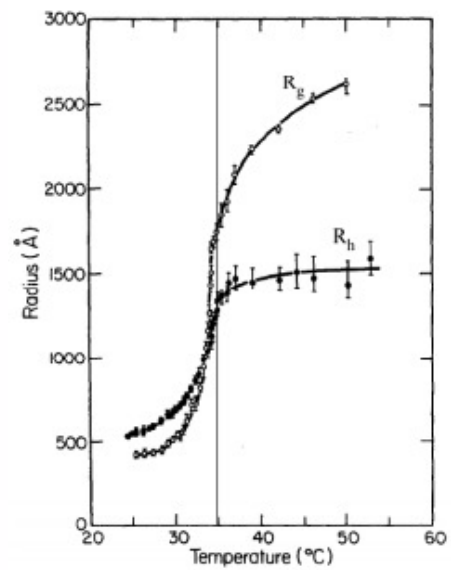

$$\eta_0 = A \exp\left(\frac{E}{k_B T}\right)$$

Weaker and Opposite Dependency

Arrhenius Behavior $$\eta_0 = A\exp\left(\frac{E}{k_B T}\right)$$

Williams-Landel-Ferry (WLF) Equation $$\log(a_T) = \frac{-C_1(T - T_\mathrm{r})}{C_2 + (T - T_\mathrm{r})}$$

$$\mu(T) = \mu_0 10^{\left(\frac{-C_1(T-T_r)}{C_2+T-T_r}\right)}$$

$$\frac{\eta}{\eta_0} = \exp\left(\frac{H_a}{kT}\right) \Rightarrow \exp\left(\frac{H_a}{k(T-T_V)}\right) \Rightarrow \exp\left(\frac{E_a}{k(T-T_V)}\right) \Rightarrow \exp\left(\frac{H_a - TS_a}{k(T-T_V)}\right)$$

3 constants T_r, H_a, S_a; WLF has 3 constants T_V, C_1, C_2

If exp(x) =10y then y =x/(ln(10)) = x/2.30

$T_V = (C_2 - T_r)$; $S_a = 2.30\ C_1$; $H_a = 2.30 C_1 T_r$

If you choose $T_r = T_g$ then $C_1 \sim 17.44$ and $C_2 \sim 51.6$

If you choose $T_r = T_g + 43$K then $C_1 \sim 8.86$ and $C_2 \sim 101.6$

It might be best to measure H and S and find the Vogel temperature experimentally

Intrinsic "viscosity" for colloids (Simha, Case Western)

https://physicstoday.scitation.org/do/10.1063/pt.4.2224/full/

$$\eta = \eta_0 (1 + v\phi) \qquad \eta = \eta_0 (1 + [\eta] c)$$

$$[\eta] = \frac{v N_A V_H}{M}$$

For a solid object with a surface, v is a constant in molecular weight, depending only on shape

For a symmetric object (sphere) $v = 2.5$ (Einstein) $[\eta] = \frac{2.5}{\rho}\ ml/g$

For ellipsoids v is larger than for a sphere,

$$v = \frac{J^2}{15(\ln(2J) - 3/2)}$$

prolate

a, b, b :: a>b

J = a/b

$$v = \frac{16J}{15\tan^{-1}(J)}$$

oblate

a, a, b :: a<b

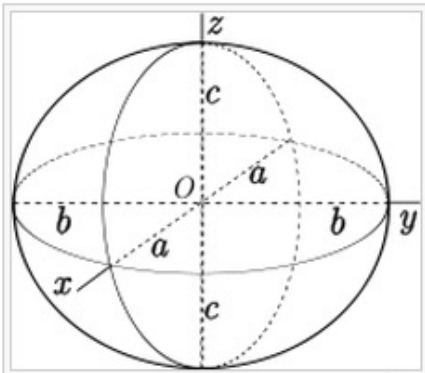

Tri-axial ellipsoid with distinct semi-axes *a*, *b* and *c*

Intrinsic "viscosity" for colloids (Simha, Case Western)

$$\eta = \eta_0 \left(1 + v\phi\right) \qquad \eta = \eta_0 \left(1 + [\eta] c\right)$$

$$[\eta] = \frac{v N_A V_H}{M}$$

Hydrodynamic volume for "bound" solvent

$$V_H = \frac{M}{N_A}\left(\bar{v}_2 + \delta_S v_1^0\right)$$

Partial Specific Volume	$\bar{v}_2$
Bound Solvent (g solvent/g polymer)	δ_S
Molar Volume of Solvent	v_1^0

Intrinsic "viscosity" for colloids (Simha, Case Western)

$$\eta = \eta_0 \left(1 + v\phi\right) \qquad \eta = \eta_0 \left(1 + [\eta] c\right)$$

$$[\eta] = \frac{v N_A V_H}{M}$$

Long cylinders (TMV, DNA, Nanotubes)

$$[\eta] = \frac{2}{45} \frac{\pi N_A L^3}{M\left(\ln J + C_\eta\right)}$$

J=L/d

C_η End Effect term ~ 2 ln 2 – 25/12 Yamakawa 1975

Shear Rate Dependence for Polymers

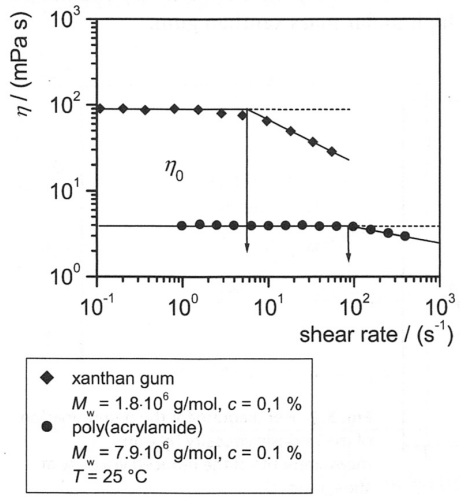

Fig. 5.8. Dynamic viscosity η as a function of the shear rate $\dot{\gamma}$ for an aqueous xanthan gum and an aqueous poly(acrylamide) solution of a comparable degree of polymerization and the same concentration c=0.1 wt% data from [92]. The viscosity depends on the shear rate above a critical shear rate $\dot{\gamma}_{crit}$

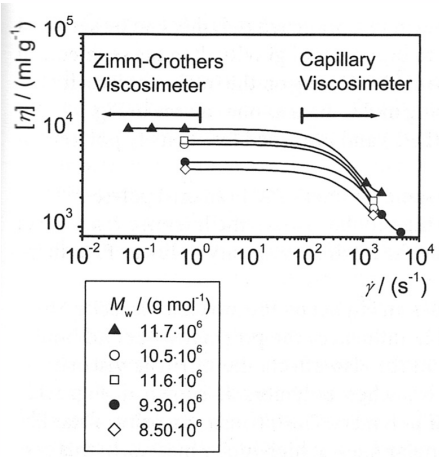

Fig. 5.10. Intrinsic viscosity $[\eta]$ determined at high shear rates $\dot{\gamma}$ with a capillary viscosimeter and at lower shear rates with a Zimm-Crothers viscosimeter for different xanthan gums in 0.1 mol/l sodium chloride (NaCl) solution at 25 °C. Data from [93]. For strongly shear thinning polymer solutions, only low shear viscosimeters reach the shear rate independent viscosity region

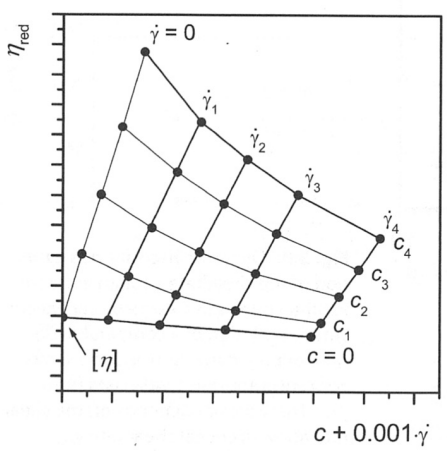

Fig. 5.9. Net diagram for the determination of the intrinsic viscosity $[\eta]$ from measurements of the reduced viscosity at shear rates≠0

Capillary Viscometer

$$\frac{Volume}{time} = \frac{\pi R^4 \Delta p}{8\eta l}$$

$$\Delta p = \rho g h$$

$$\dot{\gamma}_{Max} = \frac{4 Volume}{\pi R^3 time}$$

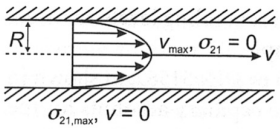

Fig. 3.2. Velocity profile in a capillary viscosimeter. The fluid velocity v has a parabolic profile with a maximum in the middle of the capillary; the shear rate $\dot{\gamma}$ and the shear stress τ have a maximum at the capillary wall and are zero in the middle of the capillary

Kulicke & Clasen "Viscosimetry of Polymers and Polyelectrolytes (2004)

Branching and Intrinsic Viscosity

5.5 Branching

Branching in a polymer coil leads for polymers of the same molar mass to changes of the intrinsic viscosity. Although the chemical composition is the same, branched polymers have a higher density ρ_{equ} in solution than linear polymers and therefore

$$[\eta] \approx \frac{V_{Molecule}}{M_{Moledule}}$$

$V_{Molecule} = 4/3\ \pi R_H^3$

R_H is smaller for a branched chain

$$[\eta] \sim M_{Molecule}^{\frac{3}{d_f}-1}$$

$[\eta]$ is constant for a 3d object

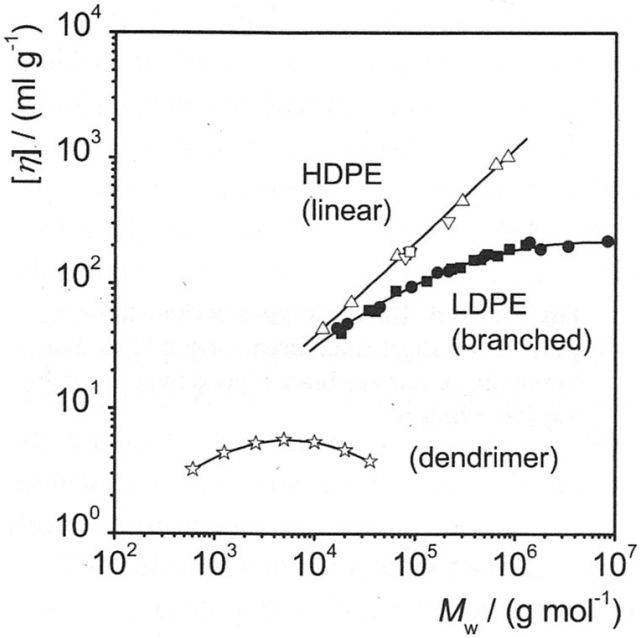

Fig. 5.11. Intrinsic viscosity $[\eta]$ as a function of the molar mass M for linear poly(ethylene) (high density poly(ethylene), HDPE) and longchain branched poly(ethylene) (low density poly(ethylene), LDPE) in tetraline at T=120 °C (data from [47, 94]) as well as for a dendrimer with 3,5-dioxybenzylidene units in tetrahydrofuran at T=30 °C (data from [47, 95])

Gen. 4 is 3d then dendrimer collapses for higher generations

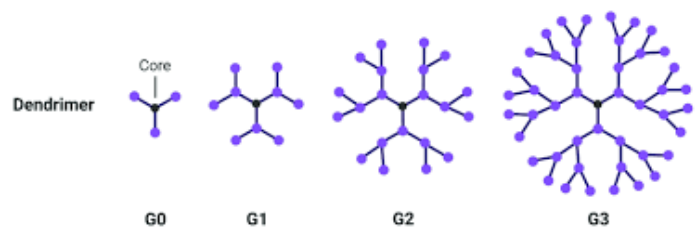

Kulicke & Clasen "Viscosimetry of Polymers and Polyelectrolytes (2004)

How Complex Mass Fractal Structures Can be Decomposed

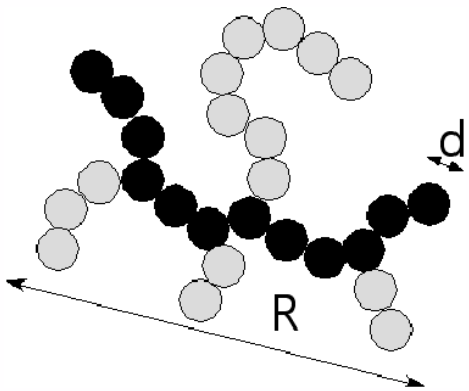

Tortuosity

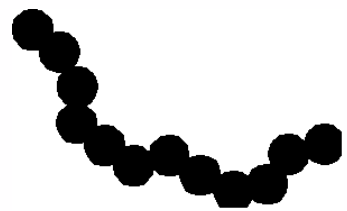

Connectivity

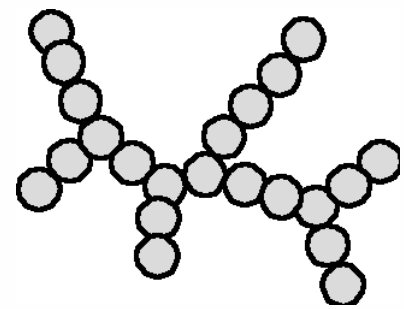

$$z \sim \left(\frac{R}{d}\right)^{d_f} \sim p^c \sim s^{d_{\min}}$$

$$p \sim \left(\frac{R}{d}\right)^{d_{\min}}$$

$$s \sim \left(\frac{R}{d}\right)^{c}$$

$$d_f = d_{\min} c$$

z	d_f	p	d_{min}	s	c	R/d
27	1.36	12	1.03	22	1.28	11.2

Branching and Intrinsic Viscosity

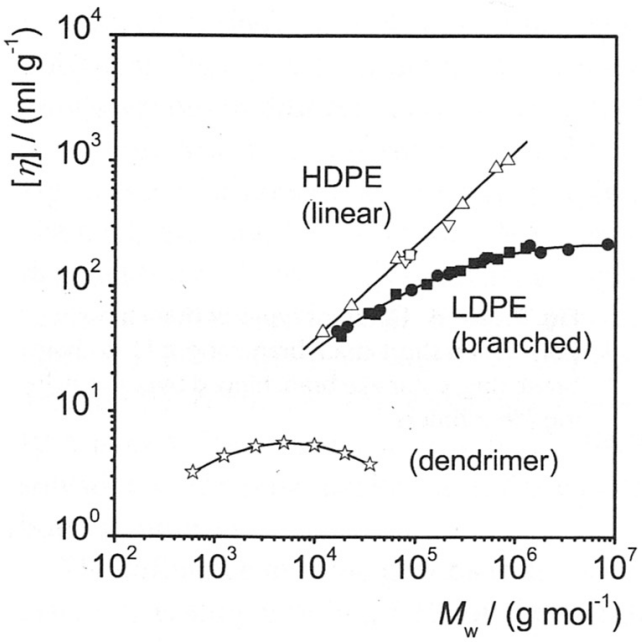

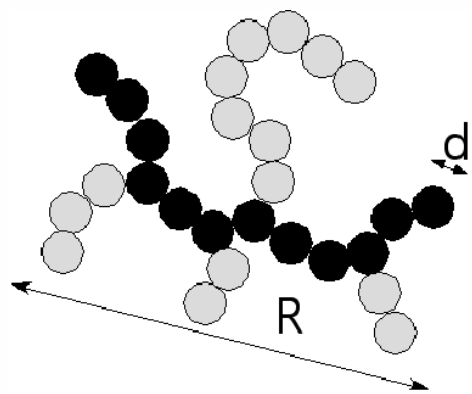

$$R_H \sim p^{1/d\min}$$

$$z \sim p^{c}$$

$$R_H \sim z^{cd\min} = z^{df}$$

At low z; $d_{\min} = 2$, $c = 1$; $d_f = d_{\min}c = 2$ (linear chain)
At high z; $d_{\min} \Rightarrow 1$, $c \Rightarrow 2$ or 3; $d_f = d_{\min}c \Rightarrow 2$ or 3
(highly branched chain or colloid)

$$[\eta] \sim M_{Molecule}^{\frac{3}{d_f}-1}$$

Branching and Intrinsic Viscosity

$$R^2_{g,b,M} \leq R^2_{g,l,M}$$

$$g = \frac{R^2_{g,b,M}}{R^2_{g,l,M}}$$

$$g = \frac{3f-2}{f^2}$$

$$g_\eta = \frac{[\eta]_{b,M}}{[\eta]_{l,M}} = g^{0.58} = \left(\frac{3f-2}{f^2}\right)^{0.58}$$

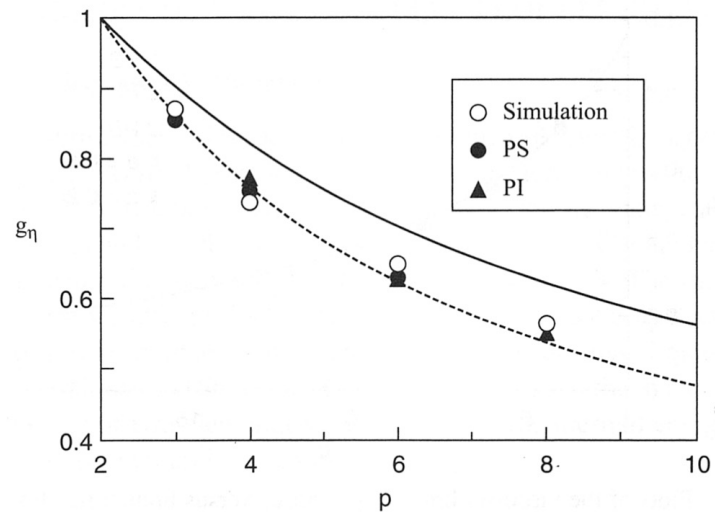

FIGURE 1.7 Plots of viscometric branching parameter, g_η, versus branch functionality, p, for star chains on a simple cubic lattice (unfilled circles), together with experimental data for star polymers in theta solvents: ●, polystyrene in cyclohexane; ▲, polyisoprene in dioxane. Solid and dashed lines represent calculated values via Eqs. (1.70) and (1.71), respectively. (Adapted from Shida et al. [2004].)

Keep in mind stars are a special case!

Utracki and Jamieson "Polymer Physics From Suspensions to Nanocomposites and Beyond" 2010 Chapter 1

Branching and Intrinsic Viscosity

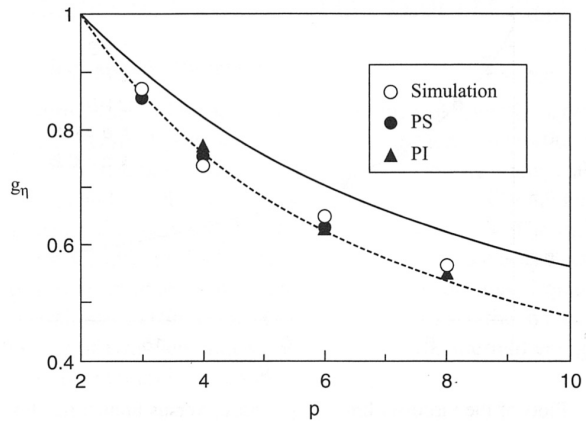

FIGURE 1.7 Plots of viscometric branching parameter, g_η, versus branch functionality, p, for star chains on a simple cubic lattice (unfilled circles), together with experimental data for star polymers in theta solvents: ●, polystyrene in cyclohexane; ▲, polyisoprene in dioxane. Solid and dashed lines represent calculated values via Eqs. (1.70) and (1.71), respectively. (Adapted from Shida et al. [2004].)

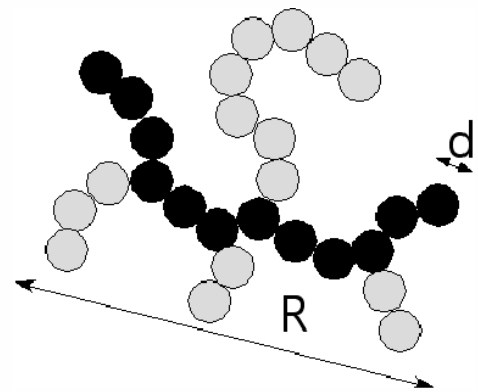

$$(R_{H,B}/ R_{H,L})^2 \sim z^{2(3/df,B - 3/df,L)}$$

This is still just looking at density! There is not topological information here which is critical to describe branching

Polyelectrolytes and Intrinsic Viscosity

Low Concentration

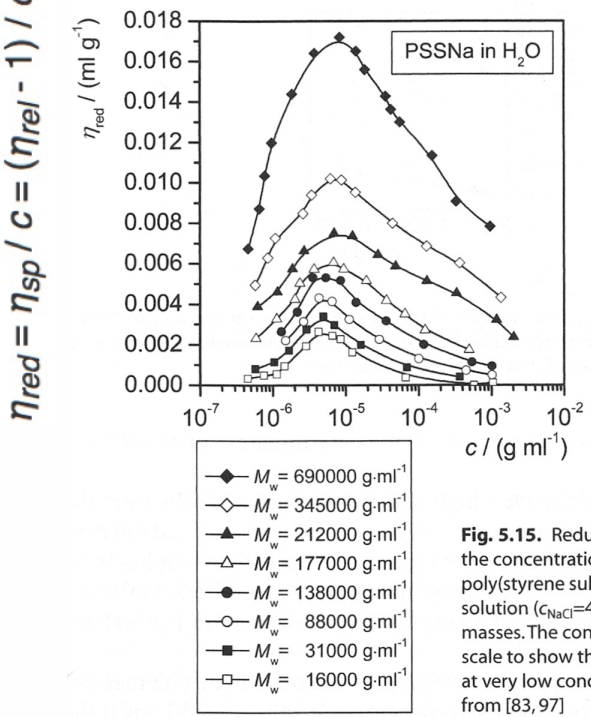

Fig. 5.15. Reduced viscosity η_{red} as a function of the concentration c for the polyelectrolyte sodium poly(styrene sulfonate) in nearly salt free aqueous solution (c_{NaCl}=4×10^{-6} mol l^{-1}) and for different molar masses. The concentration is plotted on a logarithmic scale to show the maximum behavior of the viscosity at very low concentrations of the polyelectrolyte. Data from [83, 97]

Very High Concentration

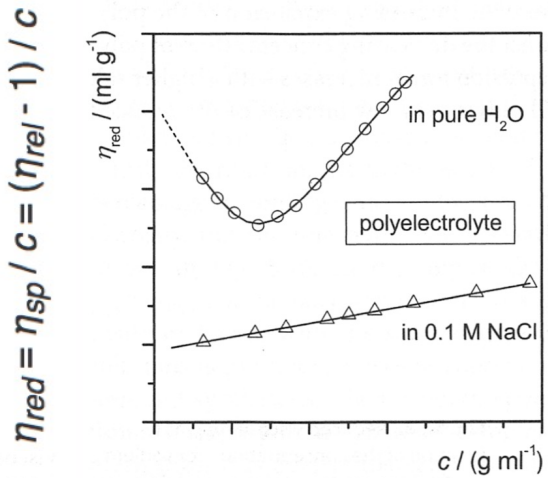

Fig. 5.16. Different behavior of a polyelectrolyte in aqueous solution and a salt solution. At high concentrations of the polyelectrolyte in aqueous solution is the concentration of counter ions inside the polymer coil higher than outside, leading to an expansion of the coil due to osmotic pressure. At low concentrations of the polyelectrolyte in aqueous solution, the polyelectrolyte is highly dissociated, leading to an expansion of the coil due to coulomb repulsion forces. Both expansion effects are compensated in the salt solution

Initially rod structures, increasing concentration
Followed by charge screening
Finally uncharged chains

Kulicke & Clasen "Viscosimetry of Polymers and Polyelectrolytes (2004)

Polyelectrolytes and Intrinsic Viscosity

$\eta_{sp} = (\eta - 1)/\eta_0$
$= \phi\,[\eta]$

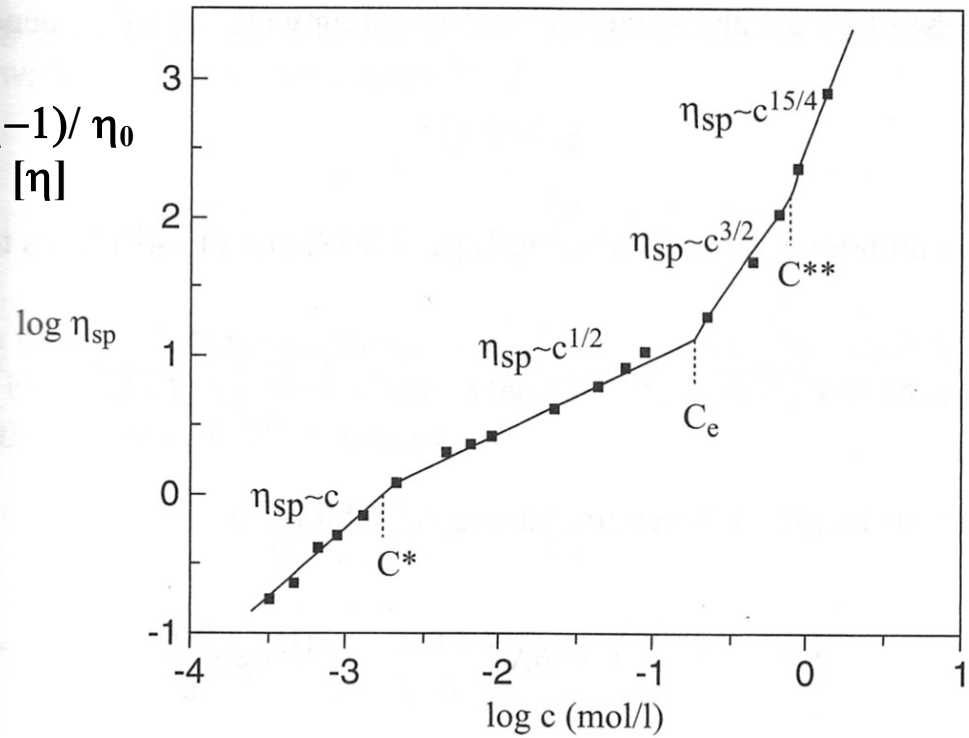

FIGURE 1.16 Determination of the chain overlap concentration c^*, the entanglement concentration c_e, the electrostatic blob overlap concentration c^{**} from the concentration dependence of specific viscosity for a 17%-quaternized P2VP copolymer (17PMVP-Cl) in solution in ethylene glycol at 25°C. Symbols are experimental data and solid lines represent the power laws predicted from scaling theory. (Adapted from Dou and Colby [2006].)

Kulicke & Clasen "Viscosimetry of Polymers and Polyelectrolytes (2004)

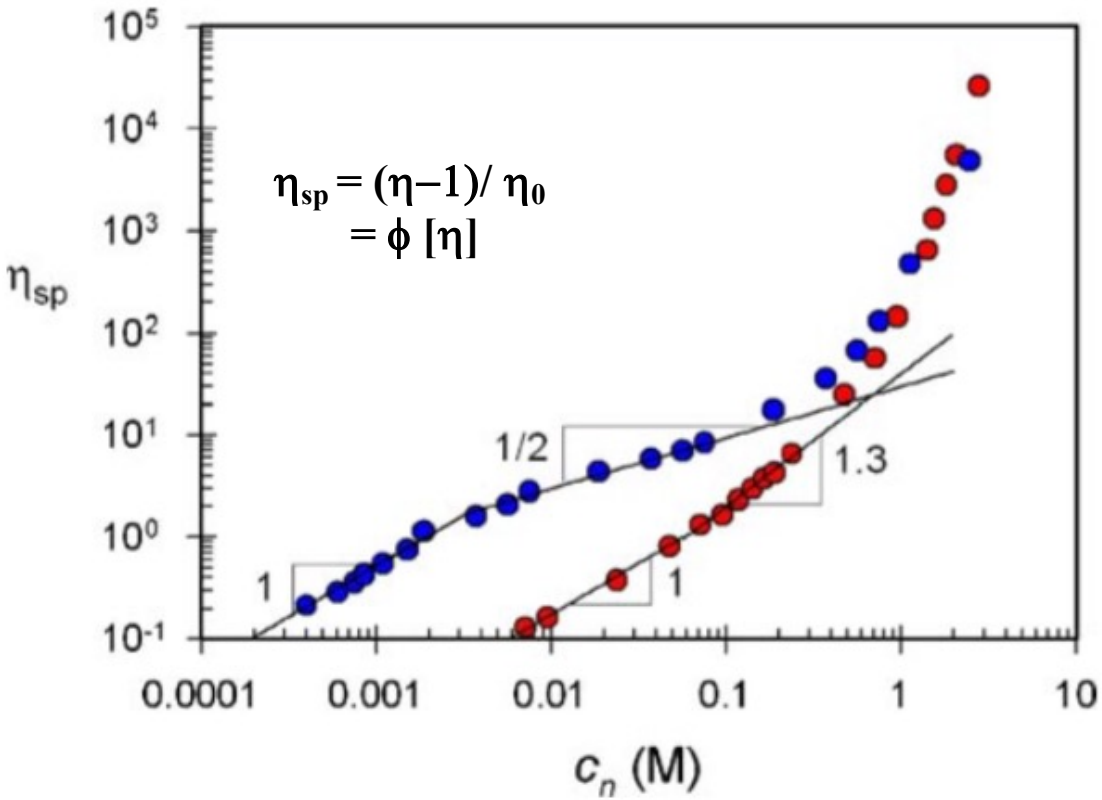

Fig. 10 Comparison of specific viscosity in the good solvent ethylene glycol of a neutral polymer (poly(2-vinyl pyridine), *red*) and the same polymer that has been 55% quaternized (poly(2-vinyl pyridine) chloride, *blue*; Dou and Colby 2006) plotted as functions of the number density of monomers with units of moles of monomer per liter. Slopes of unity for $\eta_{sp} < 1$ are expected by the Zimm model in dilute solution ($c < c^*$). Slopes of 1/2 and 1.3 for $1 < \eta_{sp} < 20$ are expected by the Rouse model for semidilute unentangled solutions of polyelectrolytes and neutral polymers, respectively. At higher concentrations, entangled solution viscosity data are shown that are consistent with the 3× larger slopes predicted for entangled solutions

Structure and linear viscoelasticity of flexible polymer solutions: comparison of polyelectrolyte and neutral polymer solutions

Ralph H. Colby

Rheol Acta (2010) 49:425–442

Hydrodynamic Radius from Dynamic Light Scattering

http://www.eng.uc.edu/~gbeaucag/Classes/Properties/HiemenzRajagopalanDLS.pdf

http://www.eng.uc.edu/~gbeaucag/Classes/Physics/DLS.pdf

http://www.eng.uc.edu/~gbeaucag/Classes/Properties/HydrodyamicRadius.pdf

Correlation Functions (Tadmor and Gogos pp. 381)

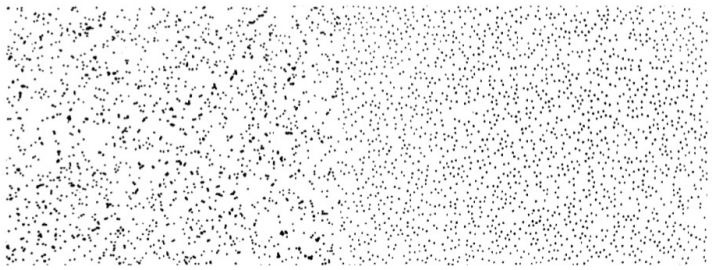

Fig. 7.32 The two textures (left field and right field) have the same first-order statistics (the same number of black dots), but they differ in second-order statistics. In the left field the dots fall at random, whereas in the right field there are at at least 10 dot diameters between dots. [Reprinted by permission from B. Julesz, "Experiments in the Visual Perception of Texture" *Sci. Am.*, **232**, 34 (1975).]

Let random variable I represents the gray levels of image region. The first-order histogram $P(I)$ is defined as:

$$P(I) = \frac{\text{number of pixels with gray level } I}{\text{total number of pixels in the region}} \tag{8}$$

Based on the definition of $P(I)$, the Mean m_1 and Central Moments μ_k of I are given by

$$m_1 = E\left[I^1\right] = \sum_{I=0}^{N_g-1} I^1 P(I) \tag{9}$$

$$\mu_k = E\left[\left(I - E[I]\right)^k\right] = \sum_{I=0}^{N_g-1} (I - m_1)^k P(I), \quad k = 2, 3, 4 \tag{10}$$

where N_g is the number of possible gray levels.

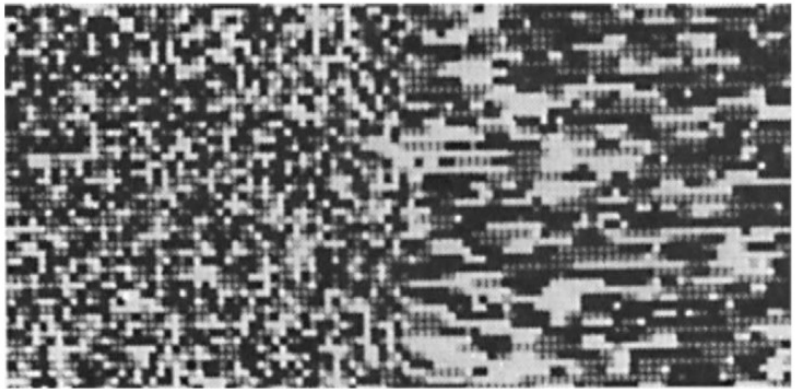

$P_{\theta,d}(I_1, I_2)$. It describes how frequently two pixels with gray-levels I_1, I_2 appear in the window separated by a distance d in direction θ. The information can be extracted from the co-occurrence matrix that measures second-order image statistics [17,24], where the pixels are considered in pairs. The co-occurrence matrix is a function of two parameters: relative distance measured in pixel numbers (d) and their relative orientation θ. The orientation θ is quantized in four directions that represent horizontal, diagonal, vertical and anti-diagonal by 0˚, 45˚ 90˚ and 135˚ respectively.

Fig. 7.33 The two textures (left field and right field) made of black, dark gray, light gray, and white squares have the same first-order statistics, but different second-order statistics, which appear as a difference in granularity. [Reprinted by permission from B. Julesz, "Experiments in the Visual Perception of Texture" *Sci. Am.*, **232**, 34 (1975).]

Journal of Signal and Information Processing, 2012, 3, 146-153
http://dx.doi.org/10.4236/jsip.2012.32019 Published Online May 2012 (http://www.SciRP.org/journal/jsip)

First and Second Order Statistics Features for Classification of Magnetic Resonance Brain Images

Namita Aggarwal, R. K. Agrawal

School of Computer and Systems Sciences, Jawaharlal Nehru University, New Delhi, India.
Email: namita_jnu@rediffmail.com, rkajnu@gmail.com

Correlation Functions (Tadmor and Gogos pp. 381)

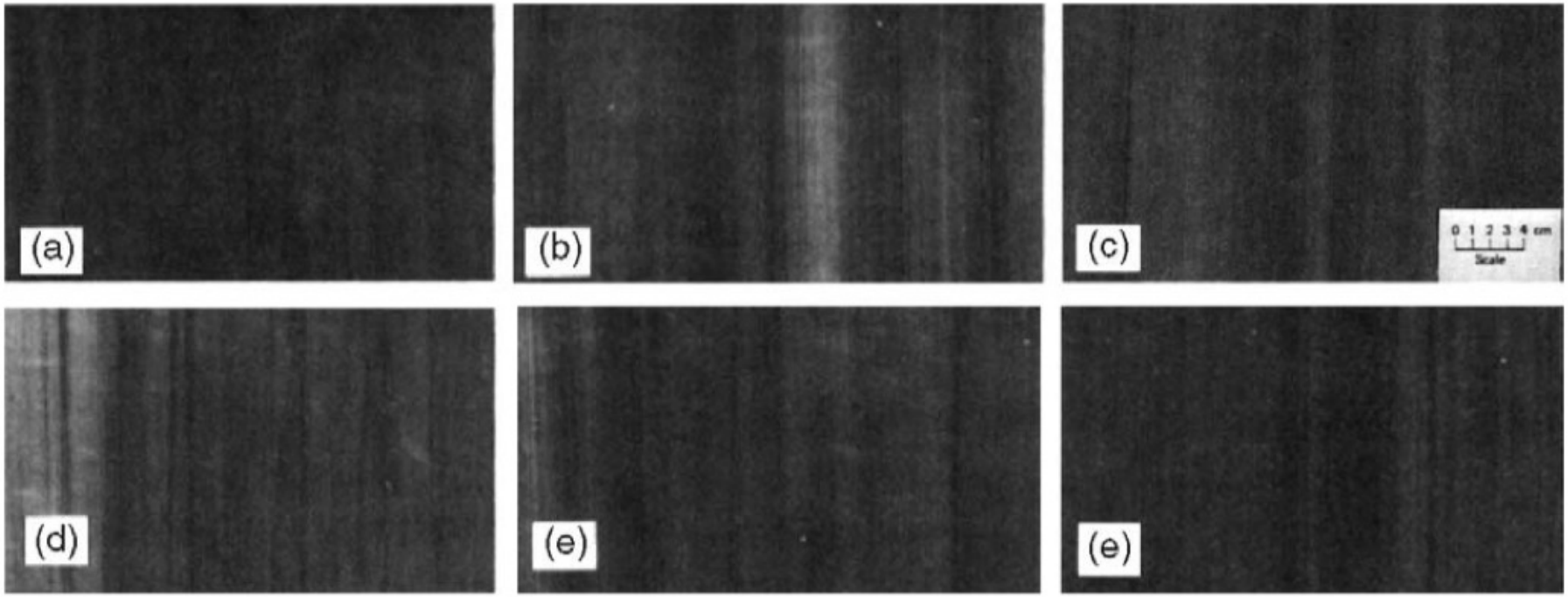

Fig. 7.34 Photographs of extruded LDPE films with carbon black concentrate extruded at various conditions. The barrel temperature (°C) and screw speed (rpm) are as follows: (a) 160°,40; (b) 160°, 60; (c) 160°, 80; (d) 180°,40; (e) 180°,60; (f) 180°, 80. [Reprinted by permission from N. Nadav and Z. Tadmor "Quantitative Characterization of Extruded Film Texture," *Chem. Eng. Sci.*, **28**, 2115 (1973).]

Correlation Functions (Tadmor and Gogos pp. 381)

Gross Uniformity: Gaussian distribution of samples, First order
Scale of Segregation: Second order

The Scale of Segregation

The *coefficient of correlation*, $R(r)$, measures the degree of correlation between the concentrations at two points separated by distance r. It is obtained by randomly "throwing" a dipole of length r, and is defined as follows:

0 to 1

$$R(r) = \frac{\sum_{i=1}^{N} (x_i' - \bar{x})(x_i'' - \bar{x})}{NS^2} \qquad (7.4\text{-}7) \qquad S^2 = \frac{\sum_{i=1}^{2N} (x_i - \bar{x})^2}{2N - 1}$$

Diffusion/Gradient
Non-reversible

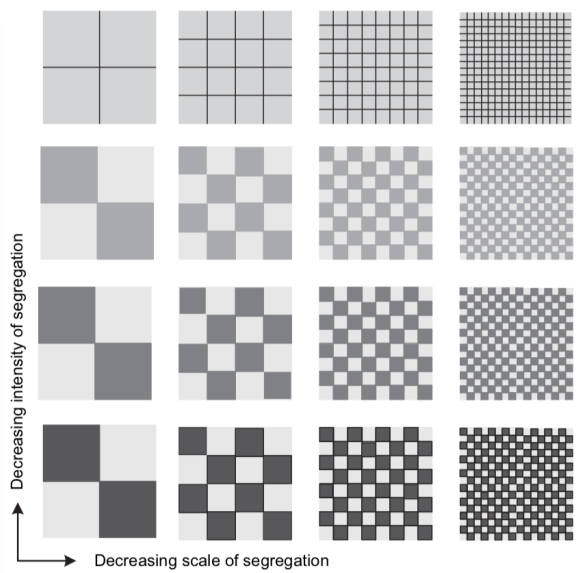

Fig. 7.36 Schematic representation of scale and intensity of segregation.

Shear strain
Reversible

$$\mathscr{s} = \int_0^{\zeta} R(r)\, dr$$

Scale of Segregation

Laminar Flow
Before/After

Correlation Functions (Tadmor and Gogos pp. 381)

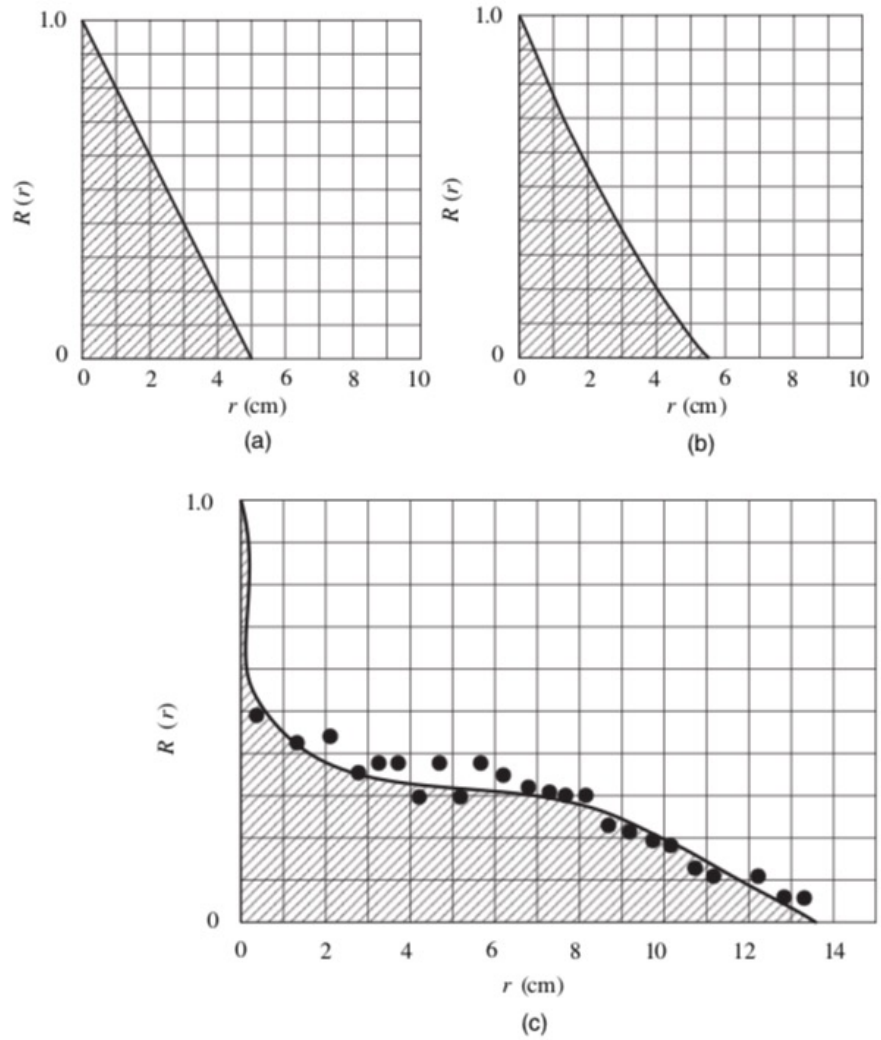

Fig. 7.37 Typical correlograms. (a) Along a line perpendicular to an equally spaced striped texture. (b) Over an area of a checkered board texture. (c) Along a line of an extruded film, as shown in Fig. 7.34, perpendicular to the extrusion direction.

Correlation Functions

DLS deals with a time correlation function at a given "q" = $2\pi/d$

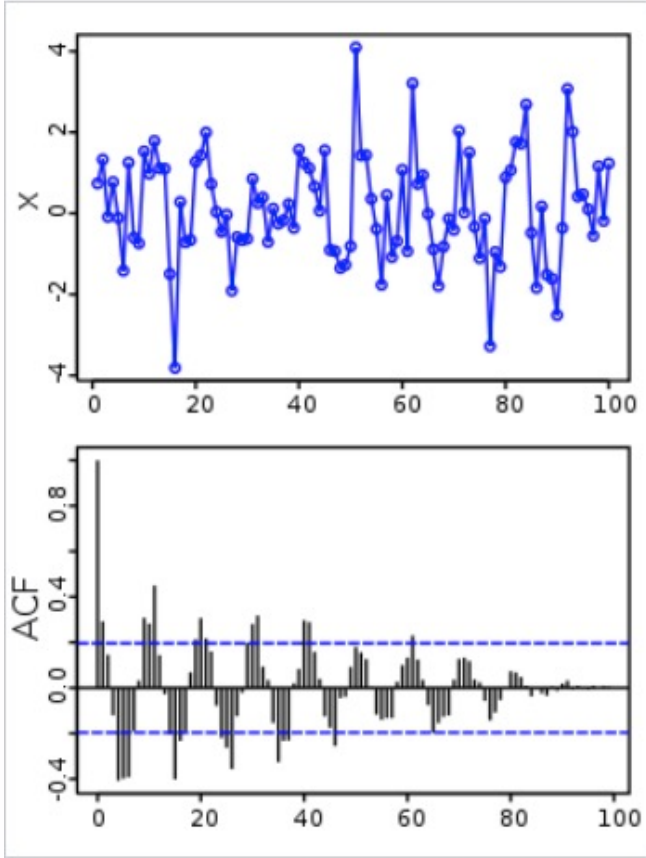

Above: A plot of a series of 100 random numbers concealing a sine function. Below: The sine function revealed in a correlogram produced by autocorrelation.

Paul Russo Lab

Dynamic Light Scattering

LSU

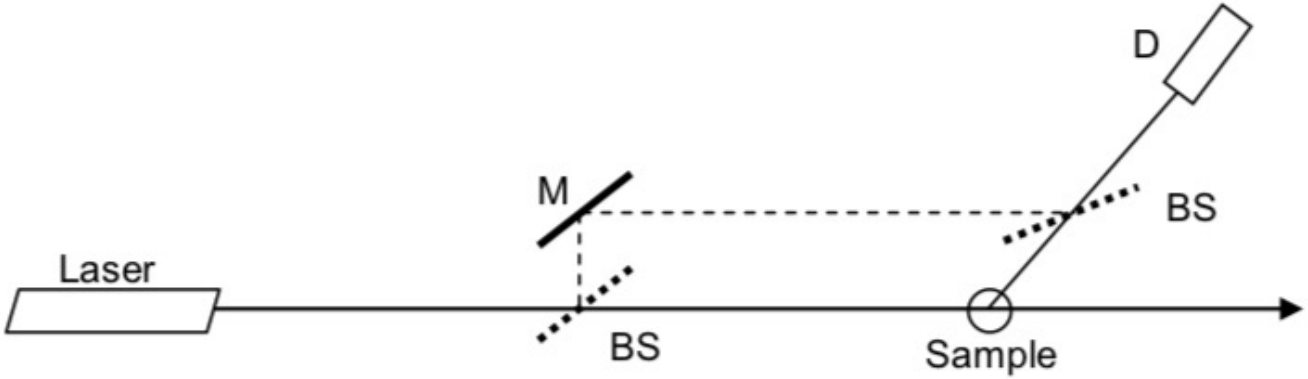

Figure 1. Heterodyne DLS apparatus. BS = beamsplitter; M = Mirror; D = detector. For a homodyne apparatus, just remove the two beamsplitters and mirror.

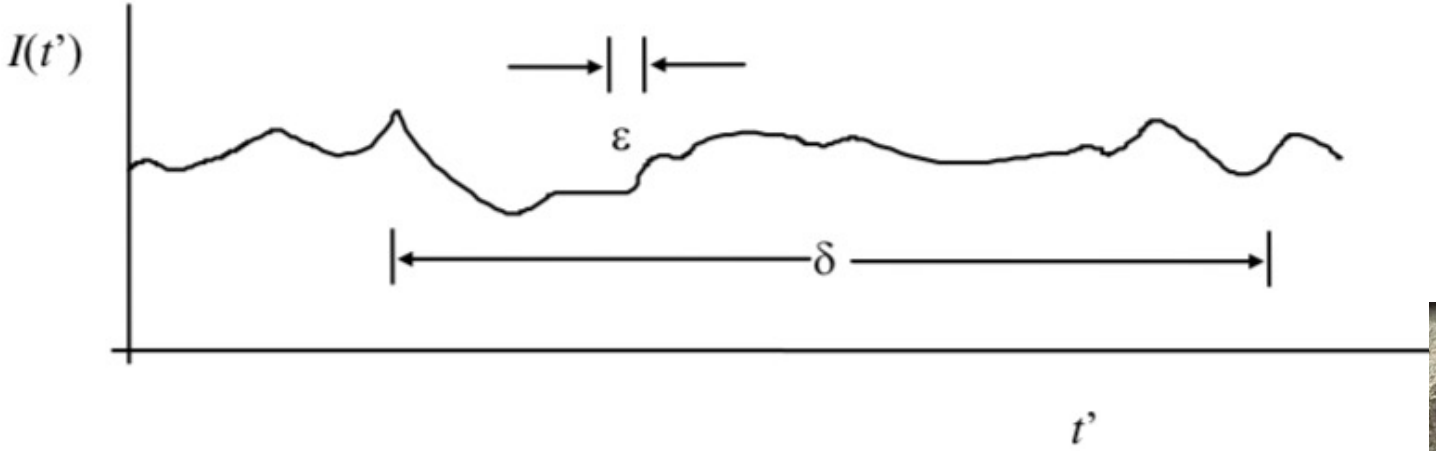

Figure 4. Intensity fluctuations are "random" on a time scale δ but "correlated" on a time scale ε.

Georgia Tech

Fick's Laws

$$J = -D\frac{d\varphi}{dx}$$

$$\frac{\partial\varphi}{\partial t} = D\,\frac{\partial^2\varphi}{\partial x^2} \qquad \varphi(x,t) = \frac{1}{\sqrt{4\pi Dt}}\exp\left(-\frac{x^2}{4Dt}\right)$$

Brownian Motion

$$\mathrm{MSD} \equiv \langle(\mathbf{x}-\mathbf{x_0})^2\rangle = 2nDt$$

Paul Russo Lab

$$G^{(2)}(t) = \langle I(0)I(t)\rangle = \lim_{T\to\infty} \frac{1}{2T}\int_{-T}^{T} I(t')\cdot I(t'+t)dt' \qquad \langle 1\rangle$$

Not normalized second order correlation function (capital G, normalized is small g)

After some time, the signal in the correlator is well approximated[2] by:

$$G^{(2)}(t) = B(1 + f|g^{(1)}(t)|^2) \qquad \langle 2\rangle$$

$$g^{(1)}(t) = e^{-\Gamma t} \qquad \langle 3\rangle$$

$$\Gamma = \tau^{-1} = q^2 D_m \qquad \langle 4\rangle \qquad \mathrm{MSD} = 2nDt$$

$$q = 4\pi\cdot n\cdot \sin(\theta/2)/\lambda_o \qquad \langle 5\rangle$$

Paul Russo Lab

$$g^{(2)}(t) = \frac{G^{(2)}(t)}{G^{(2)}(t=\infty)} = \frac{G^{(2)}(t)}{B}$$

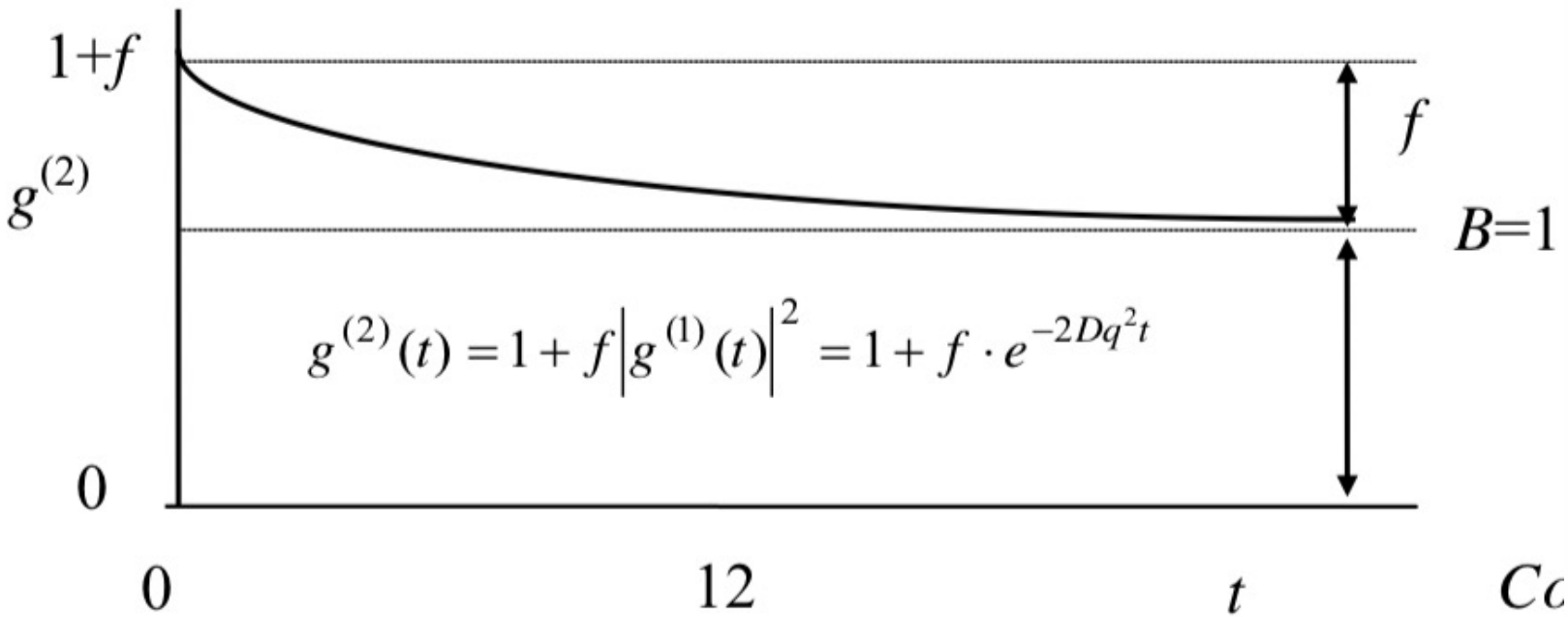

$$\sqrt{\frac{g^{(2)}(t)-1}{g^{(2)}(0)-1}} \equiv \sqrt{\frac{g^{(2)}(t)-1}{f}} \equiv g^{(1)}(t)\,. \qquad \text{<6.5>}$$

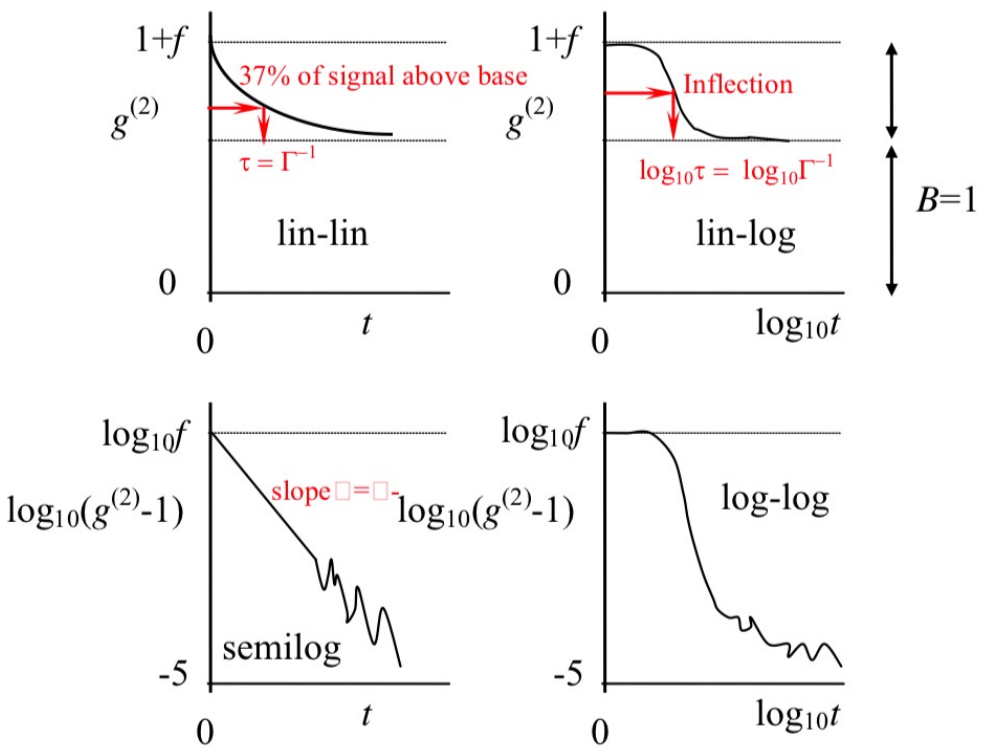

$$g^{(2)}(t) = 1 + f \cdot e^{-2Dq^2 t}$$

Figure 6. Various forms of autocorrelation function available

$$g^{(1)}(t) = e^{-\Gamma t} \qquad <3>$$

$$\Gamma = \tau^{-1} = q^2 D_m \qquad <4>$$

$$R_h = \frac{kT}{6\pi\eta_o D_o} \qquad <7>$$

What does R_h mean?

Sometimes newcomers to DLS do not know what R_h really means, so let's be very clear about that.

1. If your object is a solid sphere of radius R, then $R_h = R$.
2. If your object is spherical "bubble" (e.g., liposome) with *outer* radius R, then $R_h = R$ (exception: some liposomes may "wiggle" and that could alter R_h).
3. If your object is a sphere on the outside, but has inclusions of any shape inside, then R_h=R.
4. If your object has some other shape—such as cylinder, cube, polymer chain or star—then R_h is the radius of some hypothetical sphere that diffuses as fast as your object does.
5. If your object is a semidilute solution, gel, etc., all bets are off.

Paul Russo Lab

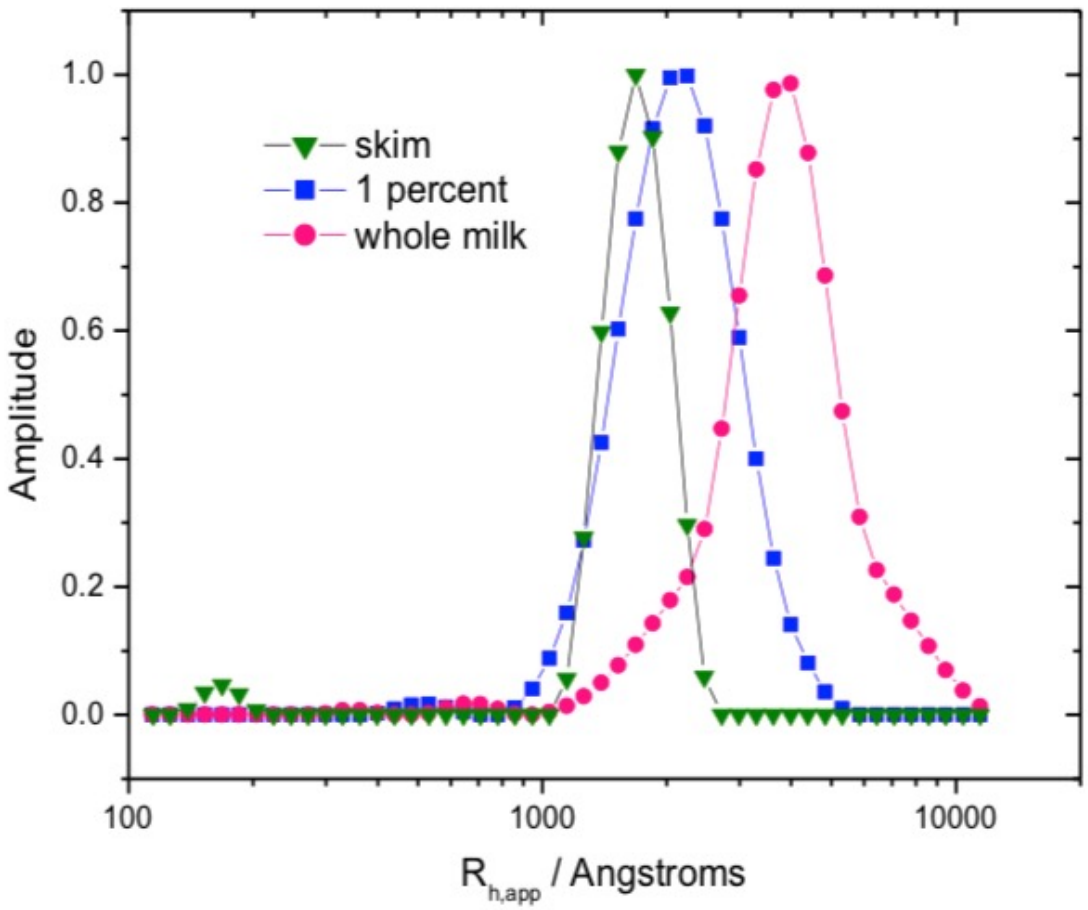

Consider motion of molecules or nanoparticles in solution

Particles move by Brownian Motion/Diffusion
The probability of finding a particle at a distance x from the starting point at t = 0 is a Gaussian Function that defines the diffusion Coefficient, D

$$\rho(x,t) = \frac{1}{(4\pi Dt)^{1/2}} e^{-x^2/2(2Dt)}$$

$$\langle x^2 \rangle = \sigma^2 = 2Dt$$

The Stokes-Einstein relationship states that D is related to R_H,

$$D = \frac{kT}{6\pi\eta R_H}$$

A laser beam hitting the solution will display a fluctuating scattered intensity at "q" that varies with q since the particles or molecules move in and out of the beam
I(q,t)
This fluctuation is related to the diffusion of the particles

Video of Speckle Pattern (http://www.youtube.com/watch?v=ow6F5HJhZo0)

For static scattering p(r) is the binary spatial auto-correlation function

We can also consider correlations in time, binary temporal correlation function
$g_1(q,\tau)$

For dynamics we consider a single value of q or r and watch how the intensity changes with time
$I(q,t)$

We consider correlation between intensities separated by t
We need to subtract the constant intensity due to scattering at different size scales
and consider only the fluctuations at a given size scale, r or $2\pi/r = q$

Dynamic Light Scattering

(http://www.eng.uc.edu/~gbeaucag/Classes/Physics/DLS.pdf)

$$I(\mathbf{R}, t) = Q_e\, \mathbf{E}_s^*(\mathbf{R}, t')^T \cdot \mathbf{E}_s(\mathbf{R}, t')$$

Q_e = quantum efficiency
$R = 2\pi/q$
E_s = amplitude of scattered wave

$$\langle I(\mathbf{R})\rangle = Q_e \langle \mathbf{E}_s^*(\mathbf{R}, t')^T \cdot \mathbf{E}_s(\mathbf{R}, t')\rangle$$

$$\langle I(0)I(t)\rangle = \langle I(0)^2\rangle + Q_e^2 \langle |\mathbf{E}^*(0)^T \cdot \mathbf{E}(t)|\, |\mathbf{E}^*(t)^T \cdot \mathbf{E}(0)|\rangle$$

If the intensity correlation function is normalized by $\langle I(0)^2\rangle$ the autocorrelation function results,

$$C(t) = \langle I(0)I(t)\rangle / \langle I(0)^2\rangle = 1 + K\, g^{(2)}(t)$$

where $g^{(2)}(t)$ is the square of the normalized autocorrelation function for electric field, $g^{(2)}(t) = |g^{(1)}(t)|^2$.

$$G_1(\mathbf{K}, t) = \langle (\Delta C(\mathbf{K}, 0))^2\rangle \exp(-D_m K^2 t)$$

$$g^{(1)}(t) = g^{(1)}(\mathbf{K}, t) = \exp(-D_m K^2 t)$$

q or K squared since size scales with the square root of time $\langle x^2\rangle = \sigma^2 = 2Dt$

Dynamic Light Scattering

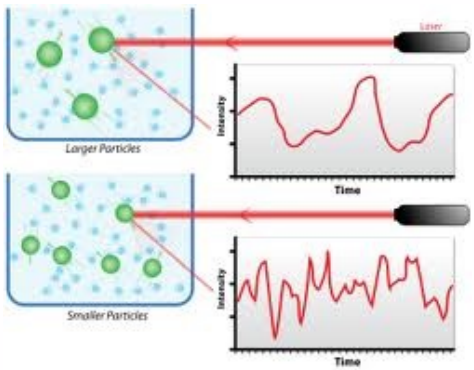

$$g^2(q;\tau) = \frac{\langle I(t)I(t+\tau)\rangle}{\langle I(t)\rangle^2}$$

$$g^2(q;\tau) = 1 + \beta\left[g^1(q;\tau)\right]^2$$

$$q = \frac{4\pi n_0}{\lambda}\sin\left(\frac{\theta}{2}\right)$$

$$g^1(q;\tau) = \exp(-\Gamma\tau)$$

$$\Gamma = q^2 D_t$$

$$D = k_B T / 6\pi\eta a$$

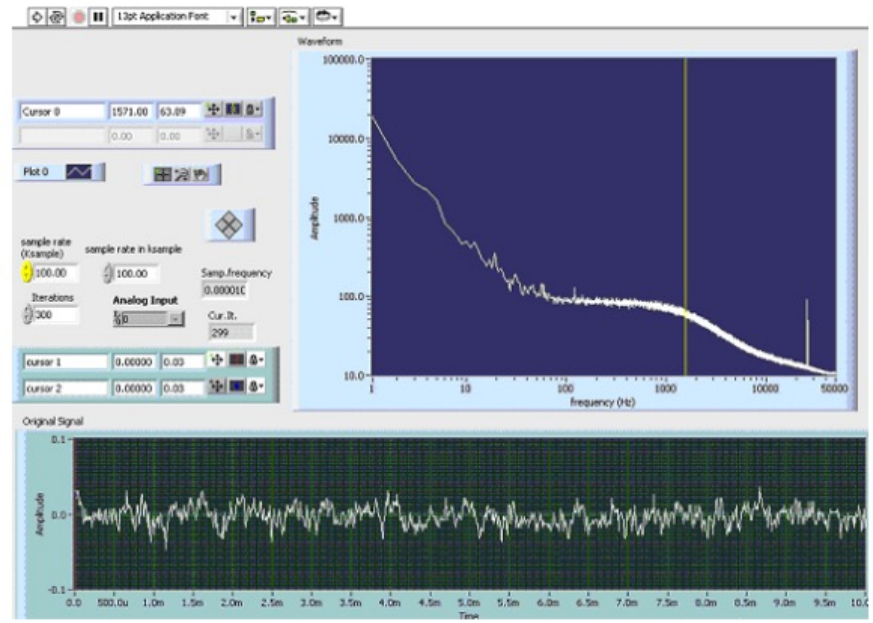

$a = R_H$ = Hydrodynamic Radius

The radius of an equivalent sphere following Stokes' Law

Dynamic Light Scattering

my DLS web page

http://www.eng.uc.edu/~gbeaucag/Classes/Physics/DLS.pdf

Wiki

https://en.wikipedia.org/wiki/Dynamic_light_scattering

Wiki Einstein Stokes

http://webcache.googleusercontent.com/search?q=cache:yZDPRbqZ1BIJ:en.wikipedia.org/wiki/Einstein_relation_(kinetic_theory)+&cd=1&hl=en&ct=clnk&gl=us

Diffusing Wave Spectroscopy (DWS)
(Passive Microrheology (there are also Two Point and Active MR))

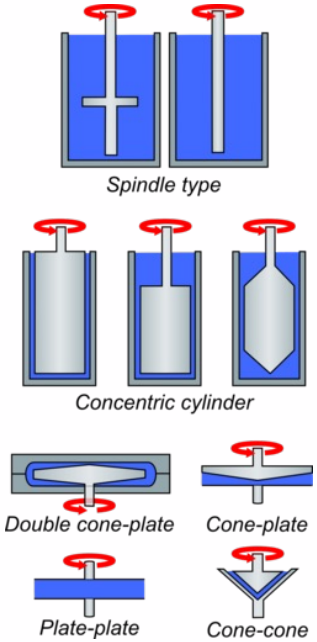

Traditional Rheology: Place a fluid in a shear field, measure torque/force and displacement

Microrheology: Observe the motion of a tracer.
Two types, passive or active microrheology. DWS is passive.

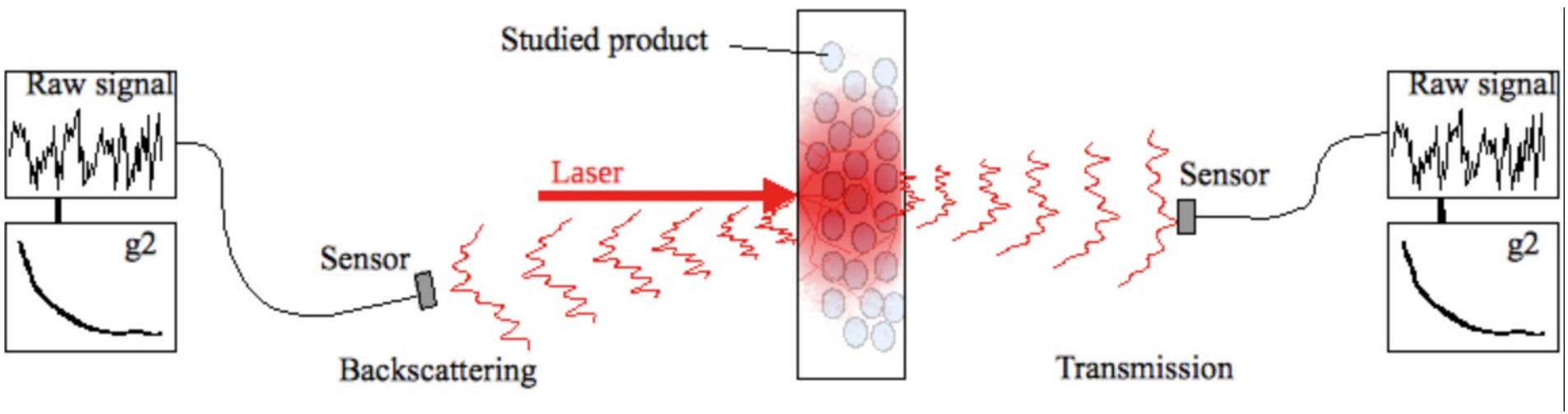

Diffusing Wave Spectroscopy (DWS)

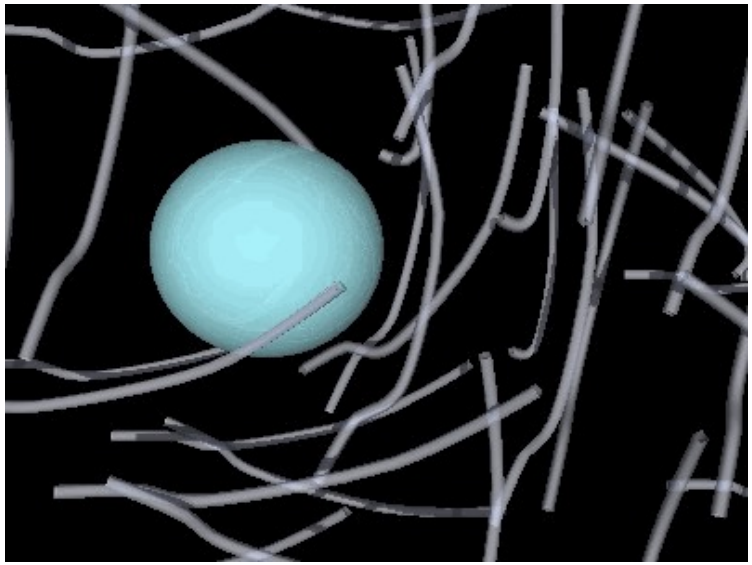

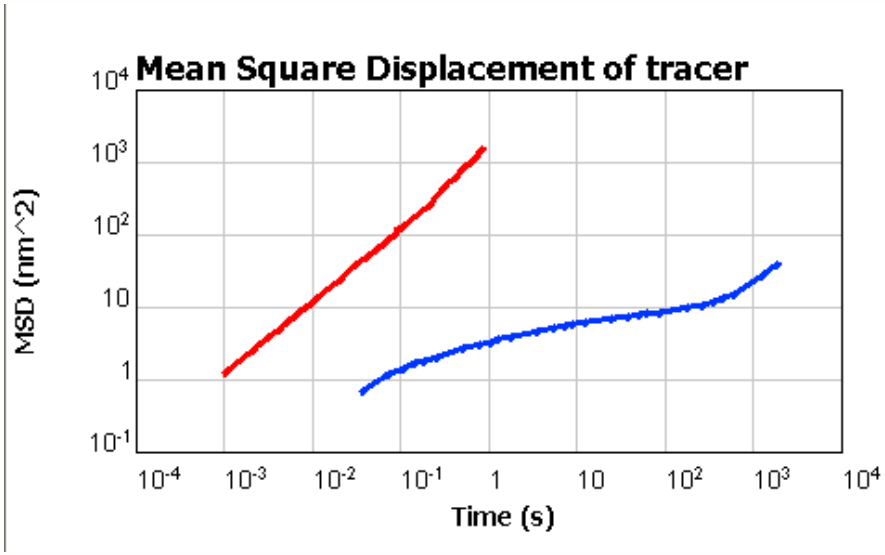

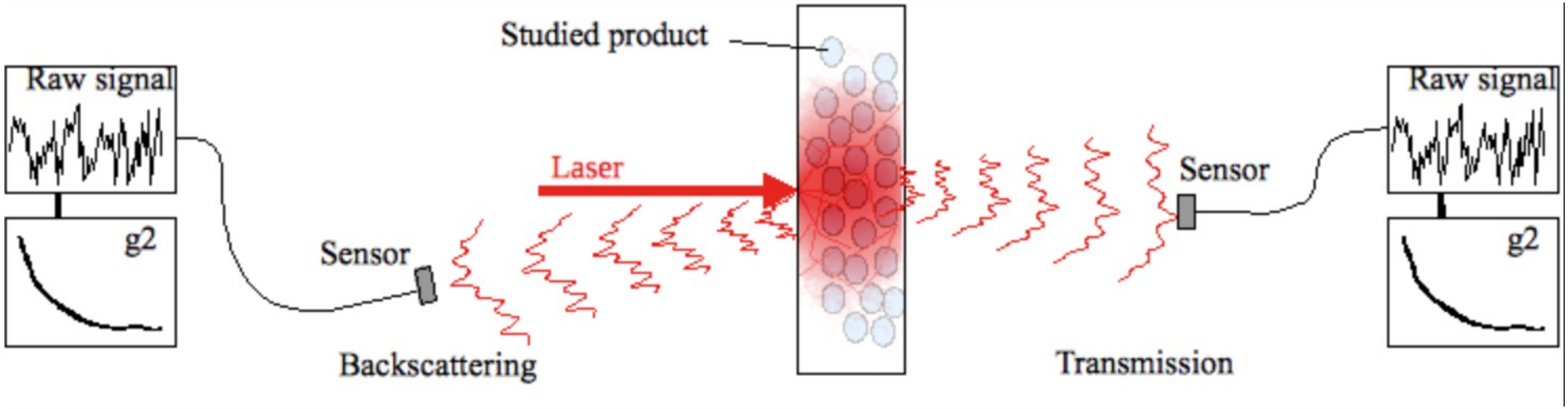

Diffusing Wave Spectroscopy (DWS)

Viscous Motion $< \Delta r^2 >= 4Dt$

Elastic Motion $< \Delta r^2 >= Const$

$$G(\omega) = G'(\omega) + iG''(\omega)$$

$$\tilde{G}(s) = \frac{k_B T}{\pi a s \langle \Delta \tilde{r}^2(s) \rangle}$$

$\tilde{G}(s)$: Laplace transform of G

k_B: Boltzmann constant

T: temperature in kelvins

s: the Laplace frequency

a: the radius of the tracer

$\langle \Delta \tilde{r}^2(s) \rangle$: the Laplace transform of the mean squared displacement

$$F(s) = \int_0^\infty f(t) e^{-st}\, dt \quad \text{(Eq.1)}$$

Diffusing Wave Spectroscopy (DWS)

$$G(\omega) = G'(\omega) + iG''(\omega)$$

$$\tilde{G}(s) = \frac{k_{\mathrm{B}}T}{\pi a s \langle \Delta \tilde{r}^2(s) \rangle}$$

$$g_2(\tau) - 1 = [\int ds P(s) \exp(-(s/l*) k_0^2 \langle \Delta r^2(\tau) \rangle)]^2$$

For back scatter: $$g_2(\tau) - 1 = \exp\left(-2\gamma\sqrt{\langle \Delta r^2(\tau) \rangle k_0^2}\right)$$

Diffusing Wave Spectroscopy (DWS)

$$G(\omega) = G'(\omega) + iG''(\omega)$$

$$k_B T$$

$$g_2(\tau)$$

$$\tau)\rangle)]^2$$

For ba

$$(\tau)\rangle k_0^2\Big)$$

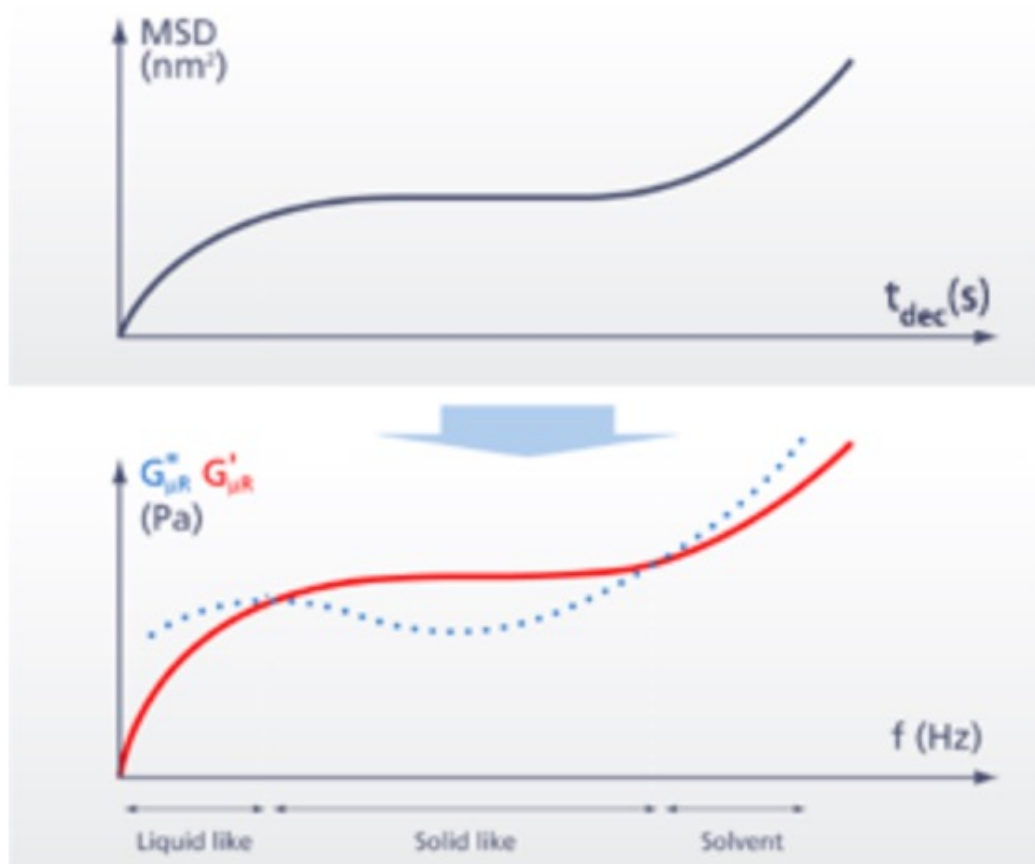

Link rheology to micelle structure

Ron Larson/Mike Weaver

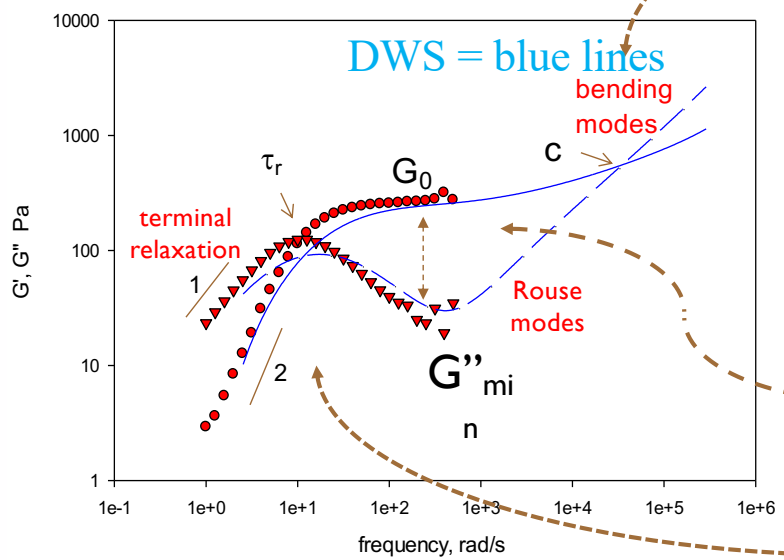

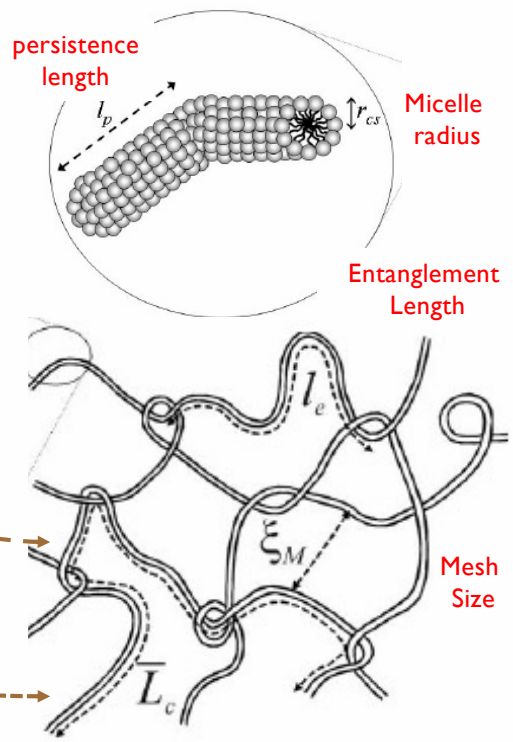

Structure inferred from rheology, using Standard Cates Model and newer developments (Larson group, others…)

Beth Schubert, 2003

Two-point Micro Rheology

A different microrheological approach studies the cross-correlation of two tracers in the same sample. In practice, instead of measuring the MSD $\langle \Delta r^2 \rangle$, movements of two distinct particles are measured - $\langle \Delta r_1 \Delta r_2 \rangle$. Calculating the G(ω) of the medium between the tracers follows:

$$\tilde{G}(s) = \frac{k_{\mathrm{B}} T}{2\pi R s \langle \Delta \tilde{r}_1(s) \Delta \tilde{r}_2(s) \rangle}$$

Notice this equation does not depend on **a**, but instead in depends on **R** - the distance between the tracers (assuming R>>a).

Active Micro Rheology

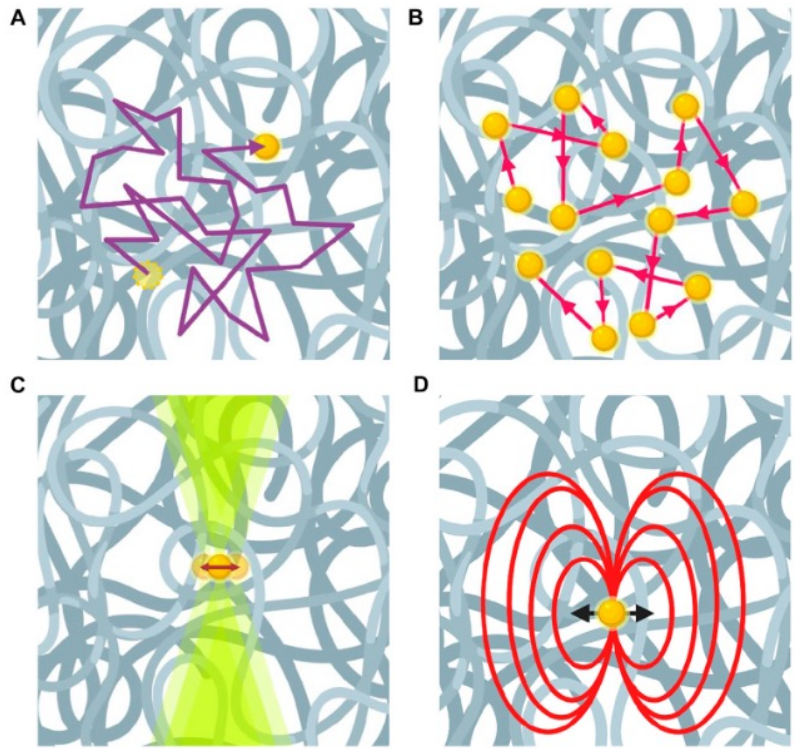

FIGURE 2 | Microrheology using different techniques for passive and active measurements. **(A)** Video particle tracking technique visually tracks the trajectories of probe particles. **(B)** Multiple-scattered laser in diffusing wave spectroscopy experiment reflect Brownian motion of probe particles. **(C)** Optical tweezers measure the force and displacement on a probe particle. **(D)** Magnetic field exerted on a probe particle by magnetic tweezers.

Quasi-Elastic Neutron (and X-ray) Scattering

In the early days of DLS there were two approaches:

Laser light flickers creating a speckle pattern that can be analyzed in the time domain
The flickering is related to the diffusion coefficient through an exponential decay of the time correlation function

A more direct method is to take advantage of the Doppler effect. Train whistle appears to change pitch as the train passes since the speed of the train is close to $1/\omega$ for the sound
If we know the frequency of the sound, we can determine the speed of the train
Measuring the spectrum from a laser, and the broadening of this spectrum after interaction with particles the diffusion coefficient can be determined from an exponential decay in the frequency, peak broadening. This is called quasi-elastic light scattering and measures the same thing as DLS by a different method.

For Neutrons and X-rays the time involved is too fast for correlators, pico- to nanoseconds. But line broadening can be observed (though **there are no X-ray or neutron lasers** i.e., monochromatic and columnated).

https://neutrons.ornl.gov/sites/default/files/QENSlectureNXS2019.pdf

Neutron and X-ray “Lasers”

For X-rays a synchrotron with an undulator insertion device can produce close to monochromatic and fairly coherent radiation. NSLS II Brookhaven National Laboratory near Stony Brook, Long Island NY (near NYC)

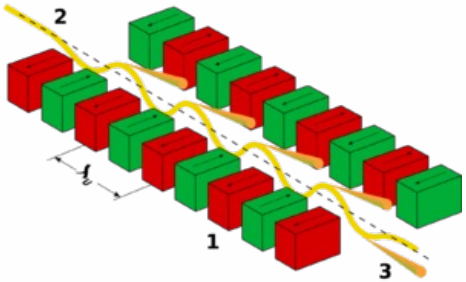

Neutron and X-ray “Lasers”

For neutrons, a spallation source with a time-of-flight detection system or a reactor with a velocity selector can result in a reasonably coherent and monochromatic (spectral in time) beam. SNS at Oak Ridge National Laboratory, Tennessee (near Knoxville) and NCNR at NIST Gaithersburg MD (near Washington DC).

Quasi Elastic Neutron Scattering QENS

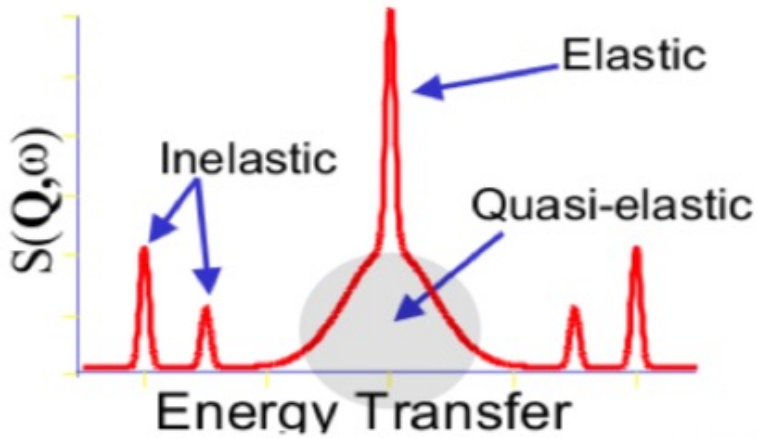

- Quasi elastic neutron scattering is a limiting case of inelastic neutron scattering
- Doppler type of broadening of the elastic line due to a small energy transfer between the neutrons and the atoms in the sample

What is QENS used for

Probes slow dynamics

- Translational diffusion
- Molecular reorientations
- Relaxation processes

Applicable to wide range of scientific topics

- ***Materials science***: fuel cells, batteries, hydrogen storage,
- ***Soft Matter***: polymer nanocomposites and blends, organic photovoltaics, polymer electrolytes
- ***Biology***: hydration water, dynamics of proteins
- ***Chemistry***: water interfaces, ionic liquids, clays, porous media, complex fluids, surface interactions

Results are comparable to Molecular Dynamics simulations

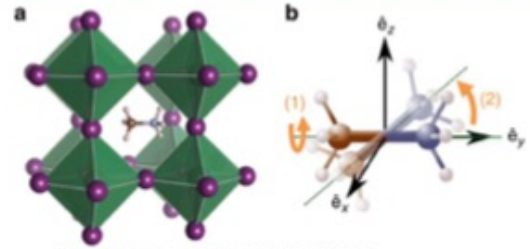

Nature Communications 6, 7124 (2015)

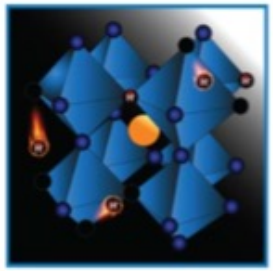

Journal of Physical Chemistry C, 123, 2019 (2019).

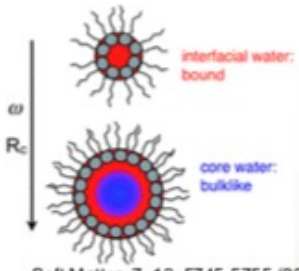

Soft Matter, 7, 12, 5745-5755 (2011)

OAK RIDGE National Laboratory

QENS spectra

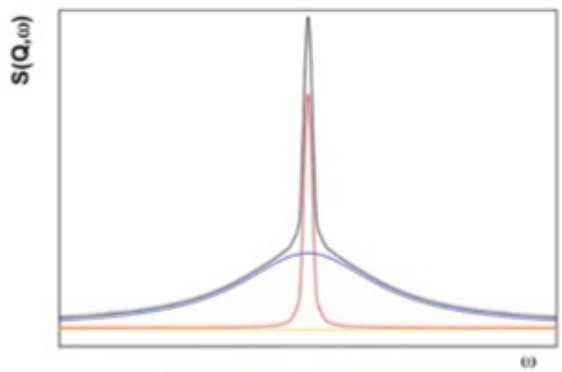

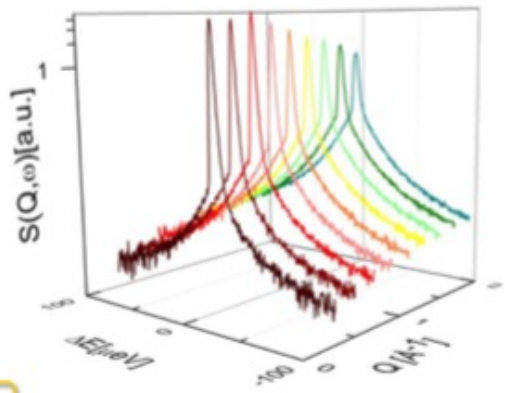

$$S(Q,\omega) = p_0\delta(\omega) + \sum_{i=1}^{n} p_i \frac{1}{\pi}\frac{\Delta_i(Q)}{\omega^2+\Delta_i^2} + B$$

Dynamic scattering function provides information on the sample states

Elastic intensity → Debye-Waller factor: Vibrational amplitudes

Quasielastic intensity → A_0 = EISF (ratio elastic/total): Geometry of motion

Quasielastic broadening → Width: Characteristic time scale / diffusion

The SNS Inelastic Instrument Suite

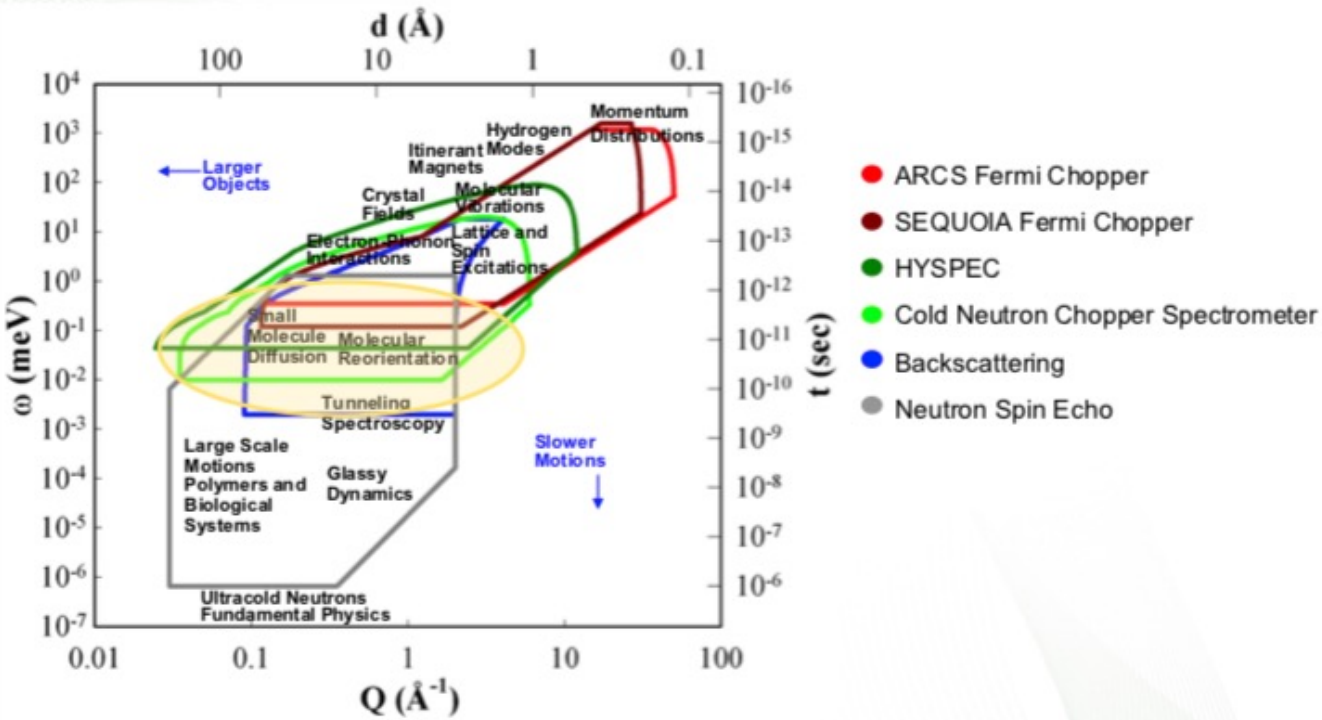

11 Presentation_name

OAK RIDGE National Laboratory

Science Example 1: Molecular Reorientation

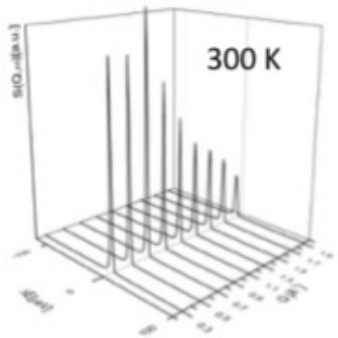

Octamethyl POSS @ BASIS

$$S(Q,\omega) = f\left[p_0\delta(\omega) + \sum_{i=1}^{n} p_i \frac{1}{\pi}\frac{\Delta_i(Q)}{\omega^2+\Delta_i^2}\right] \otimes R(Q,\omega) + B$$

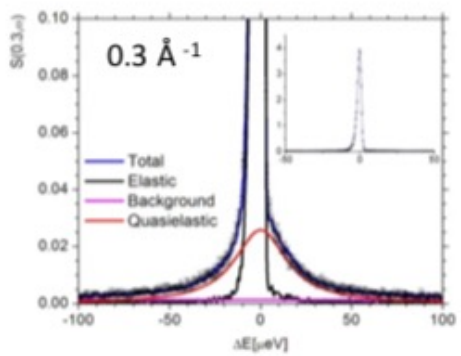

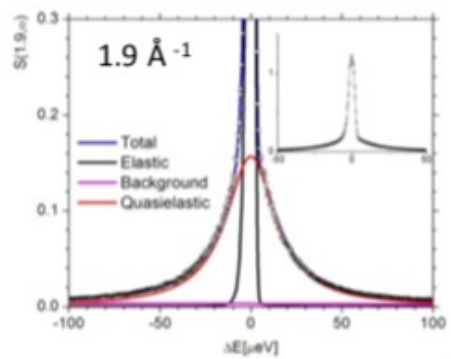

Jalarvo N., *et al*, *Journal of Physical Chemistry C*, **118**, 10, 5579-5592 (2014)

OAK RIDGE National Laboratory

Science Example 1: Molecular Reorientation

- Polyoligosilsesquioxane Ligand Dynamics
- How do ligand dynamics contribute to the functionalities of POSS?

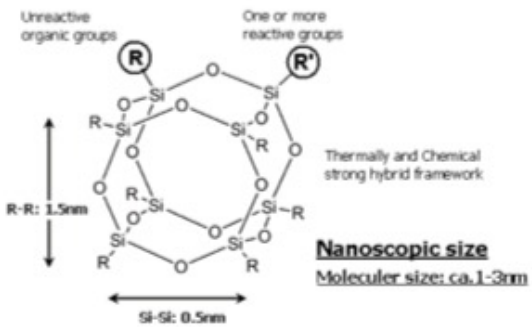

Nanoscopic size

Moleculer size: ca.1-3nm

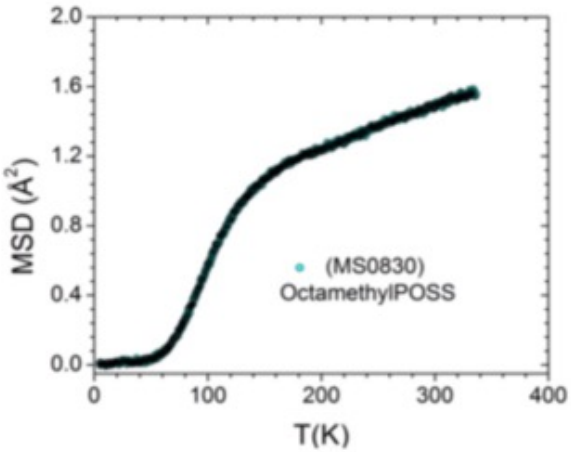

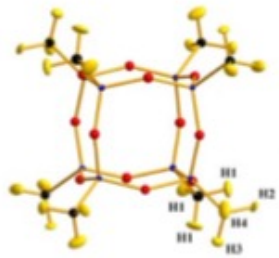

Jalarvo N., *et al*, *Journal of Physical Chemistry C*, **118**, 10, 5579-5592 (2014)

OAK RIDGE National Laboratory

Science Example 3: Water Dynamics in Anion Exchange Membranes Studied by QENS

- Ionic conductivity and water transport are key properties for applications
  - Depends on water content
- Water transport in AEM multiscale problem
  - Investigation of transport in multiple time- and length scales for structure – function insight

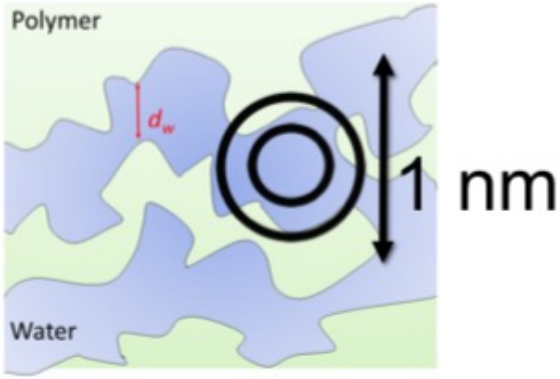

J. Melchior, *et al*, Journal of Membrane Science 586, Pages 240-247 (2019)

OAK RIDGE National Laboratory

Science Example 3: Water Dynamics in Anion Exchange Membranes Studied by QENS

TOFTOF: time-of-flight spectrometer

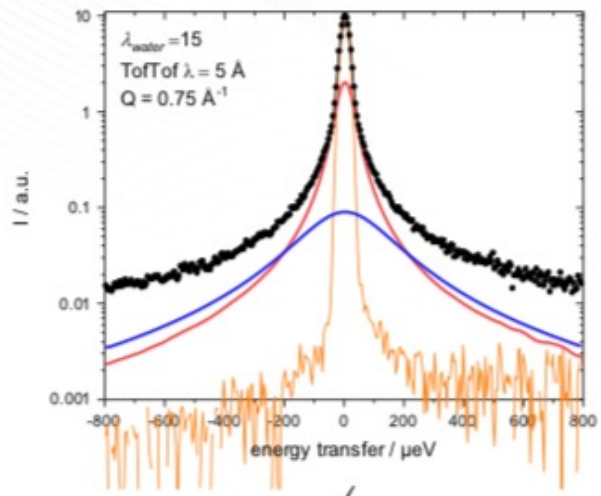

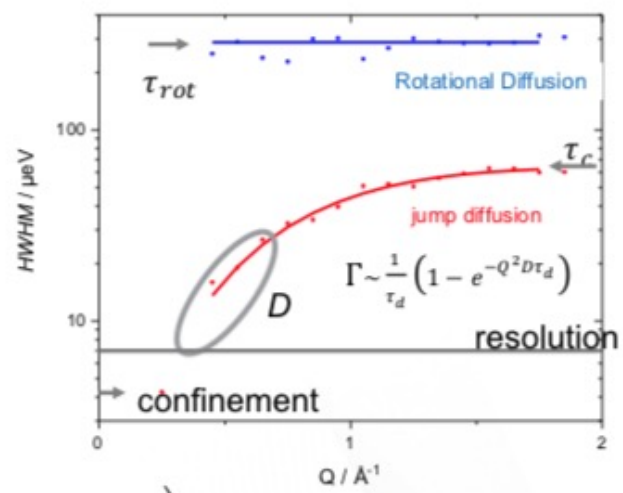

$$S(Q,\omega) = f\left(a_0(Q)\delta + \sum_n \frac{a_n(Q)}{\pi}\left(\frac{\Gamma}{\omega^2+\Gamma^2}\right)\right) \otimes Res + Backg$$

J. Melchior, *et al*, Journal of Membrane Science 586, Pages 240-247 (2019)

OAK RIDGE National Laboratory

Science Example 3: Water Dynamics in Anion Exchange Membranes Studied by QENS

$$\Gamma \sim \frac{1}{\tau_d}\left(1 - e^{-Q^2 D \tau_d}\right)$$

SPHERES: high-resolution backscattering spectrometer

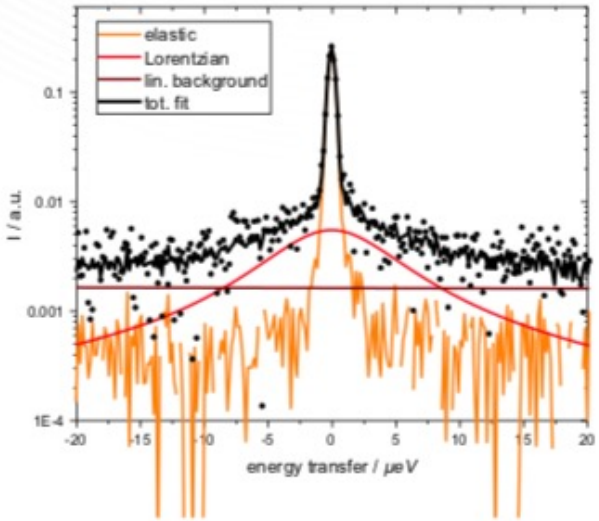

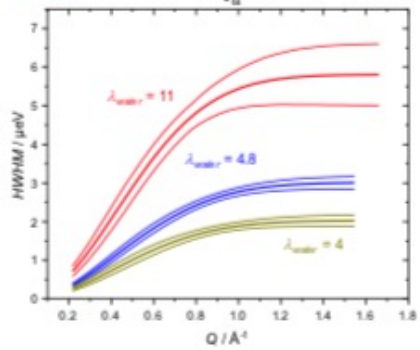

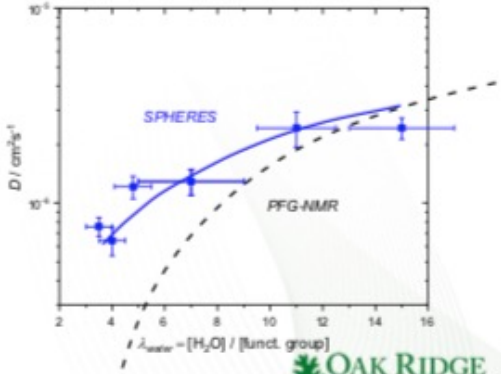

J. Melchior, *et al*, Journal of Membrane Science 586, Pages 240-247 (2019)

OAK RIDGE National Laboratory

Science Example 3: Water Dynamics in Anion Exchange Membranes Studied by QENS

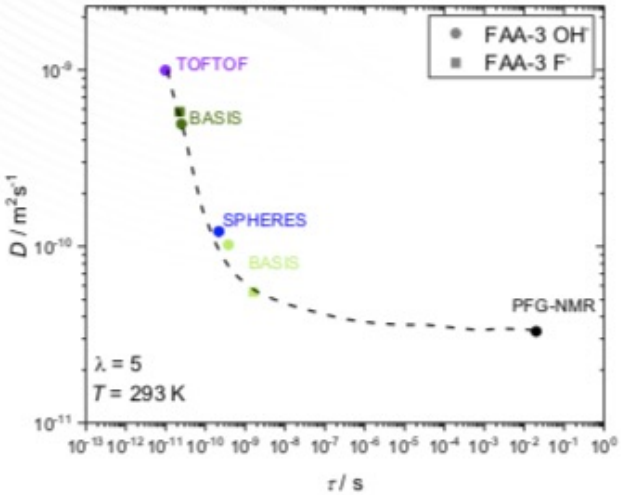

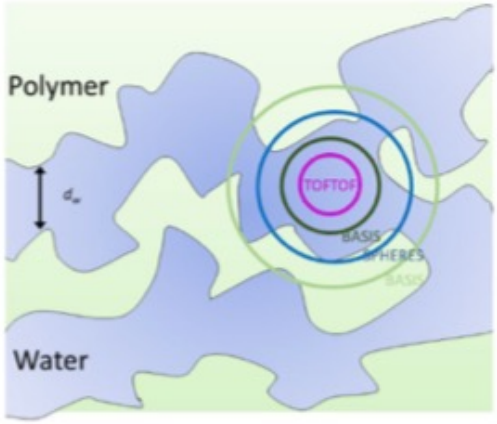

J. Melchior, *et al*, Journal of Membrane Science 586, Pages 240-247 (2019)

OAK RIDGE National Laboratory

R_g/R_H Ratio

R_g reflects spatial distribution of structure

R_H reflects dynamic response, drag coefficient in terms of an equivalent sphere

While both depend on "size" they have different dependencies on the details of structure

If the structure remains the same and only the amount or mass changes the ratio between these parameters remains constant. So the ratio describes, in someway, the structural connectivity, that is, how the structure is put together.

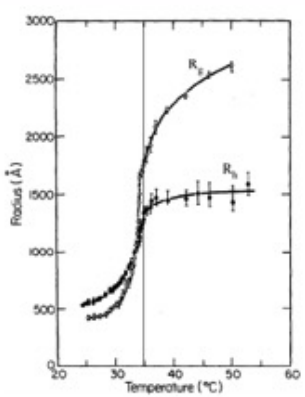

This can also be considered in the context of the "universal constant"

$$[\eta] = \Phi \frac{R_g^3}{M}$$

Lederer A et al. Angewandte Chemi 52 4659 (2013).
(http://www.eng.uc.edu/~gbeaucag/Classes/Properties/DresdenRgbyRh4659_ftp.pdf)

R_g/R_H Ratio

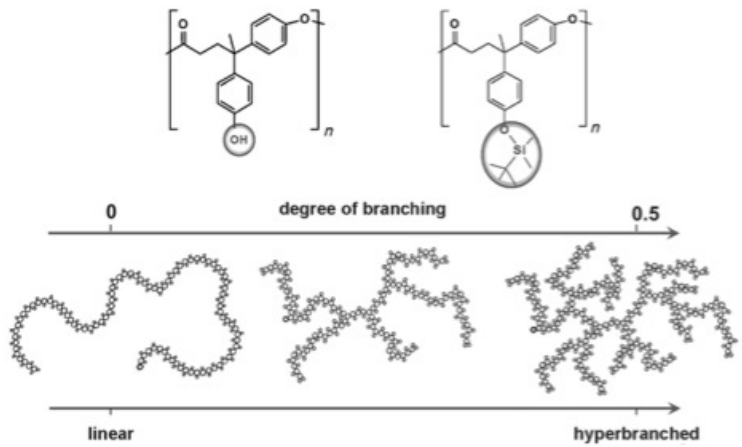

Scheme 1. Variation of the branching degree from linear to hyperbranched structures for polyesters with different functional groups.

$$\rho \equiv \frac{R_g}{R_h}$$

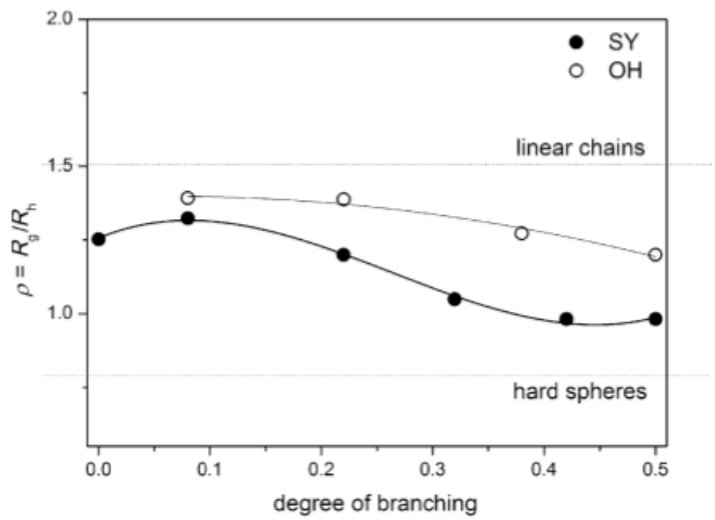

Figure 1. Dependence of the branching parameter ρ on the degree of branching for SY- and OH-terminated samples. The lines correspond to tentative fits to the measurement points.

$$\mathrm{DB} = \frac{D+T}{D+L+T} \qquad (1)$$

where D, T and L are the fractions of dendritic, terminal or linearly incorporated monomers in the resulting hyperbranched polymers obtained from integration of the respective signals in NMR-spectra. The values commonly reported for DB are in the range of 0.4 to 0.8. Equation (1) has been used

Acta Polymer., *48*, 30–35 (1997)

Lederer A et al. Angewandte Chemi 52 4659 (2013).
(http://www.eng.uc.edu/~gbeaucag/Classes/Properties/DresdenRgbyRh4659_ftp.pdf)

R_g/R_H Ratio

Table III
ρ Factor and Molecular Polydispersity P_w/P_n for Some Selected Models[a]

model		ρ	P_w/P_n
linear chains			
monodisperse	1.5	$8/3\pi^{1/2}$	1
polydisperse ($m = 1$)		$3^{1/2}$	2
polydisperse (m coupled chains)		$\frac{(m+2)^{1/2}}{m+1} 2\Sigma\left(1 + \frac{k-1}{m}\right)c(k)$	$1 + (1/m)$
star molecules			
regular stars		$\left(\frac{3f-2}{f\pi}\right)^{1/2} \frac{8}{3} \frac{(2-f) + 2^{1/2}(f-1)}{f}$	1
polydisperse stars		$\left(\frac{6f}{f+1}\right)^{1/2} \frac{f+3}{2(f+1)}$	$1 + (1/f)$
polycondensates			
A_f type	1.73	$3^{1/2}$	$P_w\left(1 - \frac{f}{2(f-1)}\right)$
ABC type		$\left(\frac{3}{4}\frac{1+2B}{1+B}\right)^{1/2}\left(\frac{2+B}{1+B}\right)$	$2(1+B)$
randomly cross-linked chains (polydisperse ($m = 1$) primary chains)		$3^{1/2}$	$2(P_w/P_w p)$
monodisperse spheres	0.77	$(^3/_5)^{1/2}$	1

[a] $\rho = \langle 1/R\rangle_z \langle S^2\rangle_z^{1/2}$; all other notation is as in Tables I and II.

Burchard, Schmidt, Stockmayer, Macro. 13 1265 (1980)
(http://www.eng.uc.edu/~gbeaucag/Classes/Properties/RgbyRhRatioBurchardma60077a045.pdf)

R_g/R_H Ratio

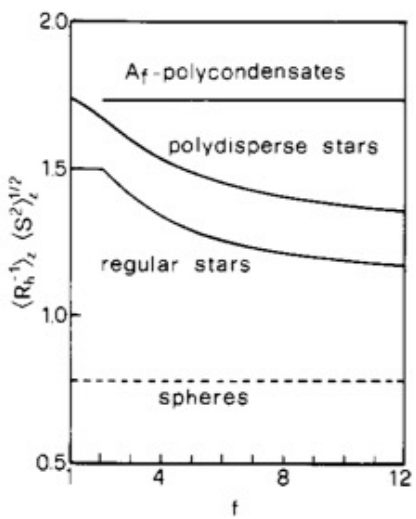

Figure 3. Dimensionless parameter $\rho = \langle R_h^{-1}\rangle_z R_g$ for three branching models and for compact spheres.

	f		B
	reg stars	polydisp stars	ABC poly-condensate
$g = 0.77 \pm 14\%$	3 ± 0.8	5.5 ± 1.4	2.25 ± 0.6
$h = 0.94 \pm 5\%$	3 ± 0.8	4.3 ± 0.9	1.65 ± 0.35
$\rho = 1.4 \pm 6\%$	3 ± 0.9	8.0 ± 2.5	3.5 ± 1.1
$C = 0.158 \pm 10\%$	3 ± 1.5	10.0 ± 5	4.5 ± 2.3

Burchard, Schmidt, Stockmayer, Macro. 13 1265 (1980)
(http://www.eng.uc.edu/~gbeaucag/Classes/Properties/RgbyRhRatioBurchardma60077a045.pdf)

R_g/R_H Ratio

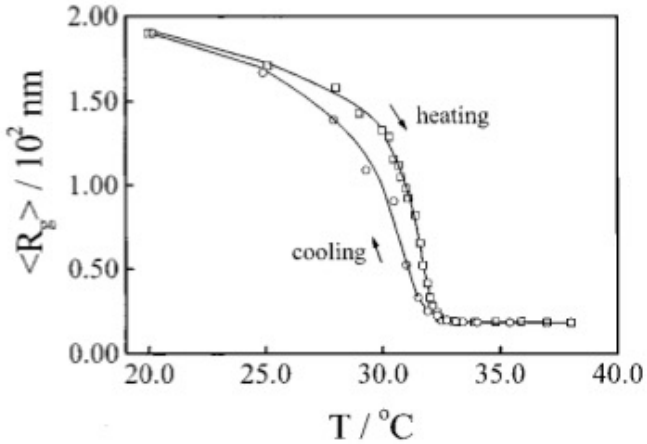

Figure 2. Temperature dependence of the average radius of gyration ($\langle R_g \rangle$) of the PNIPAM chains in the coil-to-globule (heating) and the globule-to-coil (cooling) transitions, respectively.

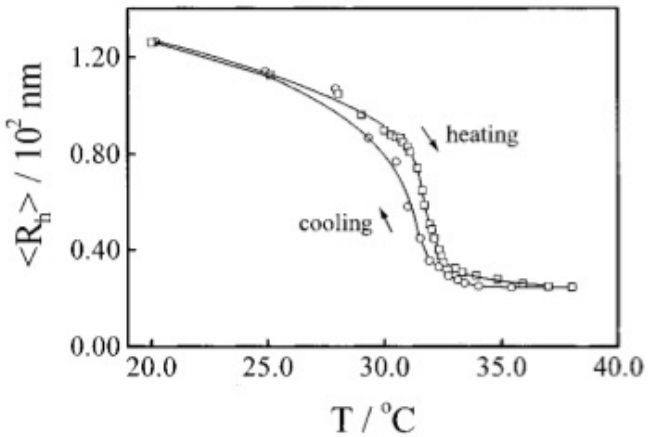

Figure 3. Temperature dependence of the average hydrodynamic radius ($\langle R_h \rangle$) of the PNIPAM chains in the coil-to-globule (heating) and the globule-to-coil (cooling) transitions, respectively.

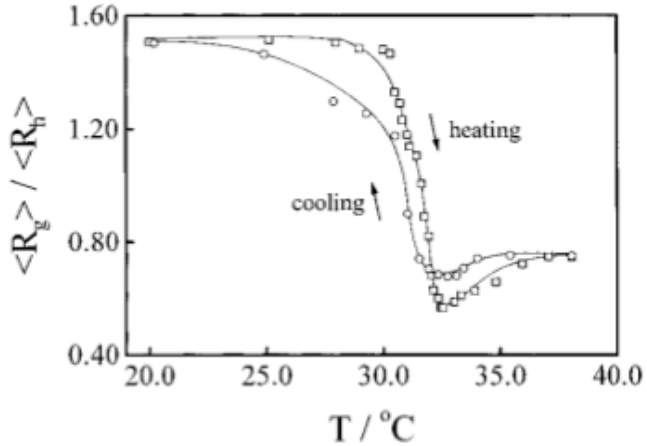

Figure 4. Temperature dependence of the ratio of radius of gyration to hydrodynamic radius ($\langle R_g \rangle / \langle R_h \rangle$) of the PNIPAM chains in the coil-to-globule (heating) and the globule-to-coil (cooling) transitions, respectively.

1.5 = Random Coil
~0.56 = Globule
Globule to Coil => Smooth Transition
Coil to Globule => Intermediate State
Less than $(3/5)^{1/2} = 0.77$ (sphere)

Wang X., Qiu X. , Wu C. Macro. 31 2972 (1998).
(http://www.eng.uc.edu/~gbeaucag/Classes/Properties/RgbyRhPNIPAAMma971873p.pdf)

R_g/R_H Ratio

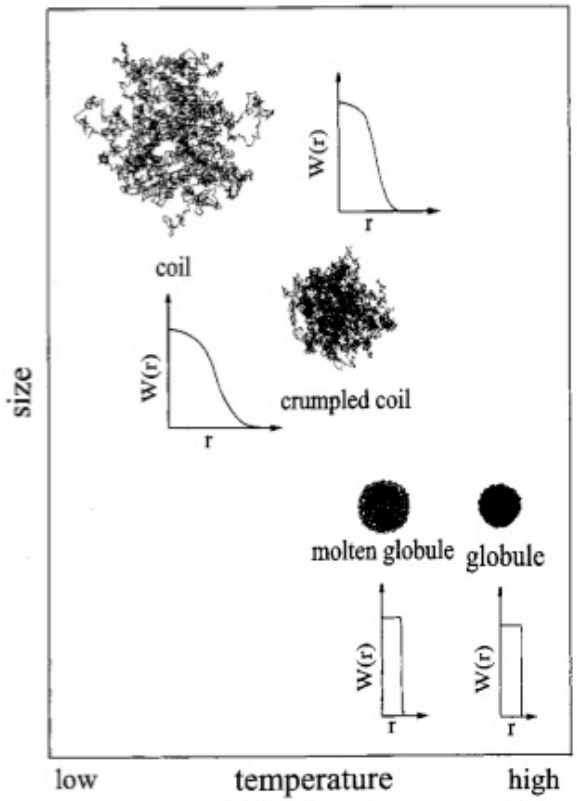

Figure 7. Schematic of four thermodynamically stable states and their corresponding chain density distributions ($W(r)$) along the radius in the coil-to-globule and the globule-to-coil transitions.

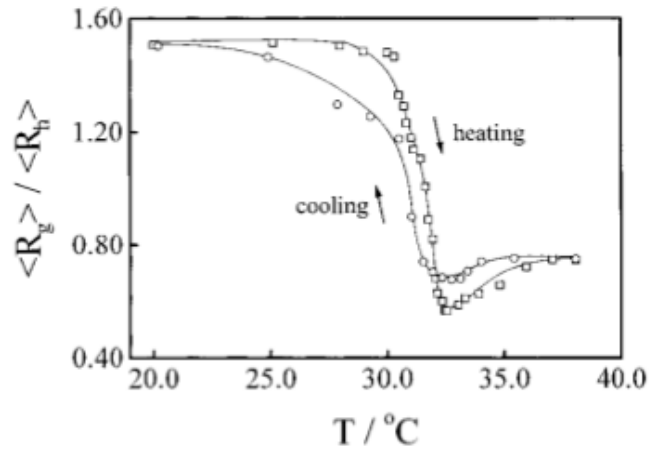

Figure 4. Temperature dependence of the ratio of radius of gyration to hydrodynamic radius ($\langle R_g \rangle / \langle R_h \rangle$) of the PNIPAM chains in the coil-to-globule (heating) and the globule-to-coil (cooling) transitions, respectively.

1.5 = Random Coil
~0.56 = Globule
Globule to Coil => Smooth Transition
Coil to Globule => Intermediate State
Less than $(3/5)^{1/2}$ = 0.77 (sphere)

Wang X., Qiu X. , Wu C. Macro. 31 2972 (1998).
(http://www.eng.uc.edu/~gbeaucag/Classes/Properties/RgbyRhPNIPAAMma971873p.pdf)

R_g/R_H Ratio

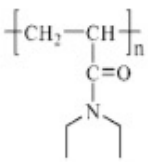

Poly(*N*,*N*-diethylacrylamide)
(PDEAM)

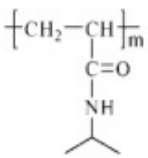

Poly(*N*-isopropylacrylamide)
(PNIPAM)

The objectives of the current study are to find whether the intrachain hydrogen boding plays a role in stabilizing individual collapsed single-chain globules, in the formation of the molten globular state during the coil-to-globule transition, and in the hysteresis of the globule-to-coil transition.

1.5 to 0.92 (> 0.77 for sphere)

It is important to note that for PDEAM $\langle R_g\rangle/\langle R_h\rangle$ finally reaches ~1.0, higher than 0.774 predicted for a uniform nondraining sphere. This means that individual PDEAM single-chain globules are not hard sphere, but still partially draining, less compact than those PNIPAM single-chain globules because its $\langle R_g\rangle/\langle R_h\rangle$ reaches ~0.78 at high temperatures.[21] We can attribute such a difference to the lacking of intrachain hydrogen bonding in PDEAM. It has been known that the hydrogen

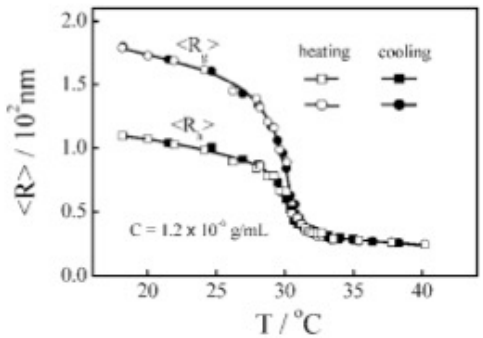

Figure 4. Temperature dependence of average radius of gyration ($\langle R_g\rangle$) and hydrodynamic radius ($\langle R_h\rangle$) of poly(*N*,*N*-diethylacrylamide) (PDEAM) chains in water in one heating-and-cooling cycle.

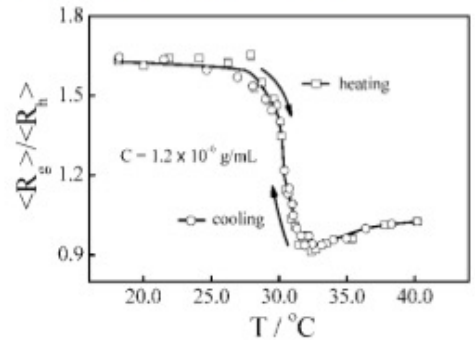

Figure 5. Temperature dependence of ratio of average radius of gyration to average hydrodynamic radius ($\langle R_g\rangle/\langle R_h\rangle$) of poly(*N*,*N*-diethylacrylamide) (PDEAM) chains in water in one heating-and-cooling cycle.

Zhou K., Lu Y., Li J., Shen L., Zhang F., Xie Z., Wu C. Macro. 41 8927 (2008).
(http://www.eng.uc.edu/~gbeaucag/Classes/Properties/RgbyRhCoiltoGlobulema8019128.pdf)

R_g/R_H Ratio

This ratio has also
been related to the
shape of a
colloidal particle

Static Scattering for Fractal Scaling

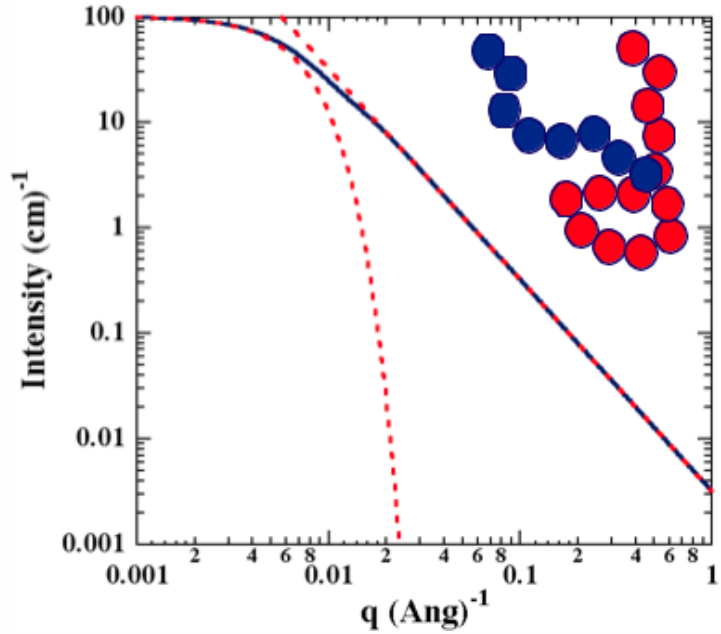

At intermediate sizes the chain is “self-similar”

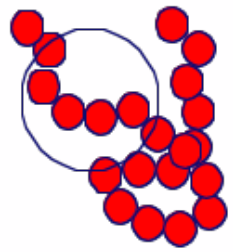

$$Mass \sim Size^{d_f}$$

$$z \sim \left(\frac{R_2}{R_1} \right)^{d_f}$$

At intermediate sizes the chain is “self-similar”

$I(q) \sim N\, n_e^2$

N = Number of Intermediate Spheres in the Aggregate

n_e = Mass of inter. sphere

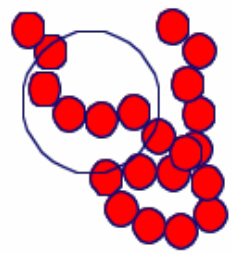

$I(q) \sim N\, n_e^2$

$$N \sim \left(\frac{R_2}{r_{\text{int}}}\right)^{d_f}$$

$$n_e \sim \left(\frac{r_{\text{int}}}{R_1}\right)^{d_f}$$

$$N n_e^2 \sim \left(\frac{r_{\text{int}}}{R_1}\right)^{d_f} \left(\frac{R_2}{R_1}\right)^{d_f} \quad \Rightarrow \quad \mathrm{I(q)} \sim \left(\frac{R_2}{R_1^2}\right)^{d_f} q^{-d_f}$$

The Debye Scattering Function for a Polymer Coil

$$I(Q) = \frac{2}{Q^2}\left(Q - 1 + \exp(-Q)\right)$$

$$Q = q^2 R_g^2$$

For $qR_g << 1$

$$\exp(-Q) = 1 - Q + \frac{Q^2}{2!} - \frac{Q^3}{3!} + \frac{Q^4}{4!} - \ldots$$

$$I(q) = 1 - \frac{Q}{3} + \ldots \approx \exp\left(-\frac{q^2 R_g^2}{3}\right)$$

Guinier's Law!

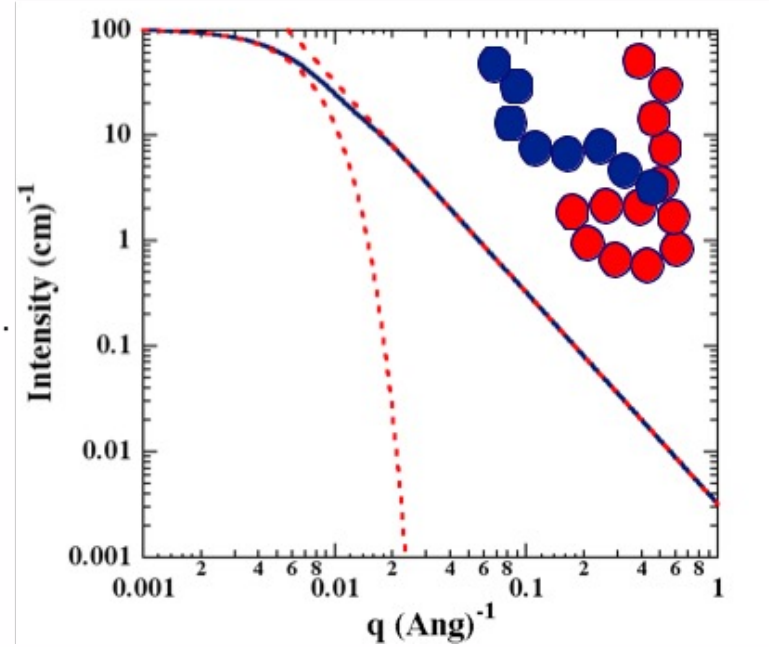

The Debye Scattering Function for a Polymer Coil

$$I(Q) = \frac{2}{Q^2}\left(Q - 1 + \exp(-Q)\right)$$

$$Q = q^2 R_g^2$$

For $qR_g >> 1$

$$I(Q) = \frac{2}{Q} = \frac{2}{q^2 R_g^2} \sim q^{-d_f}$$

$d_f = 2$

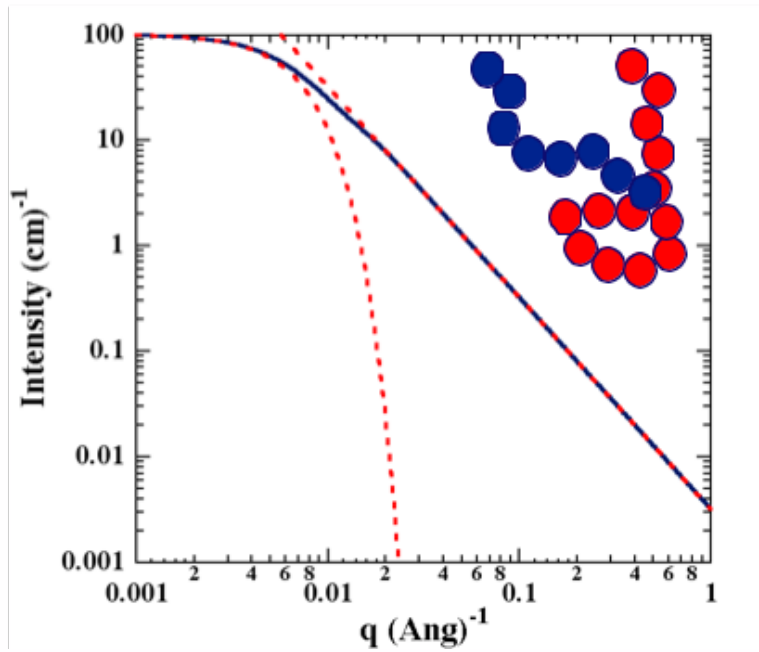

Ornstein-Zernike Equation

$$I(q) = \frac{G}{1 + q^2 \xi^2} \qquad I(q => \infty) = \frac{G}{q^2 \xi^2}$$

Has the correct functionality at high q

Debye Scattering Function =>

$$I(q) = \frac{2}{q^2 R_g^2}\left(q^2 R_g^2 - 1 + \exp\left(-q^2 R_g^2\right)\right) \qquad I(q => \infty) = \frac{2G}{q^2 R_g^2}$$

So, $$R_g^2 = 2\zeta^2$$

Ornstein-Zernike Equation

$$I(q) = \frac{G}{1 + q^2 \xi^2} \qquad I(q => 0) = G \exp\left(-q^2 \xi^2\right)$$

Has the correct functionality at low q
Debye =>

$$I(q) = \frac{2}{q^2 R_g^2}\left(q^2 R_g^2 - 1 + \exp\left(-q^2 R_g^2\right)\right) \qquad I(q => 0) = G \exp\left(-\frac{q^2 R_g^2}{3}\right)$$

$$R_g^2 = 3\zeta^2$$

The relatoinship between R_g and correlation length differs for the two regimes.

How does a polymer chain respond to external perturbation?

The Gaussian Chain

Boltzman Probability
For a Thermally Equilibrated System

$$P_B(R) = \exp\left(-\frac{E(R)}{kT}\right)$$

Gaussian Probability
For a Chain of End to End Distance R

$$P(R) = \left(\frac{3}{2\pi\sigma^2}\right)^{3/2} \exp\left(-\frac{3(R)^2}{2(\sigma)^2}\right)$$

By Comparison The Energy to stretch a Thermally Equilibrated Chain Can be Written

$$E = kT\frac{3R^2}{2nl_K^2}$$

Force

Force

$$F = \frac{dE}{dR} = \frac{3kT}{nl_K^2}R = k_{spr}R$$

Assumptions:
-Gaussian Chain
-Thermally Equilibrated
-**Small Perturbation** of Structure (so it is still Gaussian after the deformation)

Tensile Blob

For **Larger Perturbations** of Structure
-At small scales, small lever arm, structure remains Gaussian
-At large scales, large lever arm, structure becomes linear
Perturbation of Structure leads to a structural transition at a size scale ξ

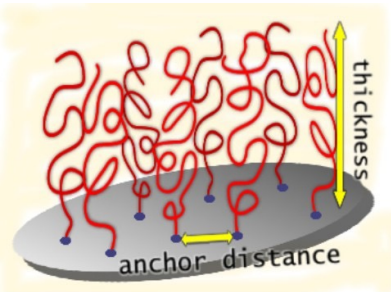

$$E = kT\frac{3R^2}{2nl_K^2} \qquad F = \frac{dE}{dR} = \frac{3kT}{nl_K^2}R$$

For weak perturbations of the chain $R \approx n^{1/2} l_K \equiv \xi_{Tensile}$

$$\xi_{Tensile} = \frac{3kT}{F}$$

Application of an external stress to the ends of a chain create a transition size where the coil goes from Gaussian to Linear called the Tensile Blob.

$$F = k_{spr} R = \frac{3kT}{R^{*2}} R$$

$$\xi_{Tensile} \sim \frac{R^{*2}}{R} = \frac{3kT}{F}$$

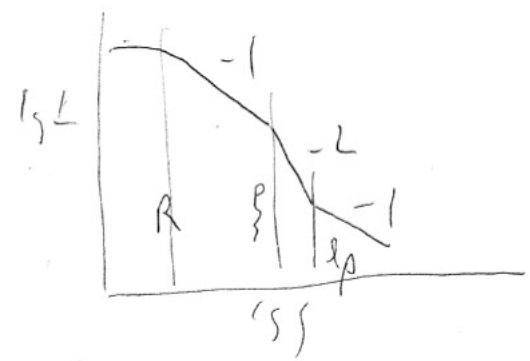

For sizes larger than the blob size the structure is linear, one conformational state so the conformational entropy is 0. For sizes smaller the blob has the minimum spring constant so the weakest link governs the mechanical properties and the chains are random below this size.

Semi-Dilute Solution Chain Statistics

In dilute solution the coil contains a concentration $c^* \sim 1/[\eta]$

$c^* = k\, n/R^3 = k\, n^{-4/5}$ for good solvent conditions

For semi-dilute solution the coil contains a concentration $c > c^*$

At large sizes the coil acts as if it were in a concentrated solution ($c >>> c^*$), $d_f = 2$. At small sizes the coil acts as if it were in a dilute solution, $d_f = 5/3$. There is a size scale, ξ, where this "scaling transition" occurs.

We have a primary structure of rod-like units, a secondary structure of expanded coil and a tertiary structure of Gaussian Chains.

What is the value of ξ?

ξ is related to the coil size R since it has a limiting value of R for $c < c^*$ and has a scaling relationship with the reduced concentration c/c^*

$$\xi \sim R\,(c/c^*)^P \sim n^{(3+4P)/5}$$

There are no dependencies on n above c^* so $(3+4P)/5 = 0$ and $P = -3/4$

$$\xi \sim R\,(c/c^*)^{-3/4}$$

Coil Size in terms of the concentration

$$\xi = b\left(\frac{N}{n_\xi}\right)^{3/5} \sim \left(\frac{c}{c^*}\right)^{-3/4}$$

$$n_\xi \sim \left(\frac{c}{c^*}\right)^{(3/4)(5/3)} = \left(\frac{c}{c^*}\right)^{(5/4)}$$

$$R = \xi n_\xi^{1/2} \sim \left(\frac{c}{c^*}\right)^{-3/4}\left(\frac{c}{c^*}\right)^{(5/8)} = \left(\frac{c}{c^*}\right)^{-1/8}$$

$$R = \xi\, n_\xi^{1/2} = R_{F0}\,(c/c^*)^{-3/4}\,(c/c^*)^{5/8} = R_{F0}\,(c/c^*)^{-1/8}$$

This is called the "Concentration Blob"

Three regimes of chain scaling in concentration.

In dilute solution the chain displays good solvent scaling in most cases, $d_f = 5/3$. When the concentration is increased above the overlap concentration, c*, a concentration blob, ξ_c, is introduced between R_g and l_p. For sizes larger than the blob size, screening of interactions leads to Gaussian scaling, $d_f = 2$. For sizes smaller than the screening length of blob size, the chains are not screened and good solvent scaling is observed. The blob size follows $\xi \sim R\left(\frac{c}{c^*}\right)^{-3/4}$ until a concentration where $\xi = l_p$. At that concentrations above c**, $c^{**} \sim c^*\left(\frac{R}{l_p}\right)^{4/3}$, the chain is in a concentrated condition and all interactions are screened so that the chain has a Gaussian configuration, $d_f = 2$.

Thermal Blob

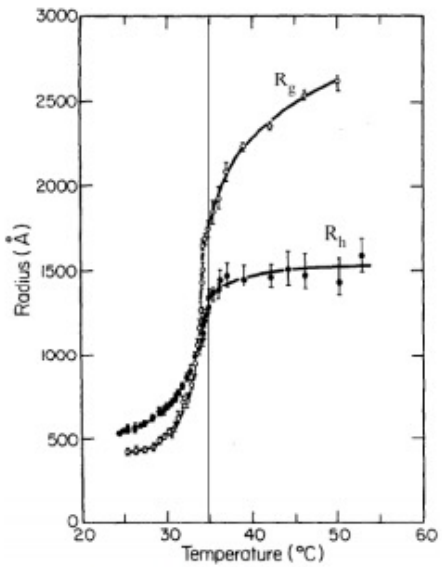

Figure 3. *Radius of gyration, R_g, and hydrodyamic radius R_h versus temperature for polystyrene in cyclohexane. Vertical line indicates the phase separation temperature. From Reference [21].*

Chain expands from the theta condition to fully expanded gradually.
At small scales it is Gaussian, at large scales expanded (opposite of concentration blob).

$$E = kT\left(\frac{3R^2}{2nl_K^2} + \frac{n^2V_c}{2R^3}\right)$$

$$E = kT\left(\frac{3R^2}{2nl_K^2} + \frac{n^2V_c(1-2\chi)}{2R^3}\right)$$

Thermal Blob

$$\Delta\varepsilon = \left(\varepsilon_{PP} + \varepsilon_{SS}\right)/2 - \varepsilon_{PS}$$

$$\chi = \frac{z\Delta\varepsilon}{kT}$$

$$V_{c,enthalpic} = V_c\left(1 - 2\chi\right)$$

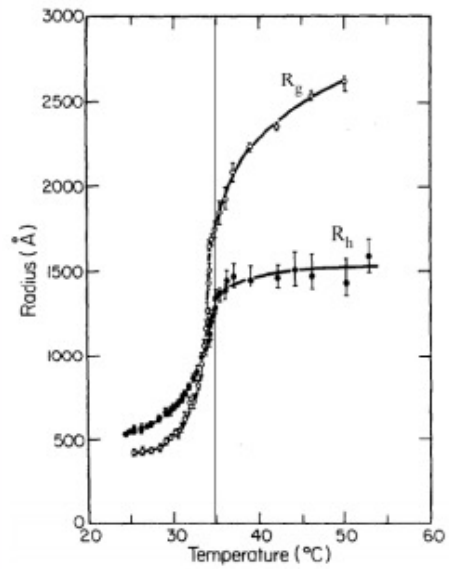

$$E = kT\left(\frac{3R^2}{2nl_K^2} + \frac{n^2V_c}{2R^3}\right)$$

$$E = kT\left(\frac{3R^2}{2nl_K^2} + \frac{n^2V_c\left(1-2\chi\right)}{2R^3}\right)$$

Thermal Blob

$$E = kT\left(\frac{3R^2}{2nl_K^2} + \frac{n^2V_c(1-2\chi)}{2R^3}\right)$$

Energy Depends on n, a chain with a mer unit of length 1 and n = 10000
could be re cast (renormalized) as a chain of unit length 100 and n = 100
The energy changes with n so depends on the definition of the base unit

Smaller chain segments have less entropy so phase separate first.
We expect the chain to become Gaussian on small scales first.
This is the opposite of the concentration blob.

Cooling an expanded coil leads to local chain structure collapsing to a Gaussian structure first.
As the temperature drops further the Gaussian blob becomes larger until the entire chain is
Gaussian at the theta temperature.

Thermal Blob

$$R = N_T^{3/5}\xi_T = \left(N/n_T\right)^{3/5}\xi_T = \left(N\Big/\left(\xi_T/l\right)^2\right)^{3/5}\xi_T = N^{3/5}\xi_T^{-1/5}l^{6/5}$$

Flory-Krigbaum Theory yields: $R = V_c^{1/5}\left(1-2\chi\right)^{1/5}N^{3/5}l^{2/5}$

By equating these:

$$\xi_T = \frac{l}{\left(1-2\chi\right)}$$

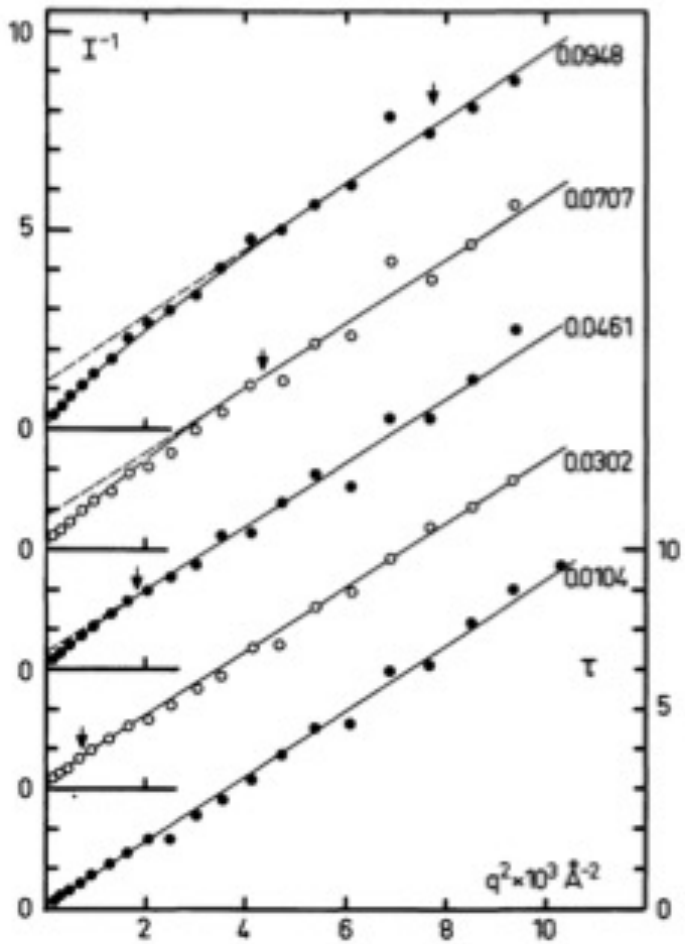

FIG. 7. — Inverse of the scattered intensity *versus* the square of the scattering vector. Points are experimental data recorded at different reduced temperatures τ as indicated on the right. The solid curves are the results of calculation using the formula (3.16). Vertical arrows show the theoretical cross-over point.

LE JOURNAL DE PHYSIQUE TOME 39, JANVIER 1978, PAGE 77

Classification
Physics Abstracts
36.20 — 64.00 — 61.40

CROSS-OVER IN POLYMER SOLUTIONS

B. FARNOUX, F. BOUÉ, J. P. COTTON, M. DAOUD, G. JANNINK, M. NIERLICH
and
P. G. DE GENNES (*)
DPh-G/PSRM, CEN Saclay, Boîte Postale n° 2, 91190 Gif sur Yvette, France

(*Reçu le 18 avril 1977, révisé le 21 juillet 1977, accepté le 8 septembre 1977*)

Digitized from Farnoux

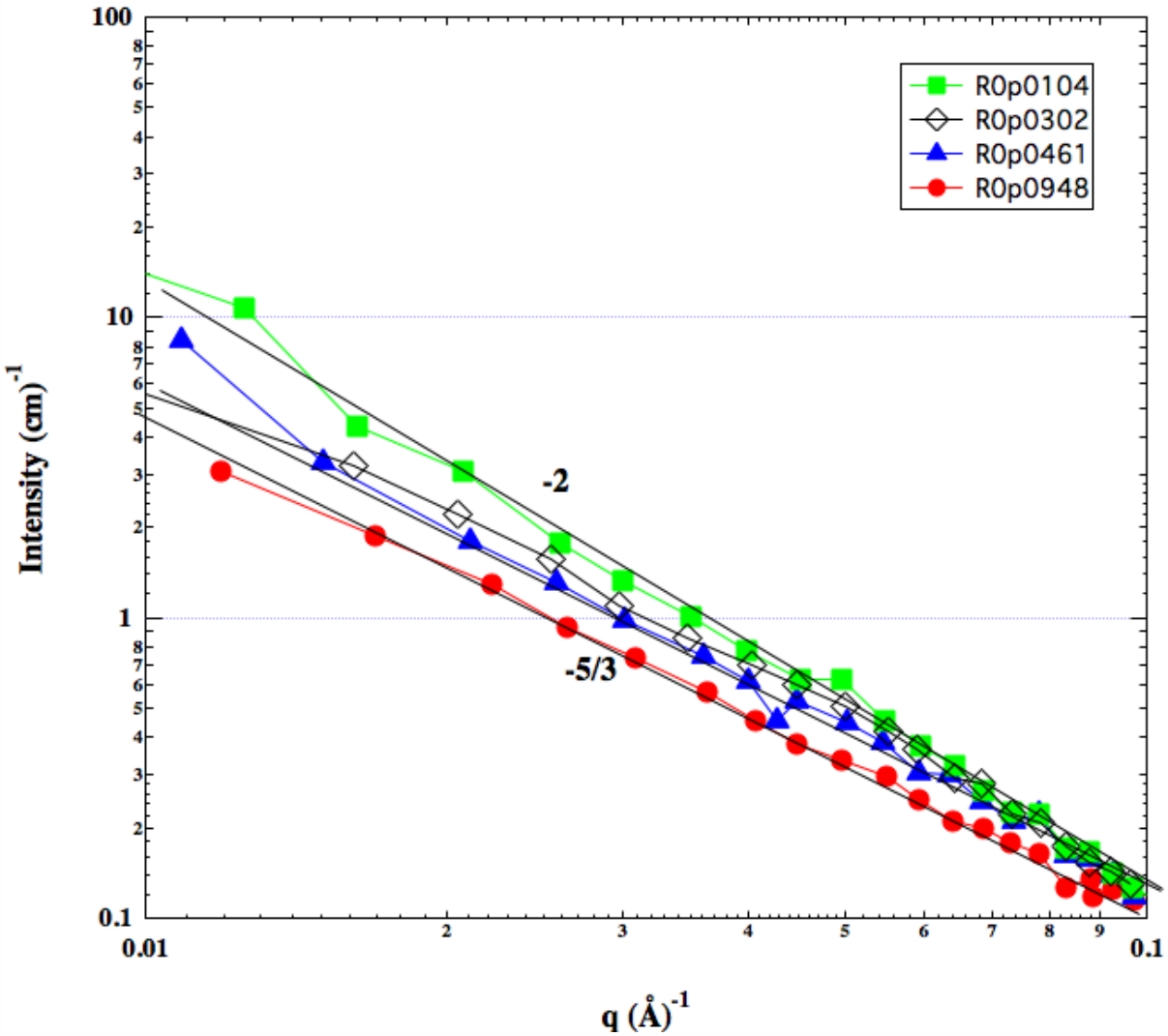

Fractal Aggregates and Agglomerates

Growth of Nanoparticles

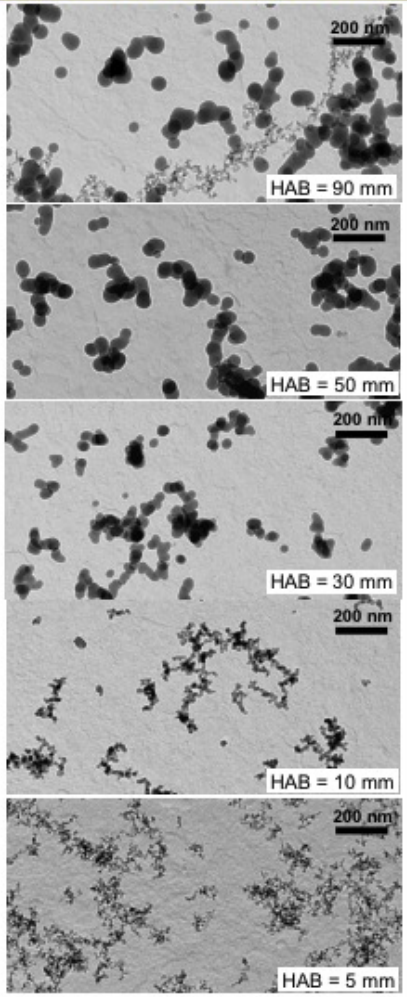

Fig. 1: Silica particles as collected by conventional thermophoretic sampling (TS) along the axis of a premixed flame of hexamethyldisiloxane and oxygen [1,2]. Using aluminum foil in-stead of TEM grids and performing multiple sampling from the same location in the flame, the Al-probe was covered with ***a silica monolayer*** *[1] (as indicated in Fig. 2).*

Spray Flame Appearance

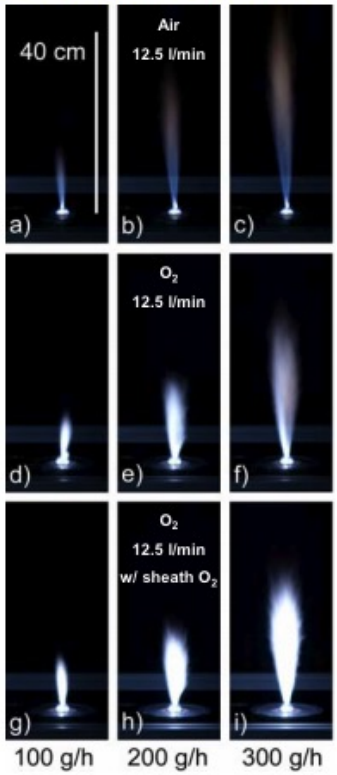

Fig. 3: Spray flames (1.26 M HMDSO in EtOH) producing 100, 200 and 300 g/h of silica using 12.5 l/min air (a-c) or O_2 as dispersion gas without (d-f) and with (g-i) additional 25 l/min of O_2 sheath flow at 1 bar pressure drop across the nozzle tip.

Powder Morphology

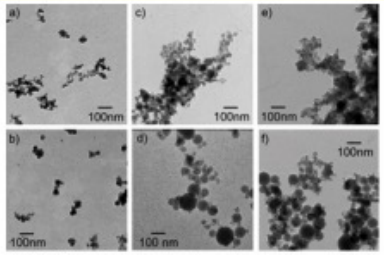

Fig. 4: Transmission electron micrographs of silica nanoparticles at production rates of 150 (top row) and 300 g/h (bottom row) using 12.5 l/min air (a,b) or O_2 as dispersion gas without (c,d) and with (e,f) additional 25 l/min of O_2 sheath flow using 1.26 M HMDSO in EtOH.

Powder Morphology

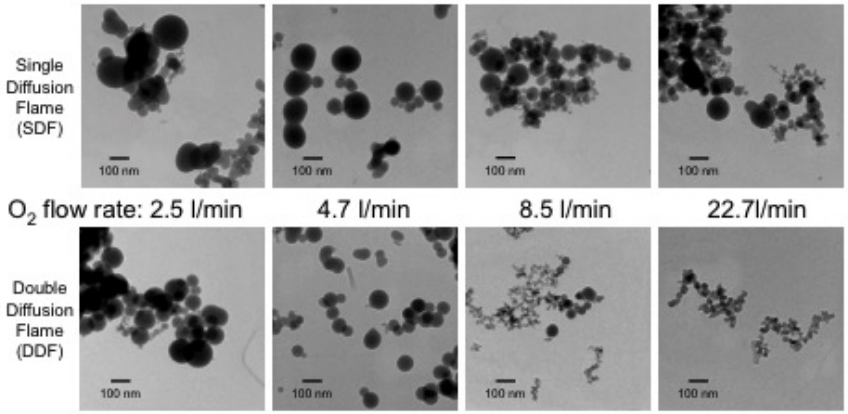

*Fig. 5: **T**ransmission **E**lectron **M**icrographs (TEM) of SiO_2 synthesized in SDF and DDF at different oxygen flow rates. Particles made in flames at low oxygen flow rates stay longer at high temperatures leading to the formation of rather big spherical, non-agglomerated particles with diameters of about 100 nm. At high oxygen flow rates the particles are agglomerates of small primary particles. Particles synthesized in DDF have narrower size distributions indicated by TEM compared to those made in SDF.*

Flame Structure

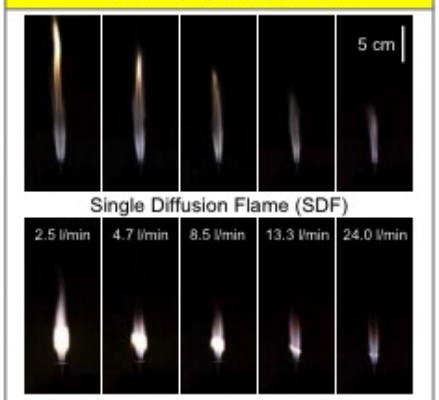

Fig. 3: Effect of oxygen flow rate on flame structure of a SDF and DDF. Increasing the oxygen flow rate decreases the flame height of the HMDSO-methane-oxygen diffusion flame as turbulence accelerates the mixing of fuel and oxidant.

Polymer Chains are Mass-Fractals

$R_{RMS} = n^{1/2}\, l$	Mass ~ Size^2
3-d object	Mass ~ Size^3
2-d object	Mass ~ Size^2
1-d object	Mass ~ Size^1
d_f-object	Mass ~ Size^{df}

This leads to odd properties:

density $$\rho = \frac{Mass}{Volume} = \frac{Mass}{Size^3} = \frac{Size^{d_f}}{Size^3} \sim Size^{d_f - 3}$$

For a 3-d object density doesn't depend on size,
For a 2-d object density drops with Size
Larger polymers are less dense

How Complex Mass Fractal Structures Can be Decomposed

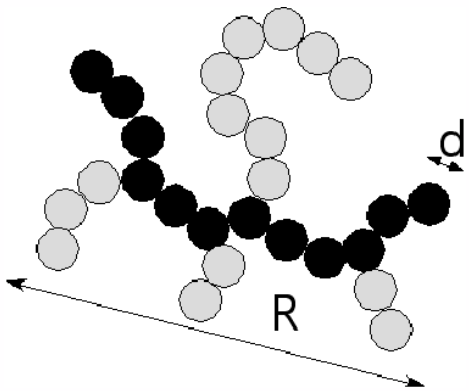

Tortuosity

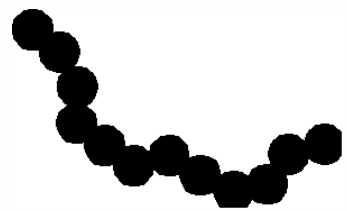

Connectivity

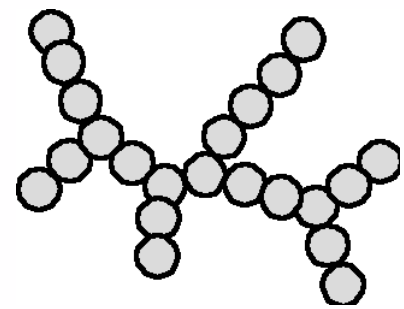

$$z \sim \left(\frac{R}{d}\right)^{d_f} \sim p^c \sim s^{d_{\min}}$$

$$p \sim \left(\frac{R}{d}\right)^{d_{\min}}$$

$$s \sim \left(\frac{R}{d}\right)^{c}$$

$$d_f = d_{\min} c$$

z	d_f	p	d_{min}	s	c	R/d
27	1.36	12	1.03	22	1.28	11.2

Disk

$$d_f = 2$$

$$d_{\min} = 1$$

$$c = 2$$

Extended β-sheet
(misfolded protein)

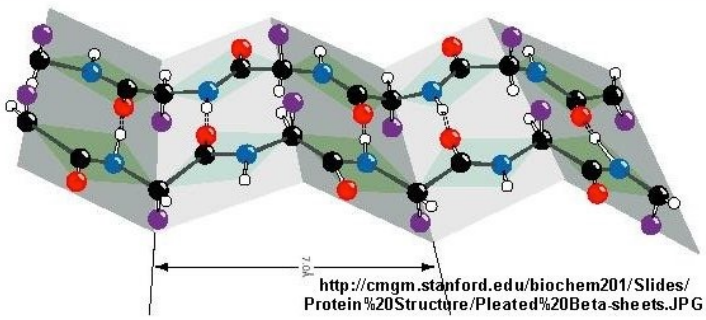

Random Coil

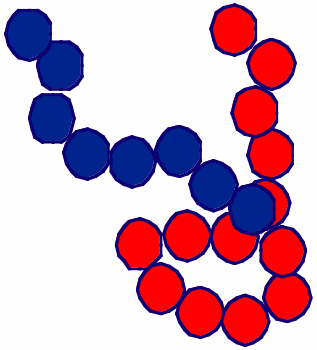

$$d_f = 2$$

$$d_{\min} = 2$$

$$c = 1$$

Unfolded Gaussian chain

Primary Size for Fractal Aggregates

Primary Size for Fractal Aggregates

- Particle counting from TEM
- Gas adsorption V/S => d_p
- Static Scattering R_g, d_p
- Dynamic Light Scattering

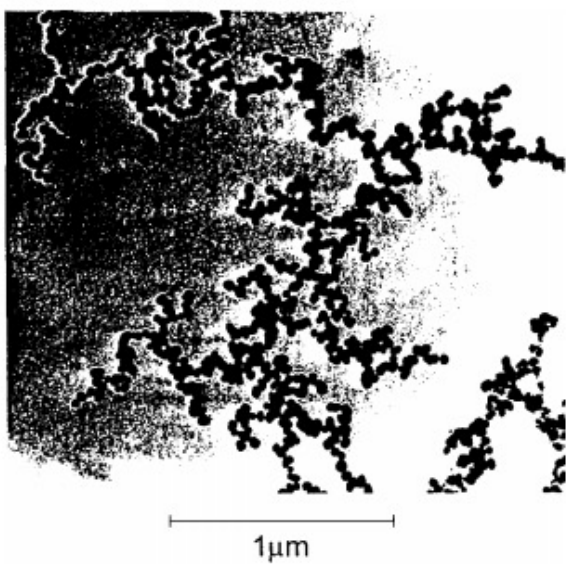

Figure 2. TEM picture of titania (TiO_2) fractal aggregates with $D \simeq 1.8$ produced by pyrolysis of Titanium Isopropoxide.

http://www.phys.ksu.edu/personal/sor/publications/2001/light.pdf

Cryo Scanning Electron Microscopy

A scanning electron micrograph of a frozen sample was taken. The sizes of the particles visible on the picture were measured individually with a ruler and used to calculate a number-mean, D(1,0), a volume-mean, D(4,3) and a number-distribution.

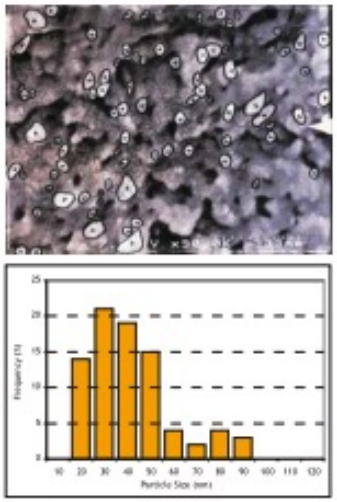

Number Mean - D(1,0) = 45.2 nm
Volume Mean - D(4,3) = 68.0 nm

Note : due to the limited number (82) of particles measured this result is only indicative.

http://www.koboproductsinc.com/Downloads/PS-Measurement-Poster-V40.pdf

Primary Size for Fractal Aggregates

- Particle counting from TEM
- Gas adsorption V/S => d_p
- Static Scattering R_g, d_p
- Dynamic Light Scattering

Dynamic Light Scattering

To evaluate repeatability and robustness, the measure was made 8 times, using 3 different dilutions. The following graph presents one of these measures, expressed as intensity-distribution, volume-distribution and number (length)-distribution.

Measure on Nicomp Model 370 - samples diluted in chloroform to 200-350 kHz.

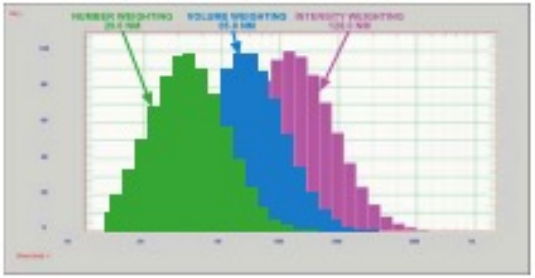

The following table shows the averaged results for the 8 measurements. Precision is calculated as the Relative Standard Deviation of the measurements.

Mean Calculation	Particle Size	Precision
Intensity Weighting	127.9 nm	2 %
Volume Weighting	71.6 nm	16 %
Number Weighting	36.2 nm	25 %

http://www.koboproductsinc.com/Downloads/PS-Measurement-Poster-V40.pdf

For static scattering p(r) is the binary spatial auto-correlation function

We can also consider correlations in time, binary temporal correlation function
$g_I(q,\tau)$

For dynamics we consider a single value of q or r and watch how the intensity changes with time
$I(q,t)$

We consider correlation between intensities separated by t
We need to subtract the constant intensity due to scattering at different size scales
and consider only the fluctuations at a given size scale, r or $2\pi/r = q$

Dynamic Light Scattering

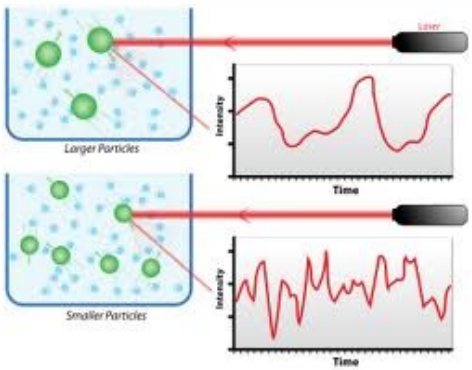

$$g^2(q;\tau) = \frac{\langle I(t)I(t+\tau)\rangle}{\langle I(t)\rangle^2}$$

$$g^2(q;\tau) = 1 + \beta\left[g^1(q;\tau)\right]^2$$

$$q = \frac{4\pi n_0}{\lambda}\sin\left(\frac{\theta}{2}\right)$$

$$g^1(q;\tau) = \exp(-\Gamma\tau)$$

$$\Gamma = q^2 D_t$$

$$D = k_B T / 6\pi\eta a$$

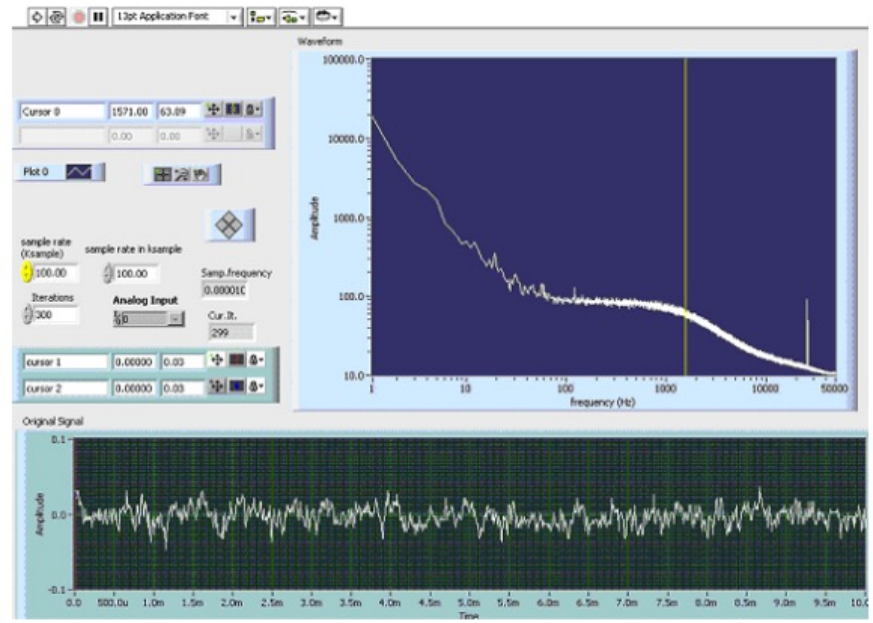

a = R_H = Hydrodynamic Radius

Dynamic Light Scattering

my DLS web page

http://www.eng.uc.edu/~gbeaucag/Classes/Physics/DLS.pdf

Wiki

http://webcache.googleusercontent.com/search?q=cache:eY3xhiX117IJ:en.wikipedia.org/wiki/Dynamic_light_scattering+&cd=1&hl=en&ct=clnk&gl=us

Wiki Einstein Stokes

http://webcache.googleusercontent.com/search?q=cache:yZDPRbqZ1BIJ:en.wikipedia.org/wiki/Einstein_relation_(kinetic_theory)+&cd=1&hl=en&ct=clnk&gl=us

Gas Adsorption

$$\theta = \frac{\text{adsorbed sites}}{\text{total sites (N)}}$$

A + S <=> AS

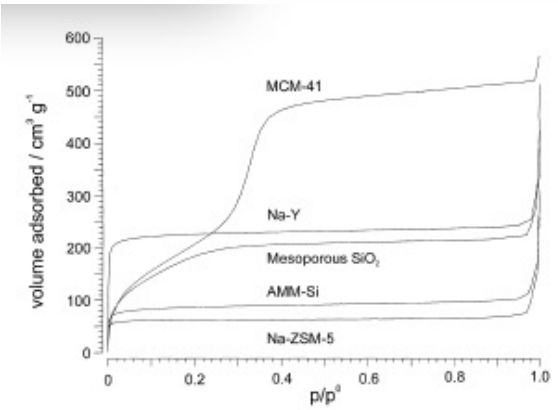

Fig. 2. Adsorption isotherms of the samples tested with Ar at 87.5 K.

http://www.chem.ufl.edu/~itl/4411L_f00/ads/ads_I.html

Adsorption

$$\frac{d\theta}{dt} = k_a p N (1-\theta)$$

Equilibrium

=

Desorption

$$\frac{d\theta}{dt} = k_d N \theta$$

$$\theta = \frac{Kp}{1+Kp}$$

$$K = k_a / k_d$$

$$\frac{\partial \ln K}{\partial T} = \frac{\Delta H_{abs}}{RT^2}$$

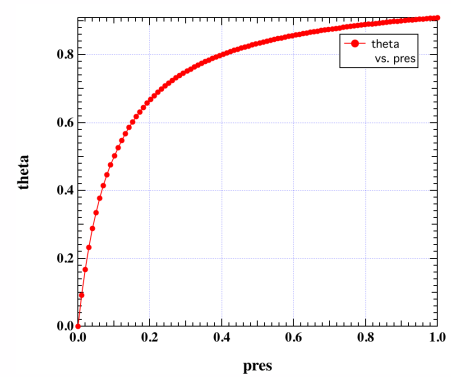

Gas Adsorption

Multilayer adsorption

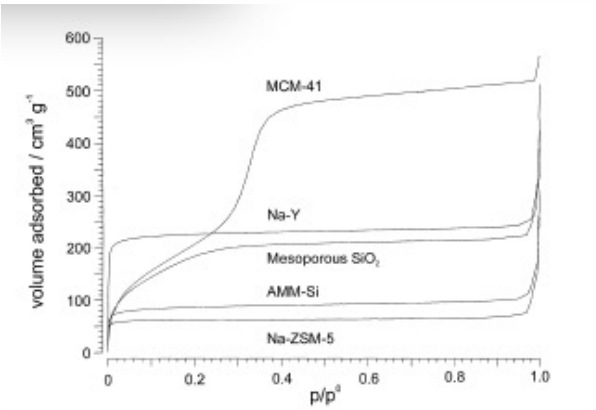

Fig. 2. Adsorption isotherms of the samples tested with Ar at 87.5 K.

BET Isotherm

Various Values of c

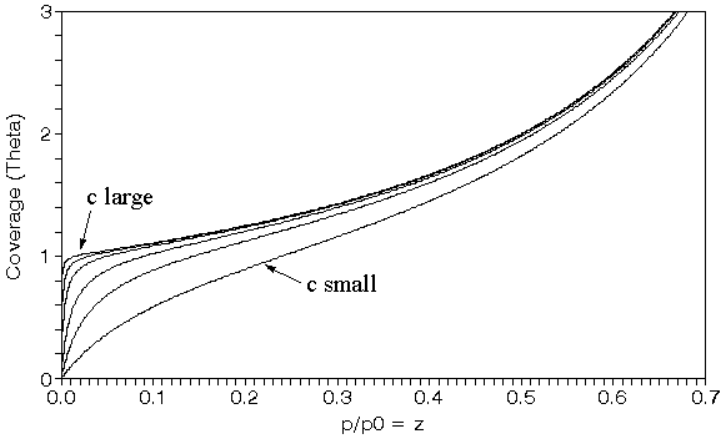

$$\frac{n}{n_{mono}} = \frac{cz}{(1-z)\,[1 - z(1-c)]} = (\theta)$$

$$c \approx \frac{e^{-\Delta H_{ads}/RT}}{e^{\Delta H_{vap}/RT}}$$

http://www.chem.ufl.edu/~itl/4411L_f00/ads/ads_I.html

S. Storck et al. / Applied Catalysis A: General 174 (1998) 137–146

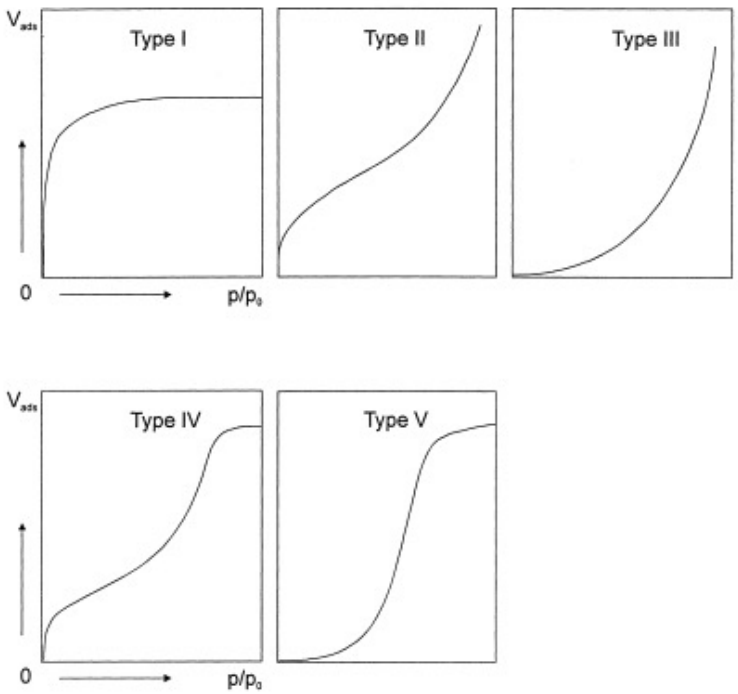

Fig. 1. Adsorption isotherm types defined by Brunauer [6].

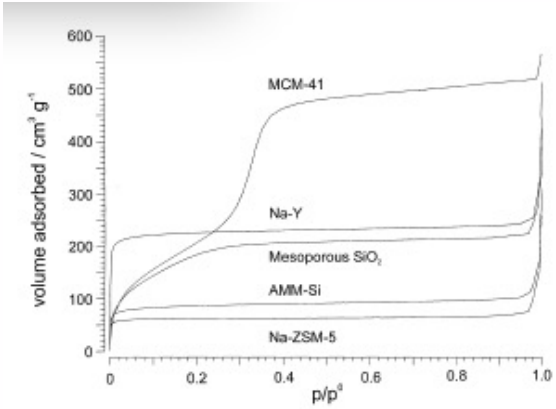

Fig. 2. Adsorption isotherms of the samples tested with Ar at 87.5 K.

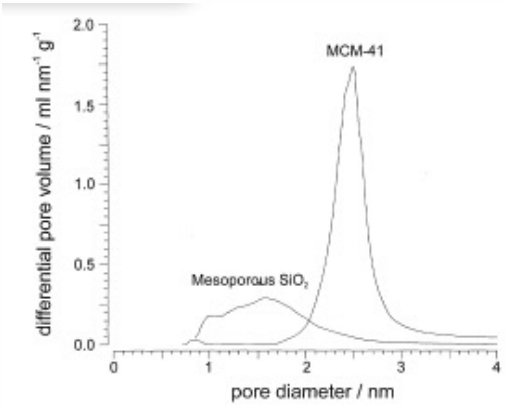

Fig. 3. Pore-size distribution according to the BJH method.

http://www.eng.uc.edu/~gbeaucag/Classes/Nanopowders/GasAdsorptionReviews/ReviewofGasAdsorptionGOodOne.pdf

From gas adsorption obtain surface area by number of gas atoms times an area for the adsorbed gas atoms in a monolayer

Have a volume from the mass and density.

So you have S/V or V/S

Assume sphere $S = 4\pi R^2$, $V = 4/3\ \pi R^3$

So $d_P = 6V/S$

Sauter Mean Diameter $d_P = \langle R^3 \rangle / \langle R^2 \rangle$

Log-Normal Distribution

$$f(R) = \frac{1}{R\sigma(2\pi)^{1/2}} \exp\left\{ -\frac{[\log(R/m)]^2}{2\sigma^2} \right\},$$

$$\langle R^r \rangle = m^r \exp\left(r^2\sigma^2/2\right) = \exp\left(r\mu + r^2\sigma^2/2\right)$$

$$\langle R \rangle = m \exp\left(\sigma^2/2\right)$$

Mean

$$\sigma_g = \exp(\sigma) \qquad x_g = \exp(m)$$

Geometric standard deviation and geometric mean (median)

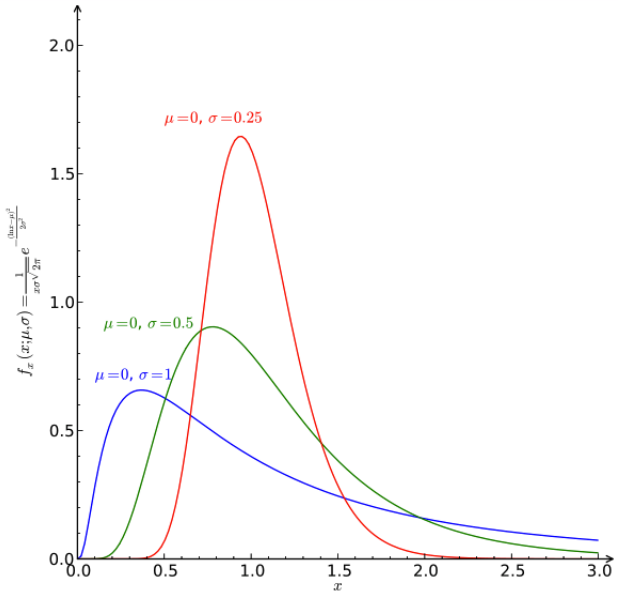

Gaussian is centered at the Mean and is symmetric. For values that are positive (size) we need an asymmetric distribution function that has only values for greater than 1. In random processes we have a minimum size with high probability and diminishing probability for larger values.

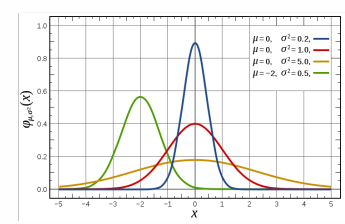

http://www.eng.uc.edu/~gbeaucag/PDFPapers/ks5024%20|applcryst%20Beaucage%20PSD.pdf

http://en.wikipedia.org/wiki/Log-normal_distribution

Log-Normal Distribution

$$f(R) = \frac{1}{R\sigma(2\pi)^{1/2}} \exp\left\{-\frac{[\log(R/m)]^2}{2\sigma^2}\right\},$$

$$\langle R^r \rangle = m^r \exp\left(r^2\sigma^2/2\right) = \exp\left(r\mu + r^2\sigma^2/2\right)$$

$$\langle R \rangle = m \exp\left(\sigma^2/2\right)$$

Mean

$$\sigma_g = \exp(\sigma) \quad x_g = \exp(m)$$

Geometric standard deviation and geometric mean (median)

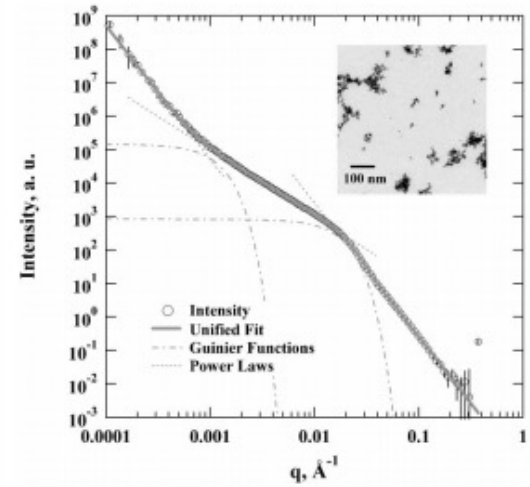

Static Scattering Determination of Log Normal Parameters

$$\ln \sigma_g = \sigma = \left\{\frac{\ln\left[B\left(R_g^2\right)^2/(1.62G)\right]}{12}\right\}^{1/2} = \left(\frac{\ln \mathrm{PDI}}{12}\right)^{1/2} \quad (17)$$

and

$$m = \left\{5R_g^2/[3\exp(14\sigma^2)]\right\}^{1/2}, \quad (18)$$

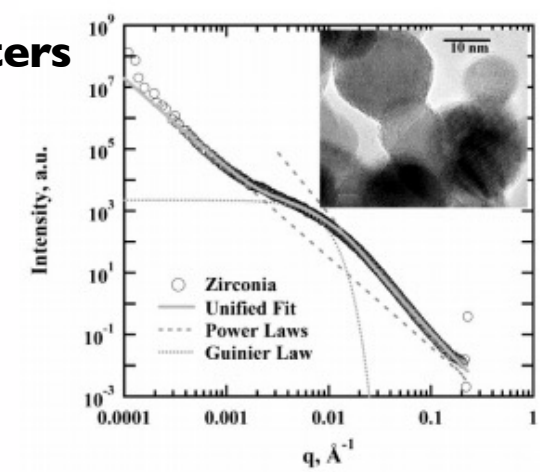

http://www.eng.uc.edu/~gbeaucag/PDFPapers/ks5024%20Jappl cryst%20Beaucage%20PSD.pdf

Primary Size for Fractal Aggregates

- Particle counting from TEM
- Gas adsorption V/S => d_p
- Static Scattering R_g, d_p
- Dynamic Light Scattering

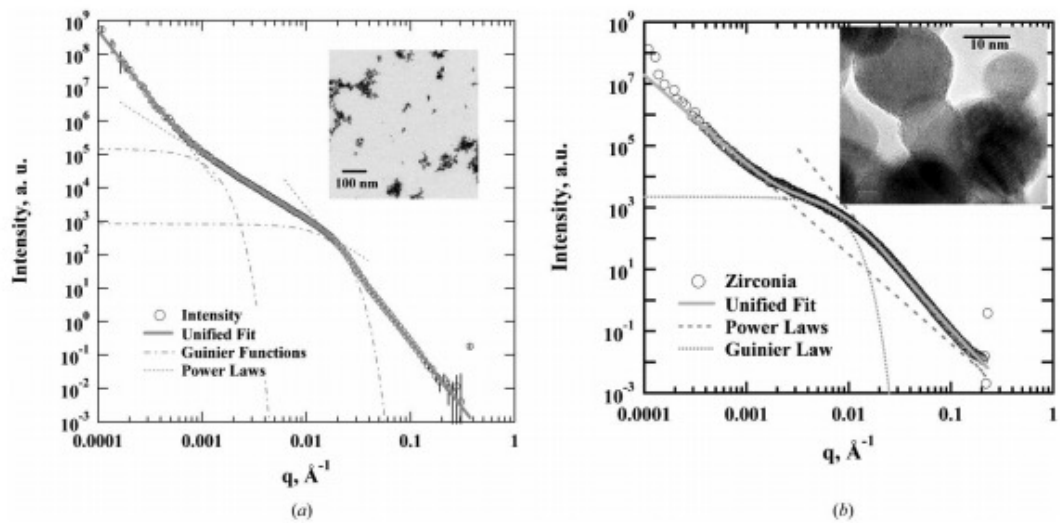

Figure 2
USAXS data from aggregated nanoparticles (circles) showing unified fits (bold grey lines), primary particle Guinier and Porod functions at high q, the intermediate mass fractal scaling regime and the aggregate Guinier regime (dashed lines). (*a*) Fumed titania sample with multi-grain particles and low-q excess scattering due to soft agglomerates. $d_{V/S}$ = 16.7 nm (corrected to 18.0 nm), PDI = 3.01 (σ_g = 1.35), R_g = 11.2 nm, d_f = 1.99, $z_{\Sigma 1}$ = 175, z_{R_g} = 226, R_{g2} = 171 nm. From gas adsorption, d_p = 16.2 nm. (*b*) Fumed zirconia sample (Mueller *et al.*, 2004) with single-grain particles, as shown in the inset. The primary particles for this sample have high polydispersity leading to the observed hump near the primary particle scattering regime. $d_{V/S}$ = 20.3 nm, PDI = 10.8 (σ_g = 1.56), R_g = 26.5 nm, d_f = 2.90. From gas adsorption, d_p = 19.7 nm.

http://www.eng.uc.edu/~gbeaucag/PDFPapers/ks5024%20JapplCryst%20Beaucage%20PSD.pdf

Primary Size for Fractal Aggregates

-Particle counting from TEM
-Gas adsorption V/S => d_p
-Static Scattering R_g, d_p

Smaller Size = Higher S/V
(Closed Pores or similar issues)

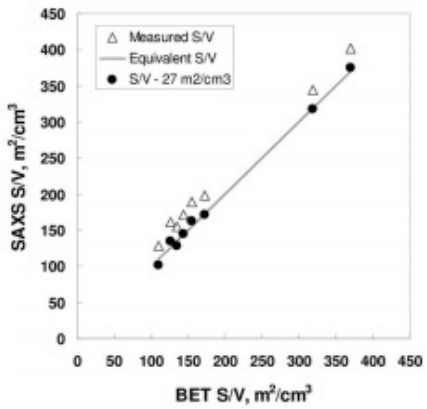

(a)

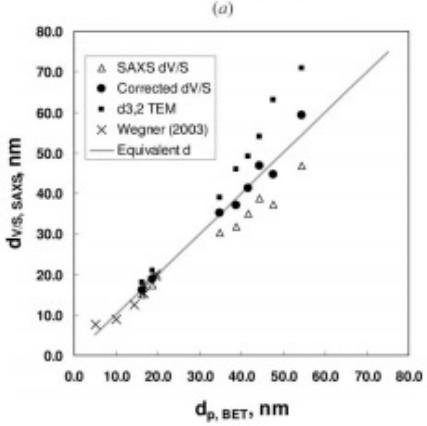

(b)

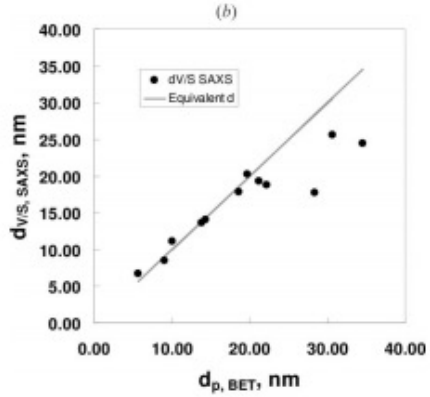

(c)

Figure 3
(*a*) *S/V* from SAXS for titania particles produced by vapor-phase pyrolysis of titania tetraisopropoxide by Kammler *et al.* (2002, 2003). The SAXS *S/V* can be made to agree with the BET value by subtraction of 27 m^2 cm^{-3}. (*b*) $d_{V/S}$ from USAXS [and corrected from (*a*)] *versus* d_p from BET analysis of gas adsorption data for a series of titania samples produced by Kammler (triangles and filled circles), and samples made in a quenched-spray flame from Wegner & Pratsinis (2003) (crosses, single-grain particles). The calculated $d_{3,2}$ from TEM micrographs for the Kammler samples is also shown (filled squares). (*c*) $d_{V/S}$ from USAXS *versus* d_p from BET for fumed zirconia samples of Mueller *et al.* (2004).

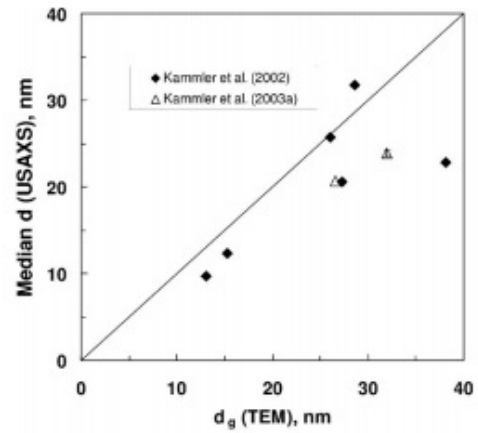

(a)

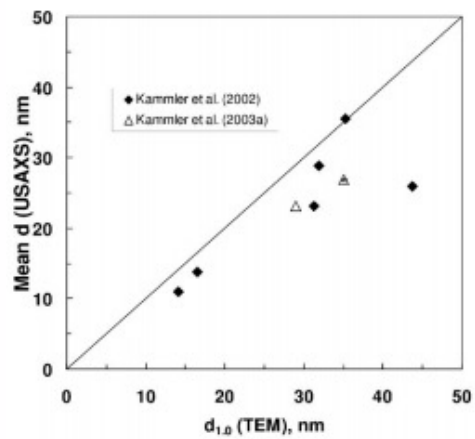

(b)

http://www.eng.uc.edu/~gbeaucag/PDFPapers/ks5024%20Japplcryst%20Beaucage%20PSD.pdf

Figure 4
(*a*) Comparison of the median particle size from exp *m*, with *m* defined by equation (18), and the median particle size calculated from an analysis of TEM data on TiO_2. (*b*) Mean particle size, $\langle R \rangle$ from USAXS, equation (2) with $r = 1$, and from TEM (Kammler *et al.*, 2003) for the same samples as Figs. 3(*a*) and 3(*b*).

Fractal Aggregates and Agglomerates

Primary Size for Fractal Aggregates

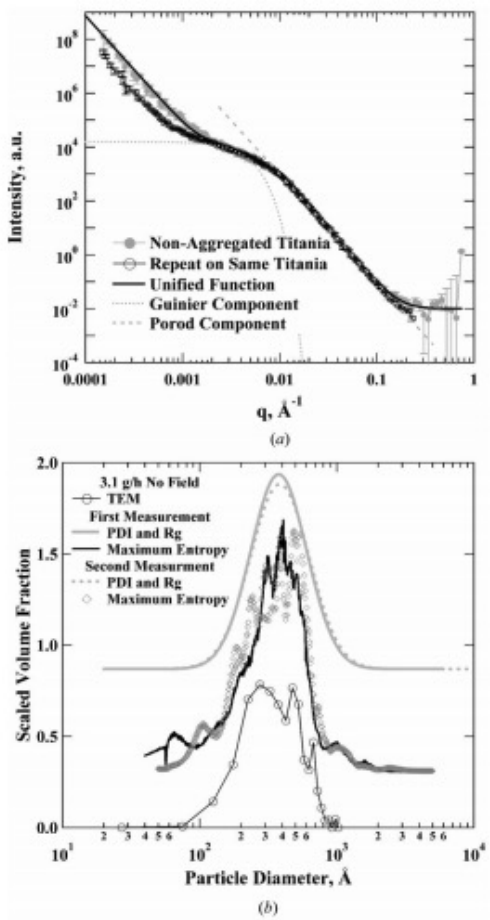

Figure 5
3.1 g h^{-1} titania. (*a*) Repeat USAXS runs on a non-aggregated titania powder (Fig. 1). (*b*) Particle size distributions from TEM (circles; Kammler *et al.*, 2003), equations (1), (2), (17) and (18) using PDI and R_g, and using the maximum-entropy program of Jemian (Jemian *et al.*, 1991). Distribution curves are shifted vertically for clarity. $d_{V/S}$ = 34.9 nm, PDI = 14.4 (σ_g = 1.60), R_g = 44.2 nm.

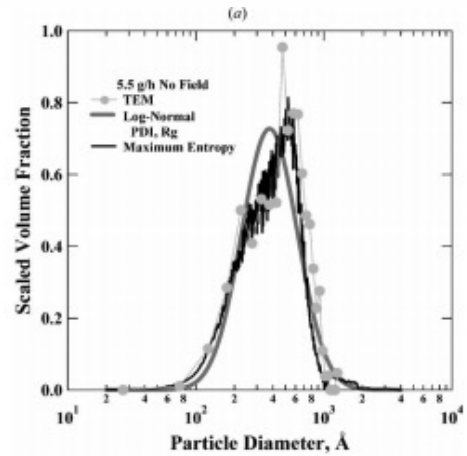

Fractal Aggregate Primary Particles

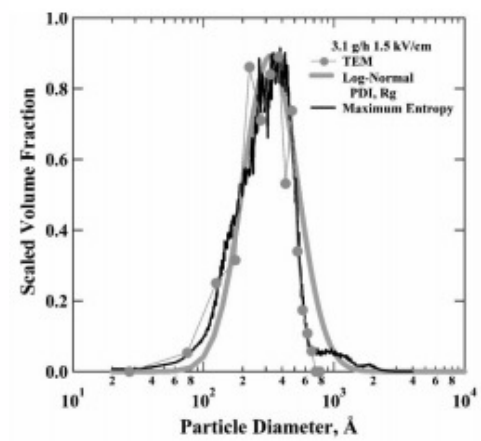

http://www.eng.uc.edu/~gbeaucag/PDFPapers/ks5024%20Japplcryst%20Beaucage%20PSD.pdf

Fractal Aggregates and Agglomerates
Aggregate growth

Some Issues to Consider for Aggregation/Agglomeration

Path of Approach, Diffusive or Ballistic (Persistence of velocity for particles)
Concentration of Monomers
persistence length of velocity compared to mean separation distance
Branching and structural complexity

What happens when monomers or clusters get to a growth site:
Diffusion Limited Aggregation
Reaction Limited Aggregation

Chain Growth (Monomer-Cluster), Step Growth (Monomer-Monomer to Cluster-Cluster)
or a Combination of Both (mass versus time plots)

Cluster-Cluster Aggregation
Monomer-Cluster Aggregation
Monomer-Monomer Aggregation

DLCA Diffusion Limited Cluster-Cluster Aggregation
RLCA Reaction Limited Cluster Aggregation

Post Growth: Internal Rearrangement/Sintering/Coalescence/Ostwald Ripening
http://www.eng.uc.edu/~gbeaucag/Classes/Nanopowders/AggregateGrowth.pdf

Fractal Aggregates and Agglomerates

Aggregate growth

Consider what might effect the dimension of a growing aggregate.

Transport Diffusion/Ballistic
Growth Early/Late (0-d point => Linear 1-d => Convoluted 2-d => Branched 2+d)
Speed of Transport Cluster, Monomer
Shielding of Interior
Rearrangement
Sintering
Primary Particle Shape

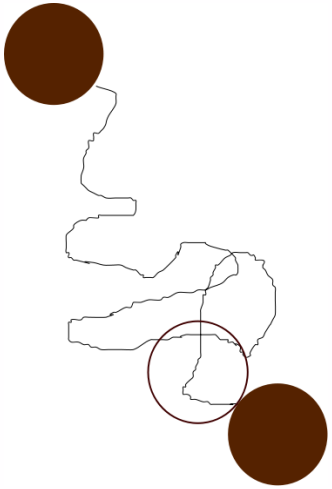

DLA df = 2.5 Monomer-Cluster (Meakin 1980 Low Concentration)
DLCA df = 1.8 (Higher Concentration Meakin 1985)

Ballistic Monomer-Cluster (low concentration) df = 3
Ballistic Cluster-Cluster (high concentration) df = 1.95

Fractal Aggregates and Agglomerates

Aggregate growth

Colloids with Strongly attractive forces

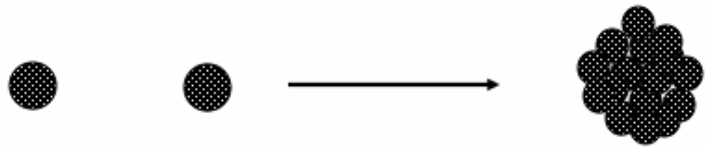

NEAR EQUILIBRIUM: Ostwald Ripening

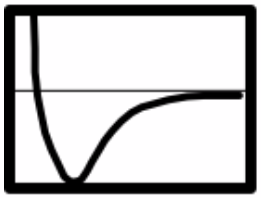

Kinetic Growth: DIFFUSION LIMITED

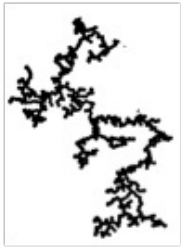

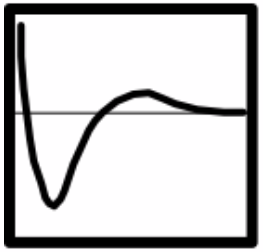

Kinetic Growth: CHEMICALLY LIMITED

Reaction Limited,
Short persistence of velocity

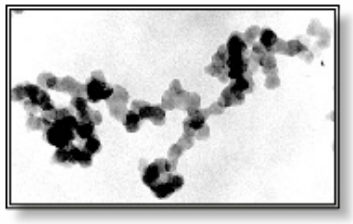

Precipitated Silica

From DW Schaefer Class Notes

Fractal Aggregates and Agglomerates

Aggregate growth

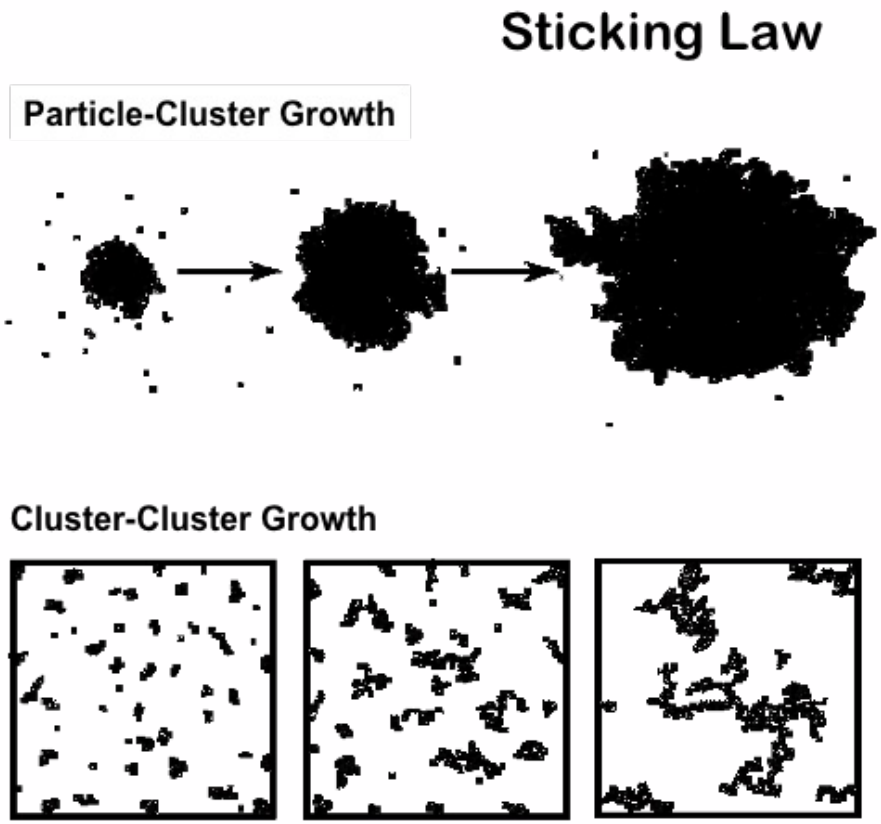

From DW Schaefer Class Notes

Fractal Aggregates and Agglomerates

Aggregate growth

Transport

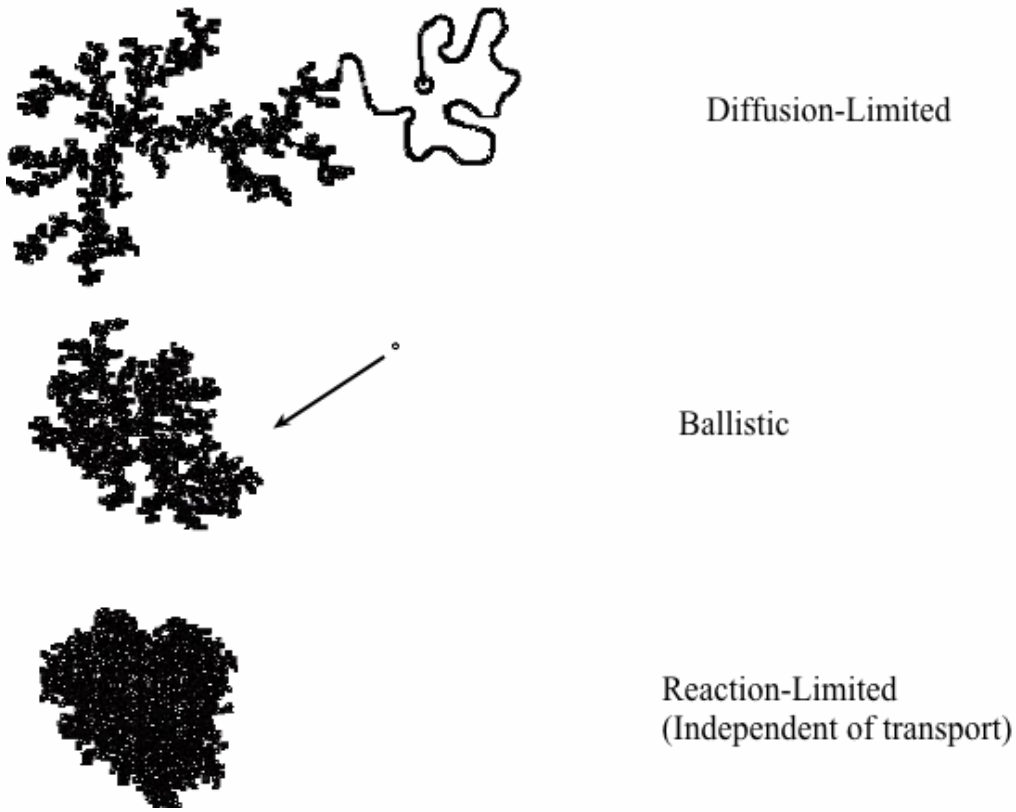

From DW Schaefer Class Notes

Fractal Aggregates and Agglomerates

Aggregate growth

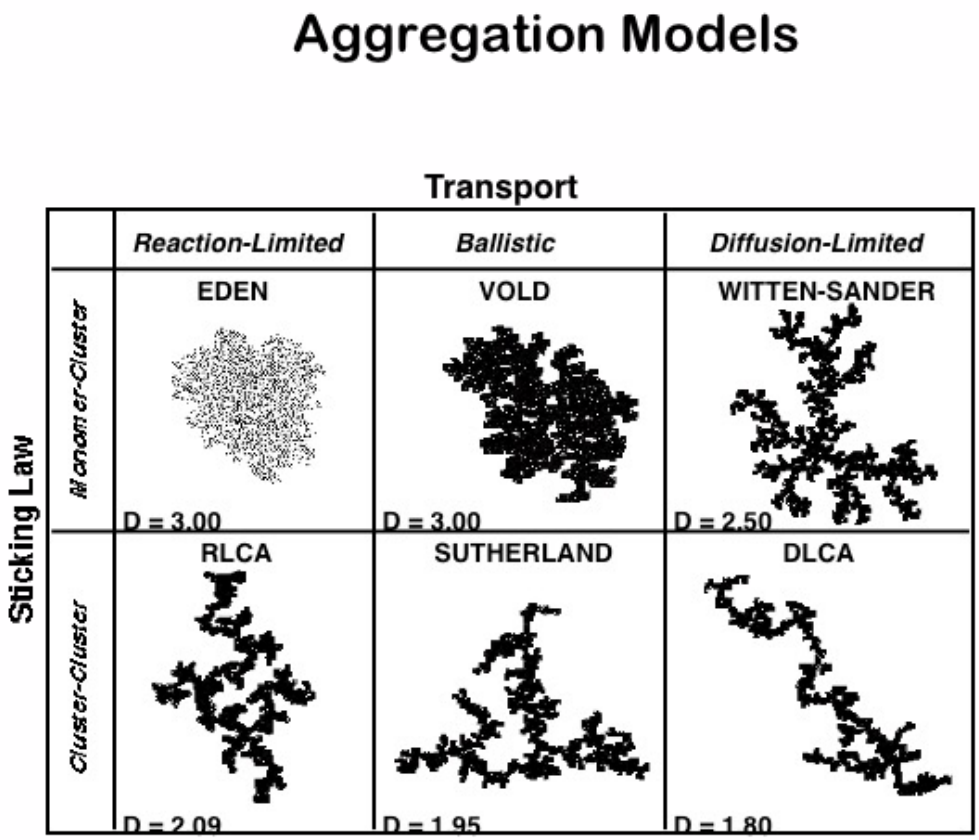

Eden Model particles are added at random with equal probability to any unoccupied site adjacent to one or more occupied sites (Surface Fractals are Produced)

Vold-Sutherland Model particles with random **linear** trajectories are added to a growing cluster of particles at the position where they first contact the cluster

Witten-Sander Model particles with random **Brownian** trajectories are added to a growing cluster of particles at the position where they first contact the cluster

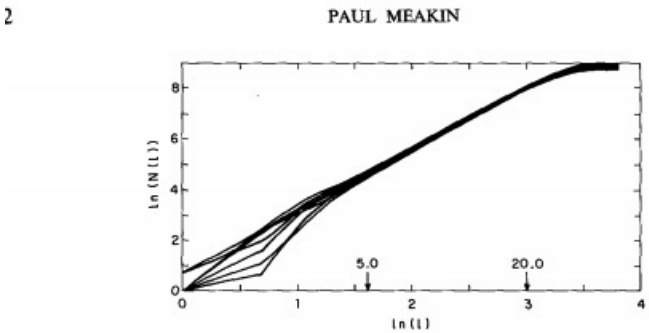

FIG. 8. Dependence of ln ($N(l)$) on ln (l) for eight clusters grown using the WS model of diffusion-limited cluster formation on a three-dimensional cubic lattice.

In RLCA a "sticking probability is introduced in the random growth process of clusters. This increases the dimension.

Sutherland Model pairs of particles are assembled into randomly oriented dimers. Dimers are coupled at random to construct tetramers, then octoamers etc. This is a step-growth process except that all reactions occur synchronously (monodisperse system).

In DLCA the "sticking probability is 1. Clusters follow random walk.

http://www.eng.uc.edu/~gbeaucag/Classes/MorphologyofComplexMaterials/MeakinVoldSunderlandEdenWittenSanders.pdf

From DW Schaefer Class Notes

Fractal Aggregates and Agglomerates

Aggregate growth

Analysis of Fractals

$$\mathrm{Log}(N) = D\,\mathrm{Log}(R)$$

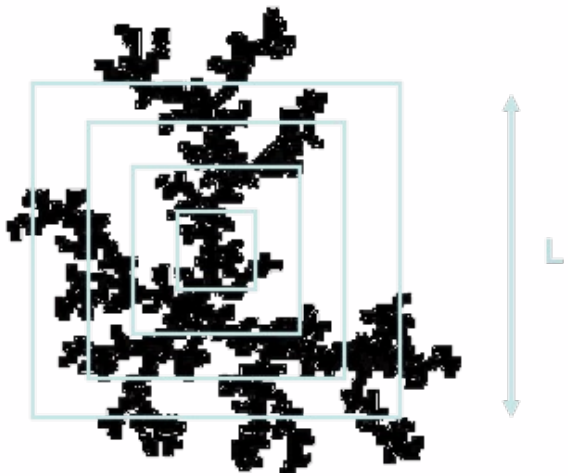

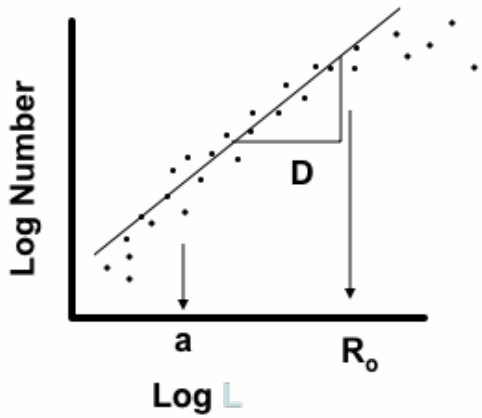

From DW Schaefer Class Notes

Fractal Aggregates and Agglomerates

Aggregate growth

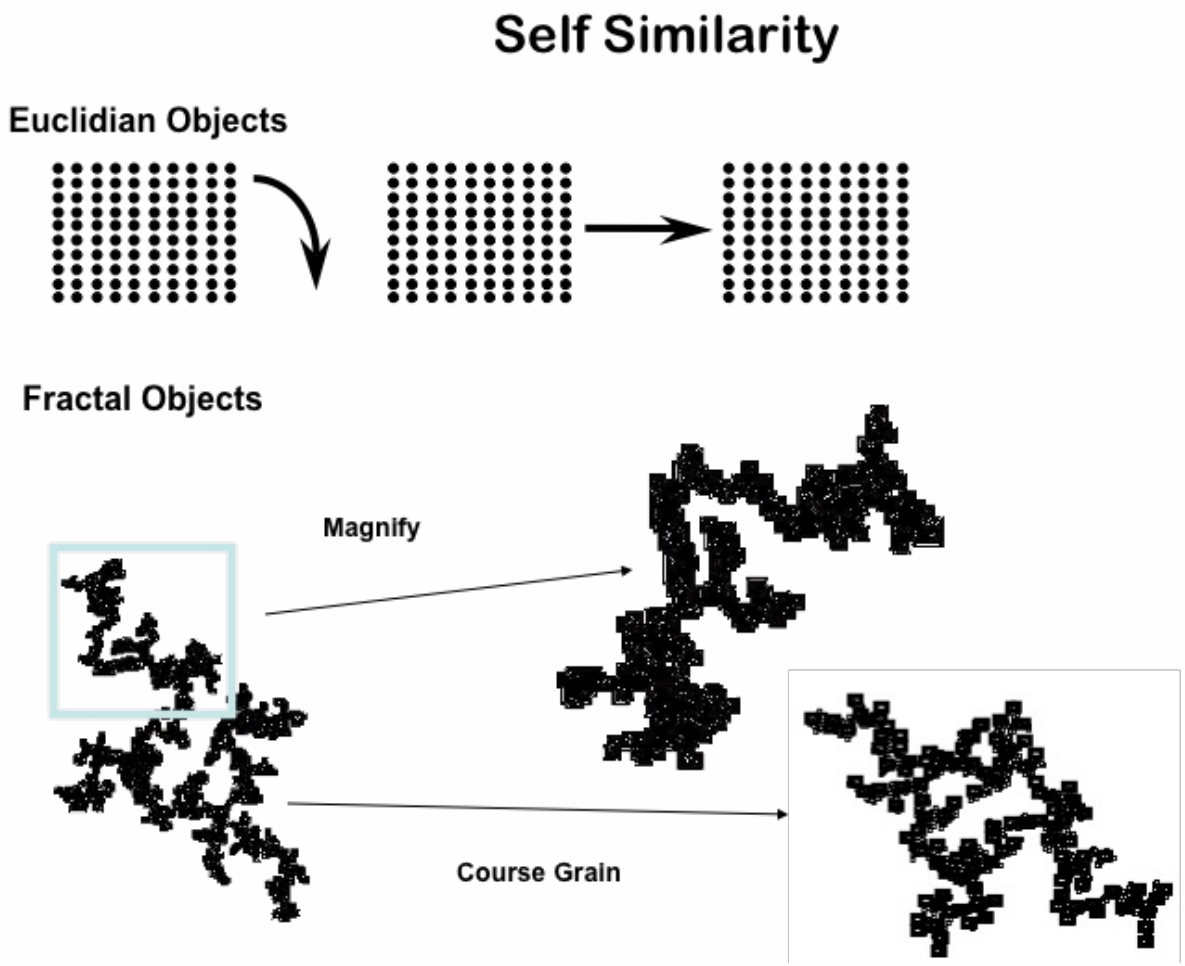

From DW Schaefer Class Notes

Fractal Aggregates and Agglomerates

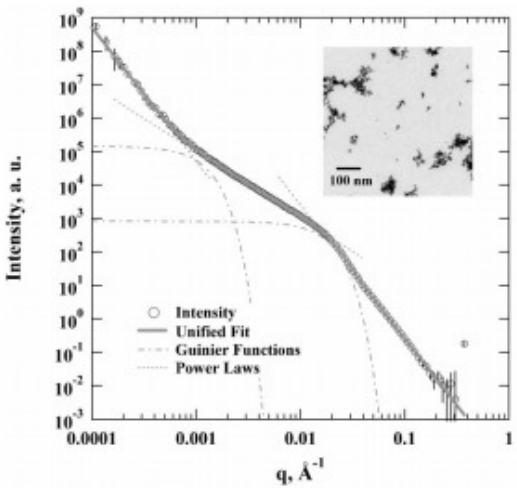

Primary: Primary Particles
Secondary: Aggregates
Tertiary: Agglomerates

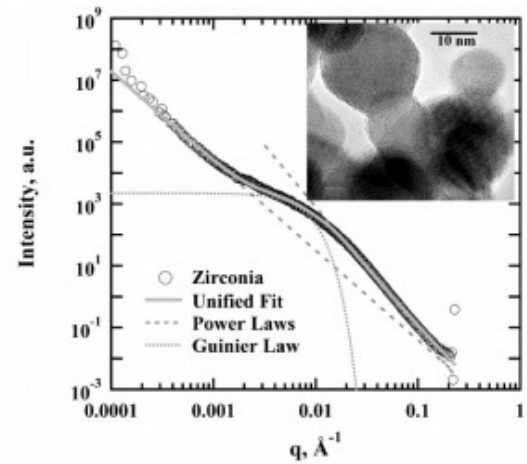

Primary: Primary Particles

Tertiary: Agglomerates

From DW Schaefer Class Notes

http://www.eng.uc.edu/~gbeaucag/PDFPapers/ks5024%20Japplcryst%20Beaucage%20PSD.pdf

Hierarchy of Polymer Chain Dynamics

Dilute Solution Chain

Dynamics of the chain

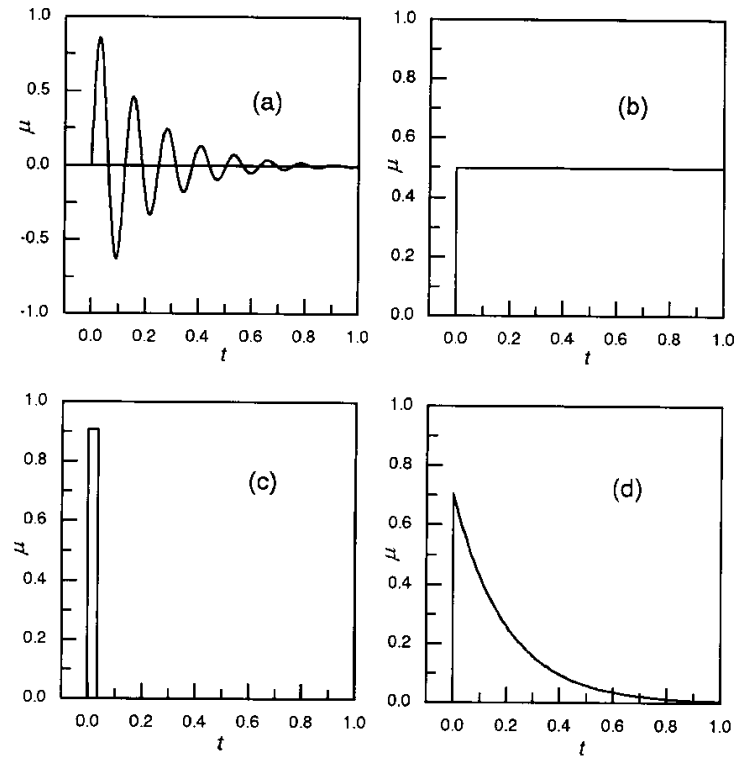

Fig. 5.4. Primary response function of a damped harmonic oscillator (a), a perfectly viscous body (b), a Hookean solid (c), a simple relaxatory system (d)

$$x(t) = \int_{-\infty}^{t} dt' \exp\left(-k_{spr}\left(t-t'\right)/\xi\right) g\left(t'\right)$$

The exponential term is the "response function"
response to a pulse perturbation

Dilute Solution Chain

Dynamics of the chain

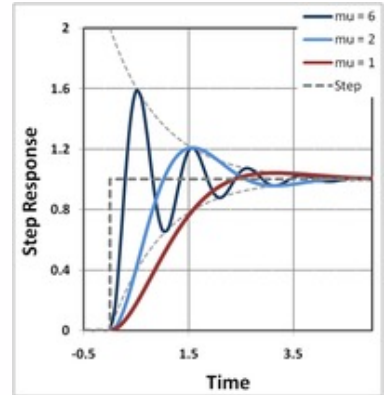

Damped Harmonic Oscillator

$$x(t) = \int_{-\infty}^{t} dt' \exp\left(-k_{spr}(t-t')/\xi\right) g(t')$$

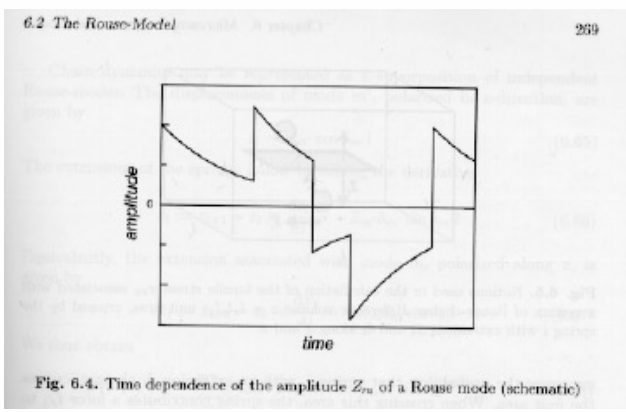

Fig. 6.4. Time dependence of the amplitude Z_n of a Rouse mode (schematic)

For Brownian motion
of a harmonic bead in a solvent
this response function can be used to calculate the
time correlation function <x(t)x(0)>
for DLS for instance

$$\langle x(t)x(0)\rangle = \int_{-\infty}^{t} dt_1 \int_{-\infty}^{0} dt_2 \exp\left[-k_{spr}(t-t_1-t_2)/\xi\right]\langle g(t_1)g(t_2)\rangle$$

$$\langle g(t_1)g(t_2)\rangle = \frac{2kT}{\xi}\partial(t_1-t_2)$$

$$\langle x(t)x(0)\rangle = \frac{kT}{k_{spr}}\exp(-t/\tau)$$

τ is a relaxation time.

$$\tau = \frac{\xi}{k_{spr}}$$

Dilute Solution Chain

Dynamics of the chain

Rouse Motion

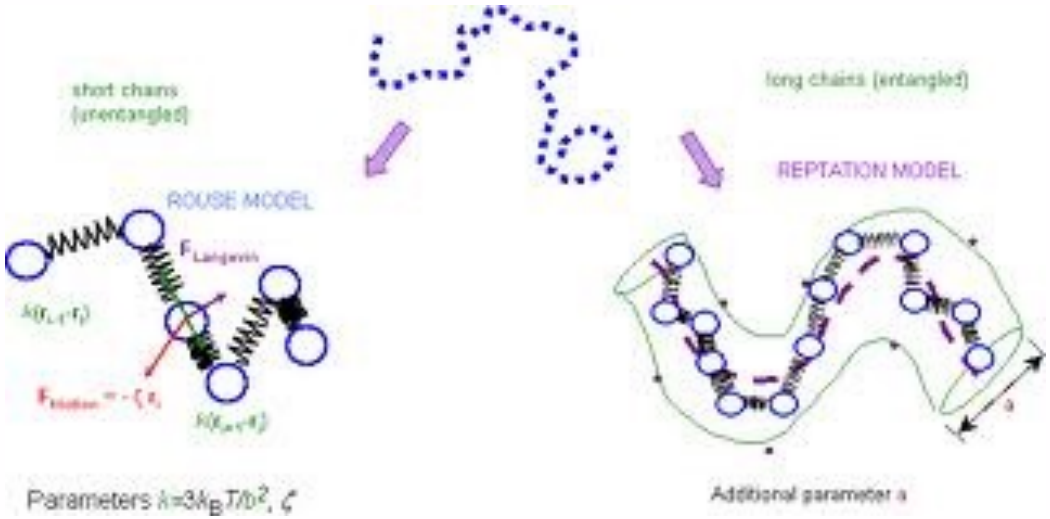

$$E = \frac{k_{spr}}{2}\sum_{i=1}^{N}\left(R_i - R_{i-1}\right)^2$$

$$\frac{dR_i}{dt} = \frac{-\left(dE/dR_i\right)}{\xi} + g_i(t)$$

$$\xi = 6\pi\eta_{solvent}a$$

Beads 0 and N are special

For Beads 1 to N-1

$$\frac{dR_i}{dt} = \frac{-k_{spr}}{\xi}\left(R_{i+1} + R_{i-1} - 2R_i\right) + g_i(t)$$

For Bead 0 use $R_{-1} = R_0$ and for bead N $R_{N+1} = R_N$

This is called a closure relationship

Dilute Solution Chain

Dynamics of the chain

Rouse Motion

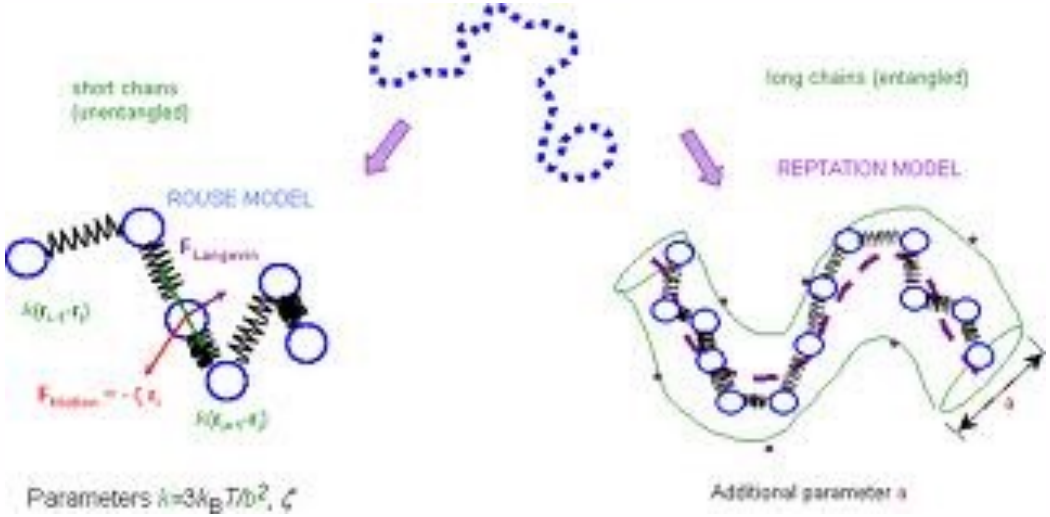

$$\frac{dR_i}{dt} = \frac{-k_{spr}}{\xi}\left(R_{i+1} + R_{i-1} - 2R_i\right) + g_i(t)$$

The Rouse unit size is arbitrary so we can make it very small and:

$$\frac{dR}{dt} = \frac{-k_{spr}}{\xi}\frac{d^2R}{di^2} + g_i(t)$$

With dR/dt = 0 at i = 0 and N

$$\frac{d^2R}{di^2}$$

Reflects the curvature of R in i,
it describes modes of vibration like on a guitar string

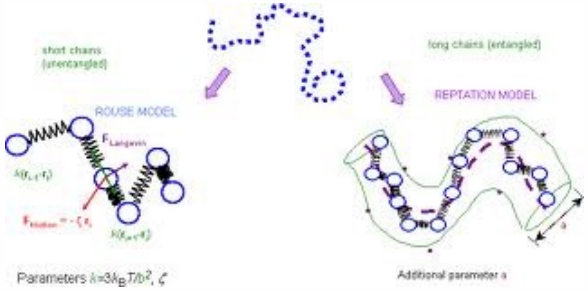

Dilute Solution Chain

Dynamics of the chain

Rouse Motion

$$\frac{d^2R}{di^2}$$ Describes modes of vibration like on a guitar string

For the "p' th" mode (0' th mode is the whole chain (string))

$$k_{spr,p} = \frac{2p^2\pi^2 k_{spr}}{N} = \frac{6\pi^2 kT}{Nb^2}p^2 \qquad \xi_p = 2N\xi \qquad \xi_0 = N\xi$$

$$\tau_p = \frac{\xi_p}{k_{spr,p}} = \frac{2N^2b^2\xi}{3\pi^2p^2kT}$$

Dilute Solution Chain

Dynamics of the chain

Rouse Motion

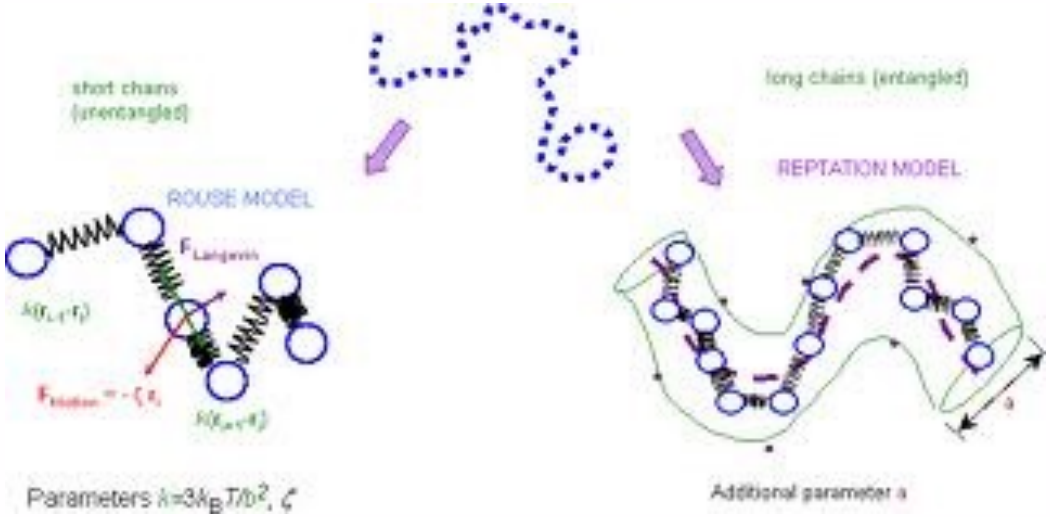

Predicts that the viscosity will follow N which is true for low molecular weights in the melt and for fully draining polymers in solution

Rouse model predicts
Relaxation time follows N^2 (actually follows N^3/df)
Diffusion constant follows 1/N (zeroth order mode is translation of the molecule) (actually follows $N^{-1/df}$)
Both failings are due to hydrodynamic interactions (incomplete draining of coil)

Dilute Solution Chain

Dynamics of the chain

Rouse Motion

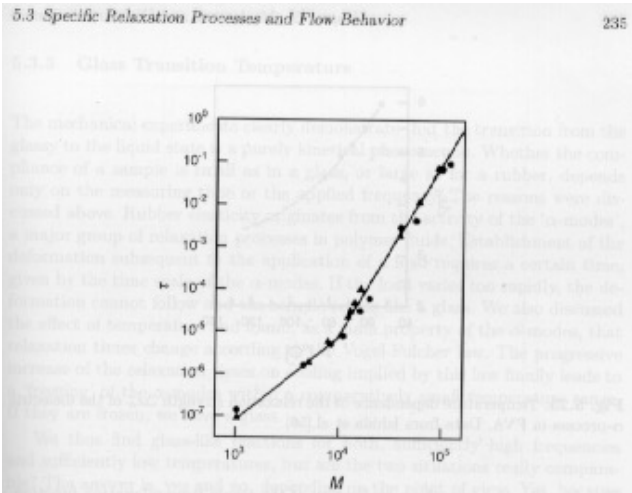

Fig. 5.21. Molecular weight dependence of the relaxation time of the dielectric normal mode in *cis*-PIP. Data from Boese and Kremer [58]

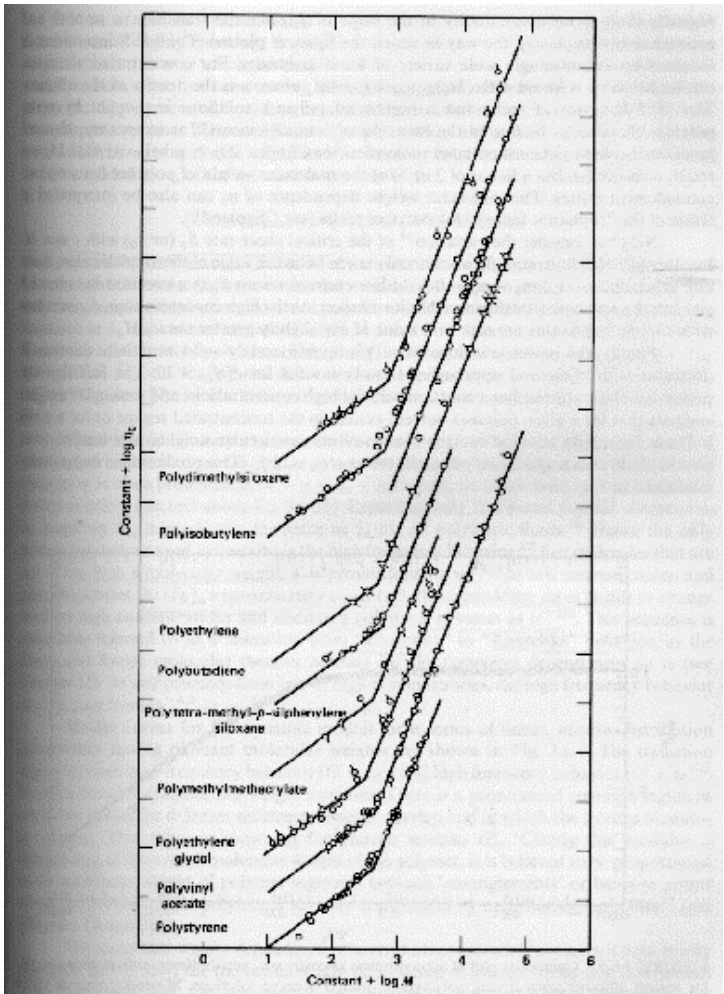

FIGURE 3.6-4. Plots of constant + log η_c vs. constant + log M for nine different polymers. The two constants are different for each of the polymers, and the one appearing in the abscissa is proportional to concentration, which is constant for a given undiluted polymer. For each polymer the slopes of the left and right straight line regions are 1.0 and 3.4, respectively. [G. C. Berry and T. G. Fox, *Adv. Polym. Sci.*, **5**, 261–357 (1968).]

Predicts that the viscosity will follow N which is true for low molecular weights in the melt and for fully draining polymers in solution

Rouse model predicts

Relaxation time follows N^2 (actually follows N^3/df)

Hierarchy of Entangled Melts

Hierarchy of Entangled Melts

Chain dynamics in the melt can be described by a small set of "physically motivated, material-specific paramters"

Tube Diameter d_T
Kuhn Length l_K
Packing Length p

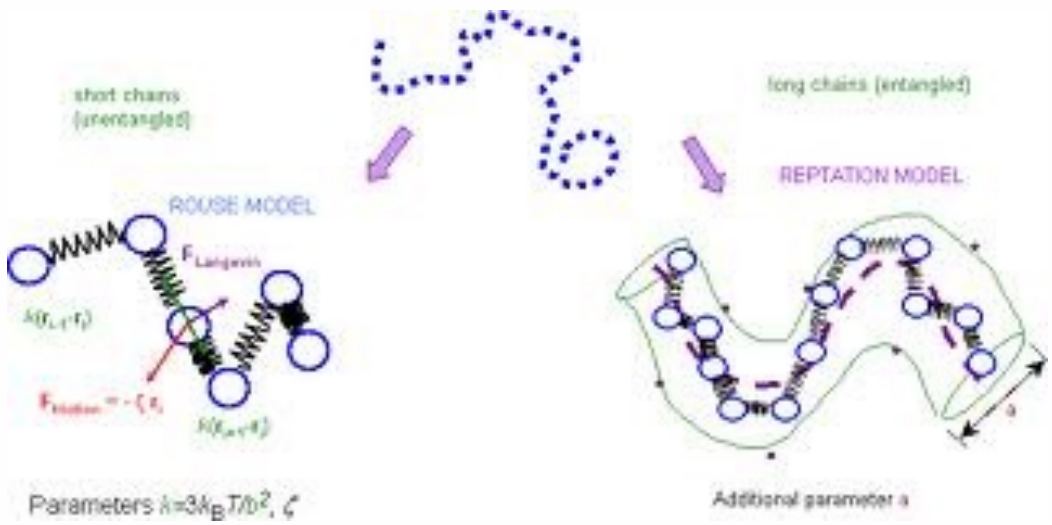

http://www.eng.uc.edu/~gbeaucag/Classes/MorphologyofComplexMaterials/SukumaranScience.pdf

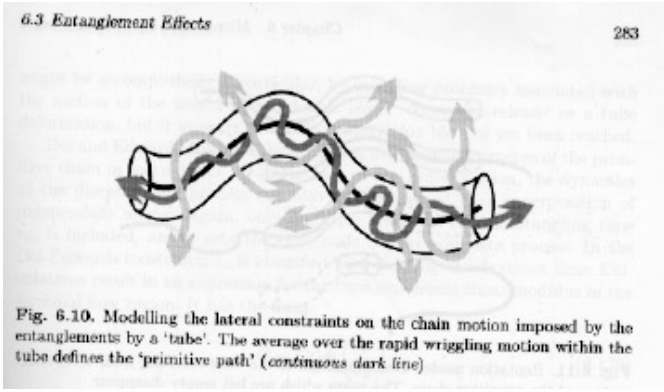

Fig. 6.10. Modelling the lateral constraints on the chain motion imposed by the entanglements by a 'tube'. The average over the rapid wriggling motion within the tube defines the 'primitive path' (*continuous dark line*)

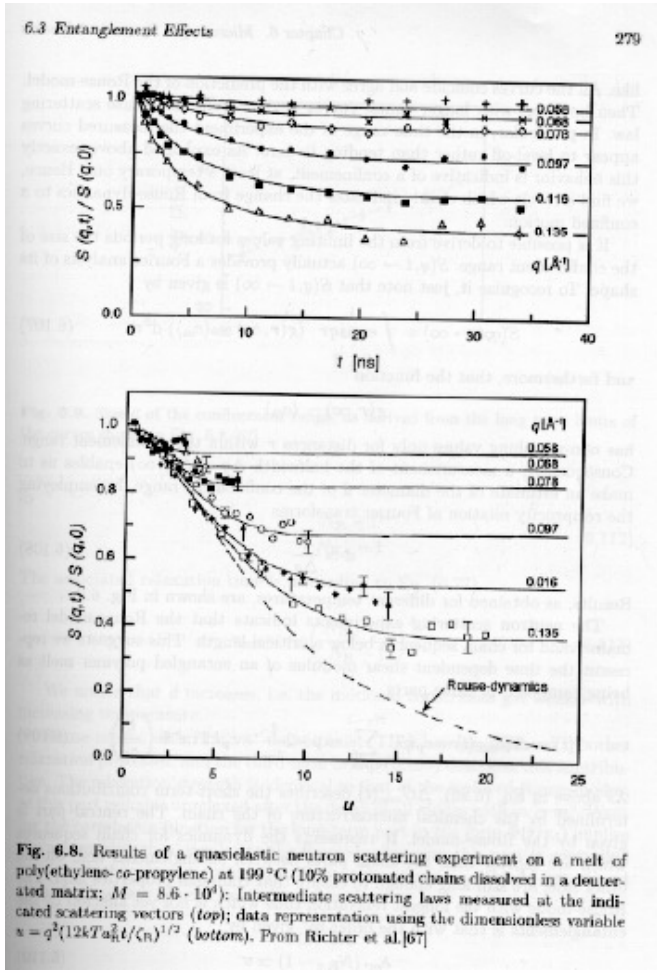

Fig. 6.8. Results of a quasielastic neutron scattering experiment on a melt of poly(ethylene-*co*-propylene) at 199 °C (10% protonated chains dissolved in a deuterated matrix; $M = 8.6 \cdot 10^4$): Intermediate scattering laws measured at the indicated scattering vectors (*top*); data representation using the dimensionless variable $u = q^2(12kTa_0^2t/\zeta_0)^{1/2}$ (*bottom*). From Richter et al.[67]

Quasi-elastic neutron scattering data
demonstrating the existence of the tube

Unconstrained motion => S(q) goes to 0 at very long times

Each curve is for a different q = 1/size

At small size there are less constraints (within the tube)

At large sizes there is substantial constraint (the tube)

By extrapolation to high times
a size for the tube can be obtained
d_T

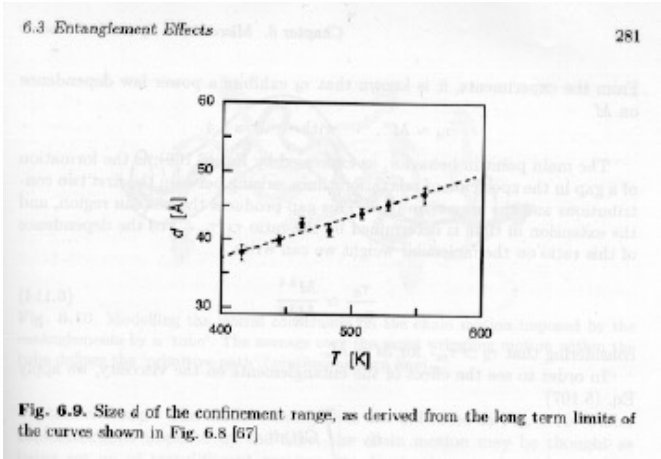

Fig. 6.9. Size d of the confinement range, as derived from the long term limits of the curves shown in Fig. 6.8 [67]

There are two regimes of hierarchy in time dependence
Small-scale unconstrained Rouse behavior
Large-scale tube behavior

We say that the tube follows a "primitive path"
This path can "relax" in time = Tube relaxation or Tube Renewal

Without tube renewal the Reptation model predicts that viscosity follows N^3 (observed is $N^{3.4}$)

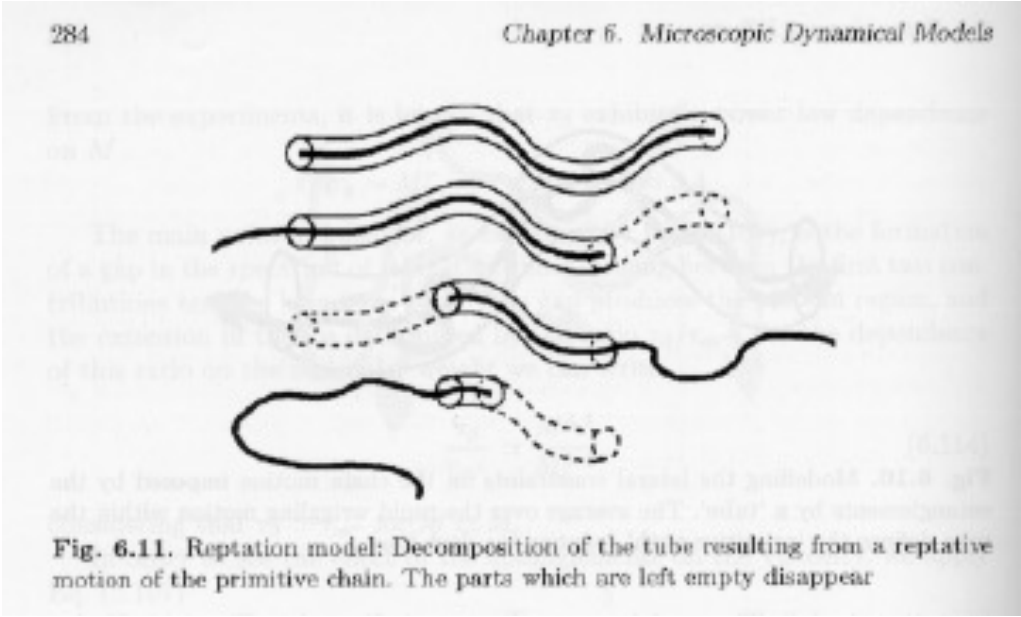

Fig. 6.11. Reptation model: Decomposition of the tube resulting from a reptative motion of the primitive chain. The parts which are left empty disappear

Without tube renewal the Reptation model predicts that viscosity follows N^3 (observed is $N^{3.4}$)

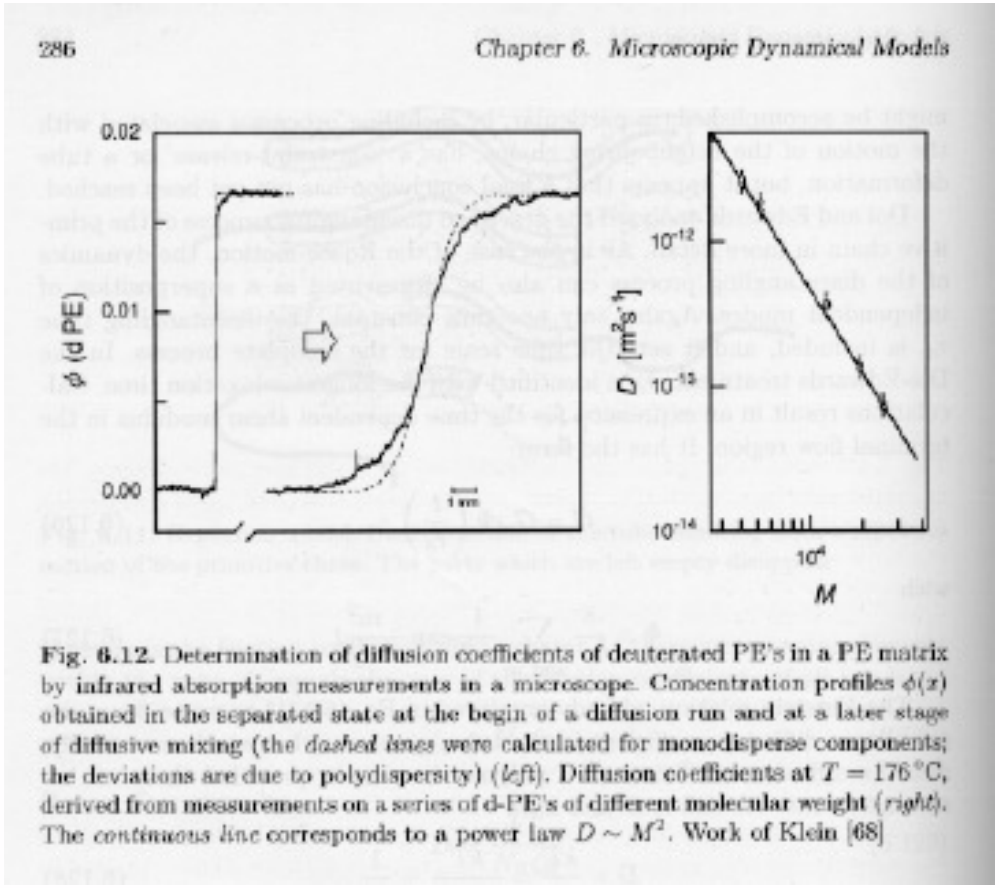

Fig. 6.12. Determination of diffusion coefficients of deuterated PE's in a PE matrix by infrared absorption measurements in a microscope. Concentration profiles $\phi(x)$ obtained in the separated state at the begin of a diffusion run and at a later stage of diffusive mixing (the *dashed lines* were calculated for monodisperse components; the deviations are due to polydispersity) (*left*). Diffusion coefficients at $T = 176\,^{\circ}\mathrm{C}$, derived from measurements on a series of d-PE's of different molecular weight (*right*). The *continuous line* corresponds to a power law $D \sim M^{2}$. Work of Klein [68]

Reptation predicts that the diffusion coefficient will follow N^2 (Experimentally it follows N^2)
Reptation has some experimental verification
Where it is not verified we understand that tube renewal is the main issue.

(Rouse Model predicts D ~ 1/N)

Reptation of DNA in a concentrated solution

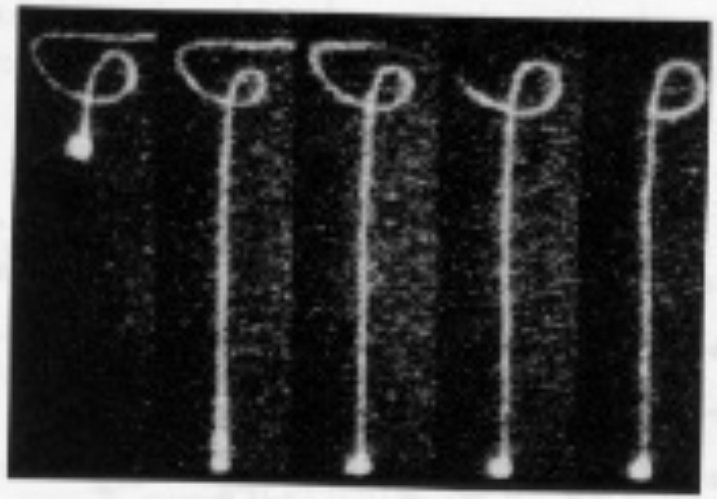

Fig. 6.13. Series of images of a fluorescently stained DNA chain embedded in a concentrated solution of unstained chains: Initial conformation (*left*); partial stretching by a rapid move of the bead at one end (*second from the left*); chain recoil by a reptative motion in the tube (*subsequent pictures to the right*). Reprinted with permission from T.Perkins, D.E.Smith and S.Chu. *Science*, 264:819, 1994. Copyright (1994) American Association for the Advancement of Science

Simulation of the tube

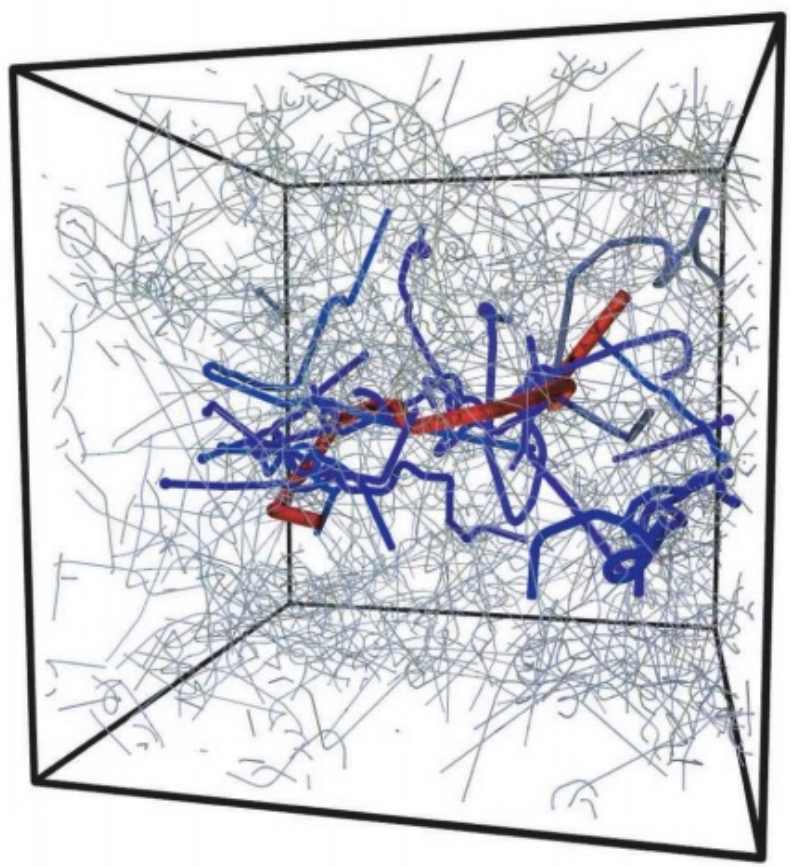

Fig. 3. Result of the primitive-path analysis of a melt of 200 chains of $N + 1 = 350$ beads. We show the primitive path of one chain (red) together with all of those it is entangled with (blue). The primitive paths of all other chains in the system are shown as thin lines.

Simulation of the tube

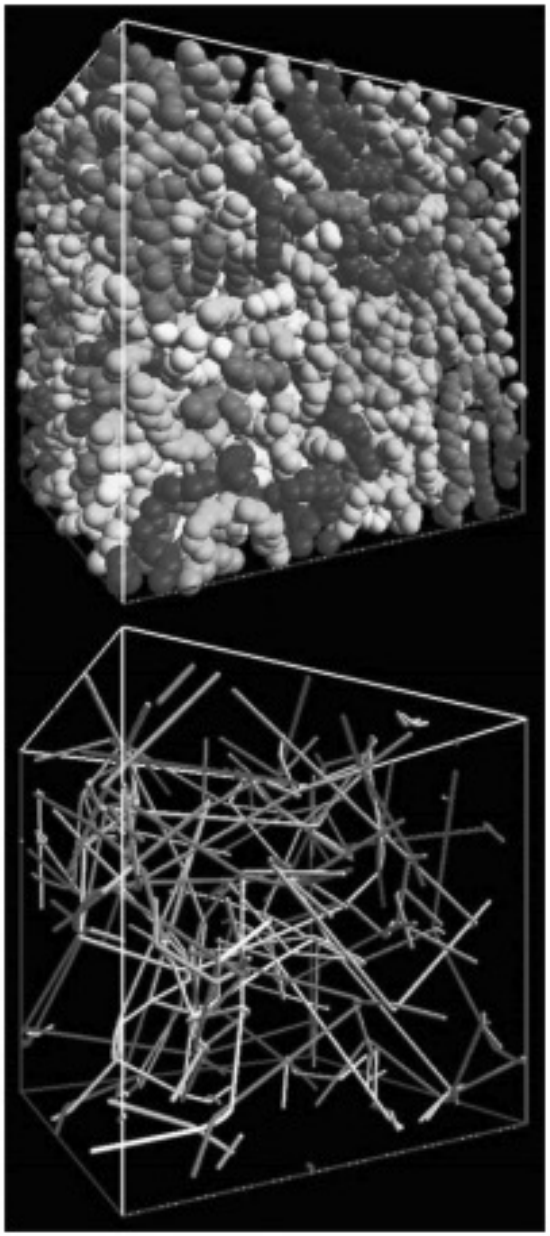

Fig. 3. A representative amorphous polymer sample and the corresponding network of primitive paths.

Plateau Modulus

Not Dependent on N, Depends on T and concentration

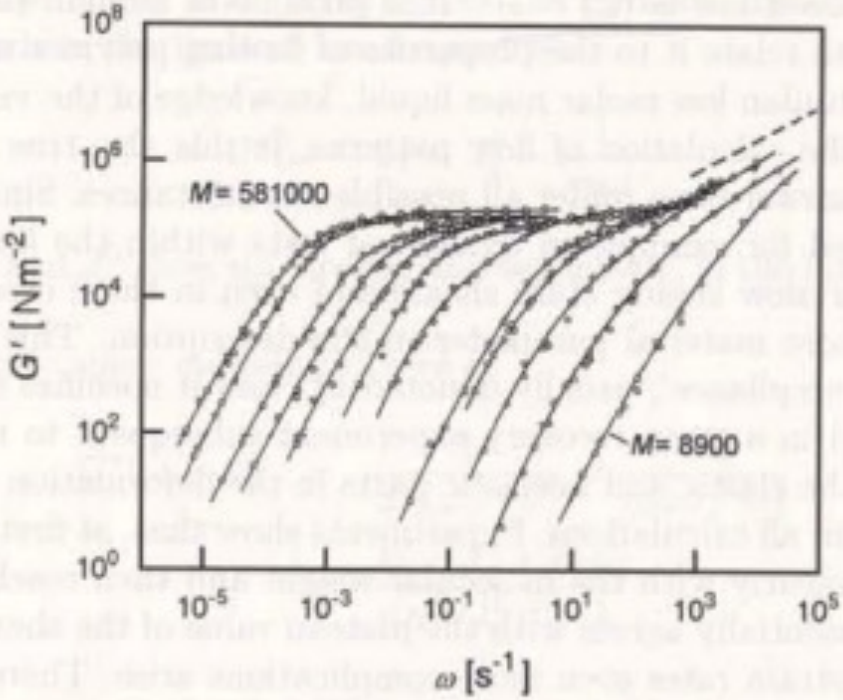

Fig. 5.15. Storage shear moduli measured for a series of fractions of PS with different molecular weights in the range $M = 8.9 \cdot 10^3$ to $M = 5.81 \cdot 10^5$. The *dashed line* in the upper right corner indicates the slope corresponding to the power law Eq. (6.81) derived for the Rouse-model of the glass-transition. Data from Onogi et al.[54]

$$G_0 = \frac{4\rho RT}{5M_e} = \frac{4RT}{5p^3}$$

Kuhn Length- conformations of chains $\langle R^2 \rangle = l_K L$

Packing Length- length were polymers interpenetrate $p = 1/(\rho_{chain} \langle R^2 \rangle)$
where ρ_{chain} is the number density of monomers

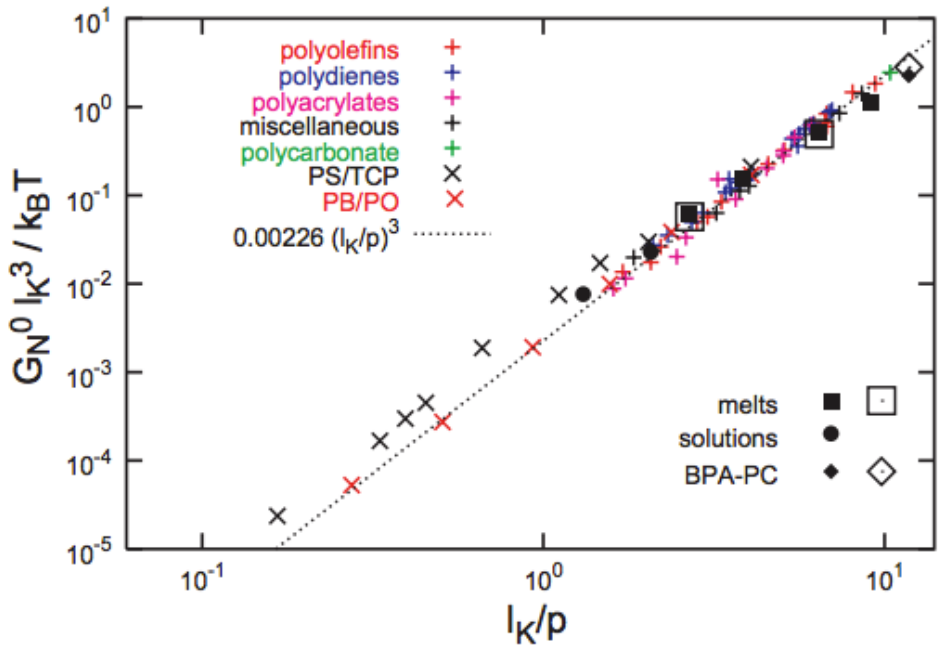

Fig. 2. Dimensionless plateau moduli Gl_K^3/k_BT as a function of the dimensionless ratio l_K/p of Kuhn length l_K and packing length p. The figure contains (i) experimentally measured plateau moduli for polymer melts (*25*) (+; colors mark different groups of polymers as indicated) and semidilute solutions (*26–28*) (×); (ii) plateau moduli inferred from the normal tensions measured in computer simulation of bead-spring melts (*35, 36*) (□) and a semi-atomistic polycarbonate melt (*37*) (◇) under an elongational strain; and (iii) predictions of the tube model Eq. 1 based on the results of our primitive-path analysis for bead-spring melts (■), bead-spring semidilute solutions (●), and the semi-atomistic polycarbonate melt (◆). The line indicates the best fit to the experimental data for polymer melts by Fetters *et al.* (*24*). Errors for all the simulation data are smaller than the symbol size.

this implies that $d_T \sim p$

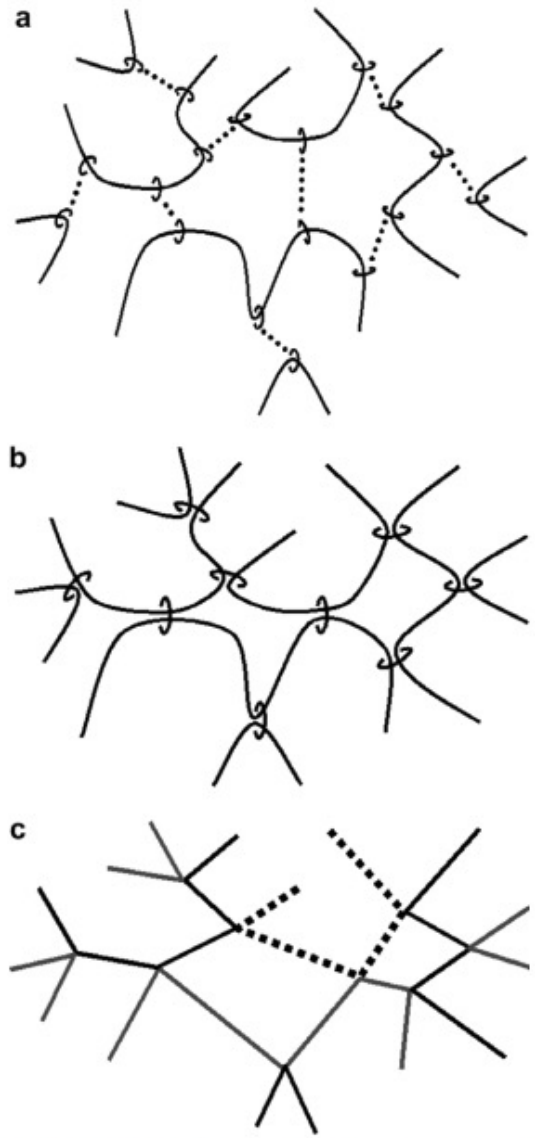

Fig. 1. Schematic representation of dual slip-links. (a) Chains coupled by virtual links. (b) Dual slip-links. (c) Real space representation of the corresponding network of primitive paths.

McLeish/Milner/Read/Larsen Hierarchical Relaxation Model

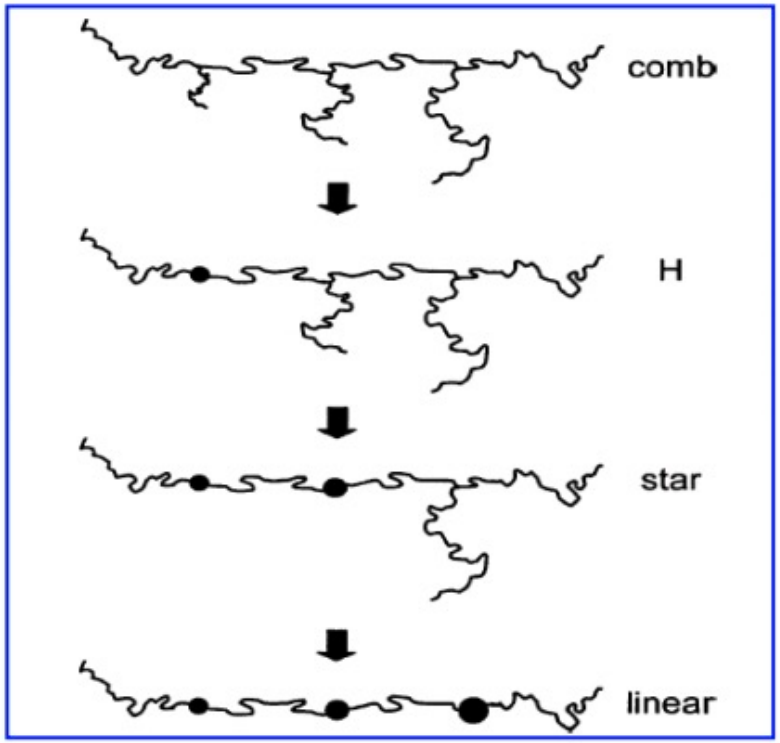

http://www.engin.umich.edu/dept/che/research/larson/downloads/Hierarchical-3.0-manual.pdf

Block Copolymers

http://www.eng.uc.edu/~gbeaucag/Classes/MorphologyofComplexMaterials/BCP%20Section.pdf

Block Copolymers

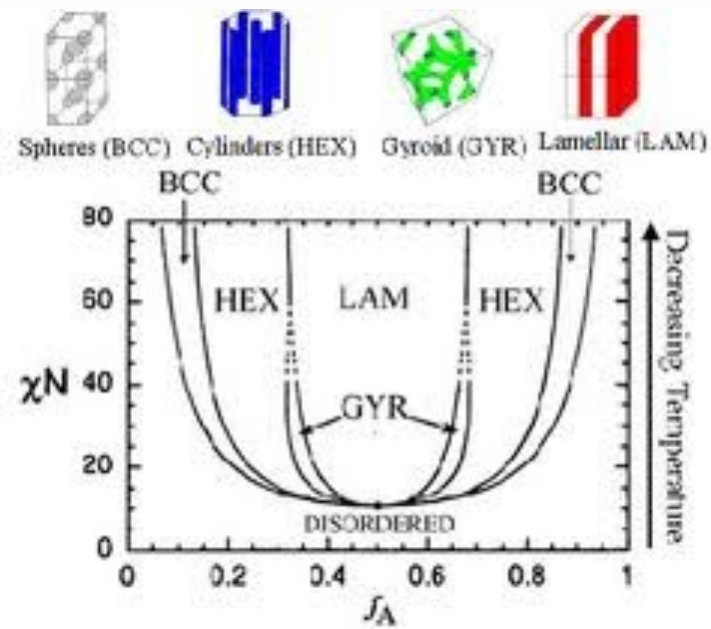

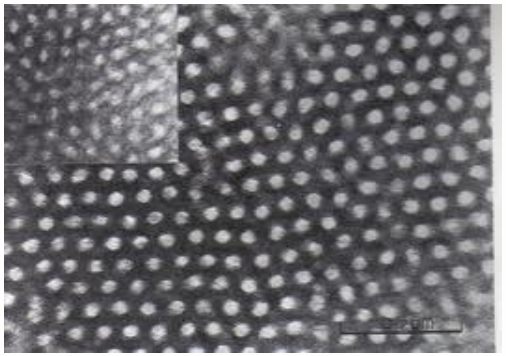

SBR Rubber

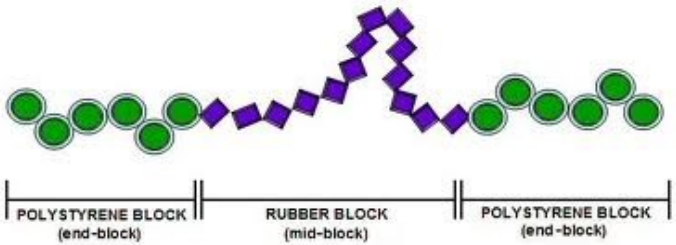

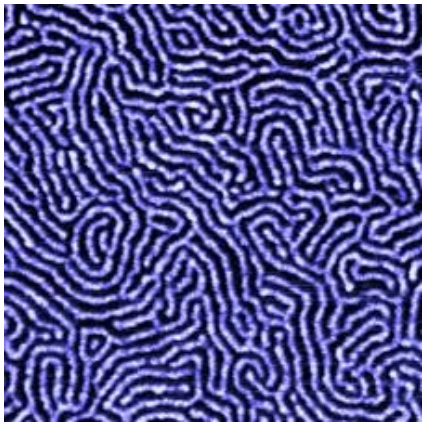

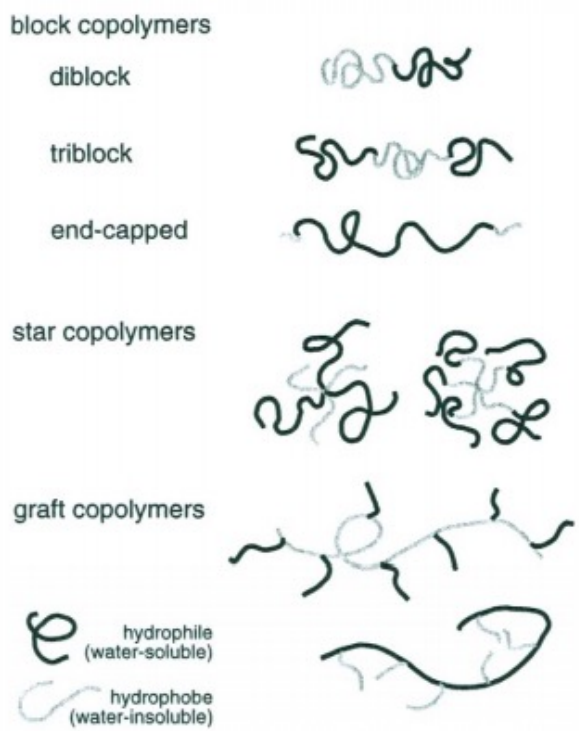

Figure 9. Schematics of block, star, and graft amphiphilic block copolymers.

http://www.eng.uc.edu/~gbeaucag/Classes/MorphologyofComplexMaterials/Amphiphilic.pdf

16

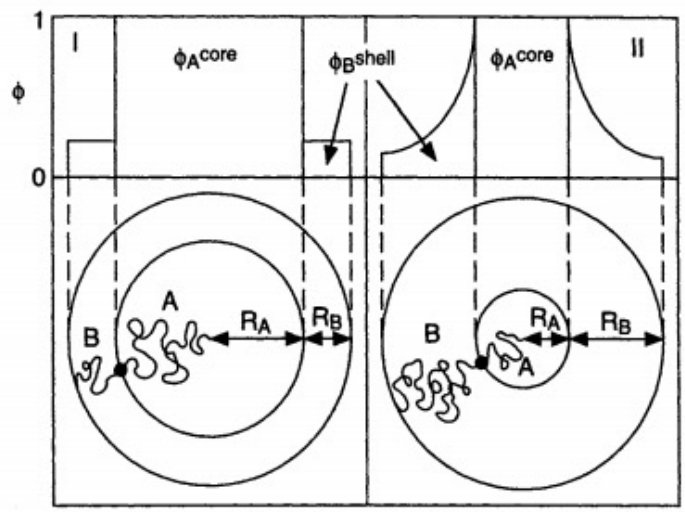

Figure 1. Illustration of model I (left) and II (right) of the AB-diblock copolymer micelle in a selective solvent (lower panel) and the volume fraction profiles of the polymer blocks (upper panel) applied for the large core case ($N_A >> N_B$) and the small core case ($N_A << N_B$), respectively.

http://www.eng.uc.edu/~gbeaucag/Classes/MorphologyofComplexMaterials/BCP%20Modeling.pdf

Hierarchy in BCP's and Micellar Systems

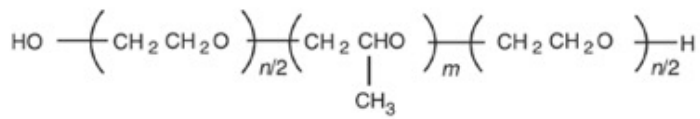

Pluronics (PEO/PPO block copolymers)

We consider primary structure as the block nature of the polymer chain.

This is similar to hydrophobic and hydrophilic interactions in proteins.

These cause a secondary self-organization into rods/spheres/sheets.

A tertiary organizaiton of these secondary structures occurs.

There are some similarities to proteins but BCP's are extremely simple systems by comparison.

What is the size of a Block Copolymer Domain?

Masao Doi, Introduction to Polymer Physics

-For and symmetric A-B block copolymer
-Consider a lamellar structure with Φ = 1/2
-Layer thickness D in a cube of edge length L, surface energy σ
- $F_{surface} \cong 2\sigma \frac{L}{D} L^2$ so larger D means less surface and a lower Free Energy F.
-The polymer chain is stretched as D increases. The free energy of a stretched chain as a function of the extension length D is given by

- $F_{stretch} \cong kT \frac{D^2}{Nb^2} \frac{L^3}{N\upsilon_c}$ where N is the degree of polymerization for A or B,

b is the step length per N unit, vc is the excluded volume for a unit step
So the stretching free energy, F, increases with D^2.

-To minimize the free energies we have $D \cong \left(\frac{\sigma N^2 b^2 \upsilon_c}{kT} \right)^{1/3} \sim N^{2/3}$

Chain Scaling (Long-Range Interactions)

Long-range interactions are interactions of chain units separated by such a great index difference that we have no means to determine if they are from the same chain other than following the chain over great distances to determine the connectivity. That is, Orientation/continuity or polarity and other short range linking properties are completely lost.

Long-range interactions occur over short spatial distances (as do all interactions).

Consider chain scaling with no long-range interactions.

The chain is composed of a series of steps with no orientational relationship to each other.

So <R> = 0

$\langle R^2 \rangle$ has a value:

$$\langle R^2 \rangle = \sum_i \sum_j r_i \bullet r_j = \sum_i r_i \bullet r_i + \sum_i \sum_{j \neq i} r_i \bullet r_j$$

We assume no long range interactions so that the second term can be 0.

$$\langle R^2 \rangle = Nr^2$$